



저작자표시-비영리-변경금지 2.0 대한민국

이용자는 아래의 조건을 따르는 경우에 한하여 자유롭게

- 이 저작물을 복제, 배포, 전송, 전시, 공연 및 방송할 수 있습니다.

다음과 같은 조건을 따라야 합니다:



저작자표시. 귀하는 원저작자를 표시하여야 합니다.



비영리. 귀하는 이 저작물을 영리 목적으로 이용할 수 없습니다.



변경금지. 귀하는 이 저작물을 개작, 변형 또는 가공할 수 없습니다.

- 귀하는, 이 저작물의 재이용이나 배포의 경우, 이 저작물에 적용된 이용허락조건을 명확하게 나타내어야 합니다.
- 저작권자로부터 별도의 허가를 받으면 이러한 조건들은 적용되지 않습니다.

저작권법에 따른 이용자의 권리는 위의 내용에 의하여 영향을 받지 않습니다.

이것은 [이용허락규약\(Legal Code\)](#)을 이해하기 쉽게 요약한 것입니다.

[Disclaimer](#)

이학박사 학위논문

I. **Studies on the potent hepatitis C virus NS5A inhibitors**

II. **Synthesis of conjugated polymers using palladium iron oxide nanocrystals**

I. **NS5A 를 타겟으로 하는 C 형 간염 치료제 연구**

II. **팔라듐 산화철 나노입자를 이용한 컨쥬게이션된 폴리머 합성법**

2017 년 2 월

서울대학교 대학원

화학부 유기화학 전공

배 일 학

Abstract

Part I. Studies on the potent hepatitis C virus NS5A inhibitors*

Hepatitis C virus (HCV) belongs to the *hepacivirus* genus in the Flaviviridae family as a single stranded RNA virus (50 nm in size) and its infection often leads to serious disorders such as liver cirrhosis, followed eventually by hepatocellular carcinoma. HCV RNA consists of structural and nonstructural proteins. Especially, several non-structural proteins (NS2, NS3, NS4A, NS4B, NS5A and NS5B) involved in the reproduction of HCV are of great importance for the identification of new therapeutic targets. However, current standard of anti-viral therapy has been the combination of pegylated interferon- α with ribavirin (Peg-IFN/RBV), until a recent addition of the HCV protease inhibitors such as Boceprevir and Telaprevir. However, even with the protease inhibitors, sustained virologic response (SVR) for genotype 1 is still about 60~80%. Therefore development of effective anti-HCV drug candidates is urgently needed. In this chapter, we report the discovery of a series of extremely potent HCV NS5A inhibitors based on the symmetrical benzidine and fluorine prolinamide skeleton. Taking a simple synthetic route, we established a library of novel potent HCV NS5A inhibitor platform, which allows easy modification, and through optimization of the diversity of the region, we identified some compounds exhibiting highly potent anti-HCV activities. Furthermore, through

a battery of studies including hERG ligand binding assay, CYP₄₅₀ binding assay, rat plasma stability test, human liver microsomal stability test, and pharmacokinetic studies, the identified some compounds are found to be nontoxic, and are expected to be effective therapeutic anti-HCV agents.

Key words: HCV, NS5A inhibitor, Antiviral agent, Benzidine, Diaminofluorene, Structure-activity relationship

*Part I of this thesis was published in *ACS Med. Chem. Lett.* **2014**, 5, 255–258, and *Eur. J. Med. Chem.* **2015**, 101, 163-178.

Part II. Synthesis of conjugated polymers using palladium iron oxide nanocrystals[†]

Conjugated polymers (CP) have attracted much interest in academic and industrial fields due to their electrical and optoelectronic properties. Most of CP's have been synthesized via metal-catalyzed reactions in homogeneous system such as Pd-catalyzed Suzuki, Stille, Heck, Sonogashira reactions, Ni-catalyzed Negishi, Kumada reactions, Ru-catalyzed olefin metathesis reactions (ROMP, ADMET), and Cu-catalyzed Huisgen 1,3-dipolar cycloaddition reaction. However, these homogeneous systems are mostly limited in that catalysts always remain within the CPs as ligands and metal after the reaction. These residual catalysts could reduce the electrical performance of CP, because those residual catalysts could act as a trap site of a hole or an electron. In this chapter, we report on the utilization of Pd-Fe₃O₄ heterodimer nanocrystals (HNCs) as a magnetically recyclable and effective catalyst for the repetitive synthesis of CP via Suzuki cross-coupling reactions. After optimization of various reaction conditions of the polymerization, it was found that Pd-Fe₃O₄ heterodimer nanocrystals exhibit good catalytic activity for the synthesis of CP's, can minimize the Pd content in the product CP, was magnetically recoverable through external magnet, and finally was reusable for the polymerization eleven times. Moreover, these nanocrystals have a relatively uniform size and are dispersed evenly throughout the reaction media. This

synthetic method can possibly take us one step closer to the green synthesis of CPs.

Key words: Heterodimeric nanocrystals, palladium nanoparticle, Pd-Fe₃O₄, Suzuki polycondensation, catalyst, magnetic separation, recycling

*Part II of this thesis was published in *J. Polym. Sci. A Polym. Chem.* **2014**, 52, 1525-1528.

CONTENTS

Abstract	i
List of Figures	3
List of Schemes	4
List of Tables	5

Part I. Studies on the potent hepatitis C virus

NS5A inhibitors

Chapter 1. Development of potent hepatitis C virus NS5A inhibitors containing a benzidine core

1. Introduction	8
2. Result and Discussion	11
3. Conclusion	17
4. Experimental	18

Chapter 2. New series of benzidine and diaminofluorene prolinamide derivatives as potent hepatitis C virus NS5A inhibitors

1. Introduction	30
2. Result and Discussion	32
3. Conclusion	50
4. Experimental	51
References – Part I	72

Part II. Synthesis of conjugated polymers using palladium iron oxide nanocrystals

1. Introduction	81
2. Result and Discussion	83
3. Conclusion	94
4. Experimental	95
References – Part II	98
Appendix (NMR spectra)	100
국문초록	151

List of Figures

Figure I-1. Effect of co-treatment of compound **6** and sofosbuvir on HCV replicon system. All measurements were made in triplicate.

Figure I-2. Structure of NS5A inhibitors

Figure I-3. Our strategy for producing HCV inhibitors

Figure I-4. Effect of compound **24** in combination with EC₃₀ of NS5B polymerase inhibitor (sofosbuvir) on the HCV GT-1b replicon system. Measurements were carried out in triplicate.

Figure I-5. Resistance profiles of inhibitors daclatasvir, **42**, and **43**. Measurements were carried out in triplicate.

Figure I-6. The structure of replicon NKR2AN

Figure II-1. Recovery of Pd-Fe₃O₄ HNC using external magnet after polymerization (a) without magnet (b) with magnet.

Figure II-2. TEM images of Pd-Fe₃O₄ HNC after recycling reactions in Table II-4 (a). (a) before reaction (b) after 5 runs of recycling reactions (inset : after 11 runs of recycling reactions).

List of Schemes

Scheme I-1. Synthesis of benzidine prolinamide skeleton

Scheme I-2. Synthesis of benzidine and proline derivatives from an amide skeleton

Scheme I-3. Synthesis of benzidine derivatives and prolinamide skeleton

Scheme I-4. Synthesis of fluorene-2,7-diamine derivatives

Scheme I-5. Synthesis of fluorine-containing prolinamide derivatives

List of Tables

Table I-1. Structure-Activity-Relationships of inhibitors containing a benzidine prolinamide skeleton against HCV type 2a

Table I-2. Antiviral activity in an HCV genotype 1b replicon assay

Table I-3. hERG ligand binding assay

Table I-4. Stability of compound **6** in rat plasma

Table I-5. CYP450 screening assay

Table I-6. Structure-activity relationships of inhibitors containing various proline isosteres against HCV type 2a and type 1b.

Table I-7. Structure-activity relationships of inhibitors containing substituted benzidine derivatives against HCV type 2a and type 1b.

Table I-8. Kinetic resolution of compound **24**

Table I-9. Structure-activity relationship studies of inhibitors containing a fluorene skeleton against HCV type 2a and type 1b.

Table I-10. Result of hERG ligand binding assay

Table I-11. Stability in rat plasma (% remaining)

Table I-12. Human liver microsomal stability (% remaining)

Table I-13. EC₅₀ of compounds (μM) against various subtypes of CYP₄₅₀

Table I-14. Pharmacokinetics features of selected inhibitors in rats

Table I-15. Cytotoxicity of **43** in eukaryotic cells

Table I-16. Bacterial reverse mutation assay of **43**

Table II-1. Condition optimization for Suzuki polymerization

Table II-2. Synthesis of conjugated polymers using Pd-Fe₃O₄ catalyst

Table II-3. Recycling of Pd-Fe₃O₄ HNC catalyst for Suzuki polymerization

Table II-4. Recycle test of the Pd-Fe₃O₄ HNC catalyst for compare to sonication process

Table II-5. Homogeneous Pd-catalyzed Suzuki polymerization

Part I.

Studies on the potent hepatitis C virus NS5A inhibitors

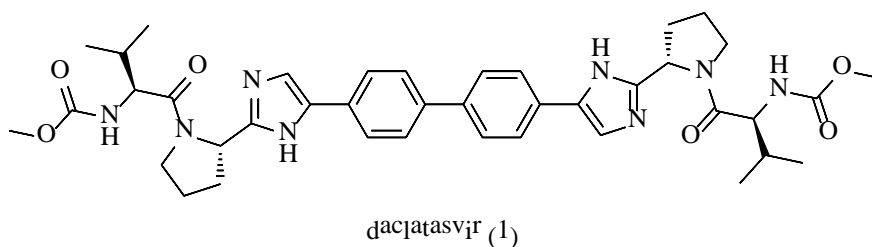
Chapter 1. Development of potent hepatitis C virus NS5A inhibitors containing a benzidine core

1. Introduction

Approximately 170 million people, including almost 4 million in the United States, are estimated to be infected with hepatitis C virus (HCV).^{1,2} It has been estimated that 75-85% of those infected with HCV will develop chronic hepatitis and more serious diseases such as liver cirrhosis and hepatocellular carcinoma.³ Until recently, therapies for HCV patients have consisted of subcutaneous injections of pegylated interferon- α (PEG-IFN- α) in combination with oral doses of ribavirin (RBV).⁴ This interferon based therapy has a limited sustained virologic response (SVR), especially in patients infected with genotype 1 HCV. In 2011, the US Food and Drug Administration (FDA) approved Boceprevir (Merck) and Telaprevir (Vertex Pharmaceuticals and Johnson & Johnson) as antiviral agents directly targeted against HCV NS3/4A protease, in combination with PEG-IFN- α and RBV. In genotype 1 patients, very promising results have been reported when either Telaprevir or Boceprevir are added to the standard of care.⁵ Although the introduction of these direct-acting antivirals (DAAs) into the regimen improves therapeutic outcome, their possible limitations include a low genetic barrier, which may result in the appearance of drug-resistant mutants during long-term treatment. The development of effective and safe small molecule antiviral agents aimed at a variety of gene targets was therefore warranted.⁶

HCV, which belongs to the *Hepacivirus* genus in the Flaviviridae family, contains a 9.8 kb, single-stranded positive sense RNA genome encoding a polyprotein of approximately 3,000 amino acids. This polyprotein encompasses structural proteins (Core, E1 and E2), virion particles and nonstructural proteins (NS2, NS3, NS4A, NS4B, NS5A and NS5B) participating in RNA replication.⁷⁻⁹ Although the precise enzymatic role of NS5A has not been clarified, it has been shown to be essential for HCV replication, virus assembly, and the host immune response related to viral resistance to IFN- α therapy. NS5A is zinc-binding phosphoprotein (56-58 kDa), consisting of 447 amino acids,^{10,11} and

associated with the membrane through an *N*-terminal amphipathic α -helix region.¹² The three principle domains in NS5A are domain I, containing a zinc binding motif required for viral RNA replication;¹³ domain II, which interacts with NS5B and cellular proteins such as PKR and PI3K, and domain III, which plays a role in infectious virus assembly, but not in RNA replication.¹⁴

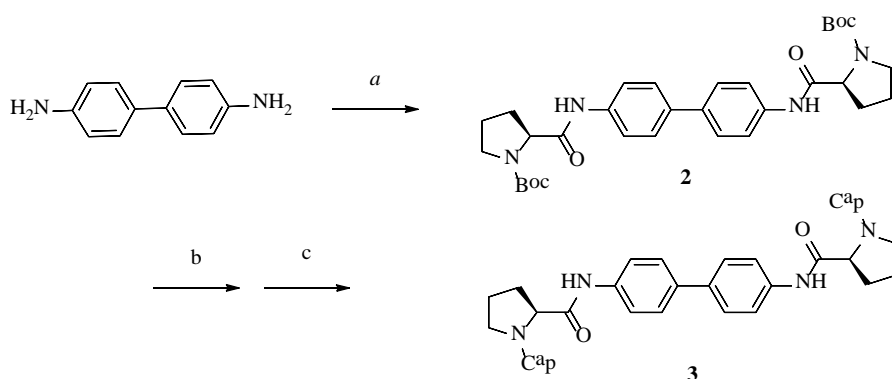


A novel NS5A inhibitor, daclatasvir (**1**, shown above; BMS-790052, combination therapy with sofosbuvir approved by Daklinza in 2015), was recently reported to exhibit strong anti-HCV activity, particularly in the case of the HCV genotype 1. The effective concentration (EC_{50}) of daclatasvir was shown to be in the picomolar range in vitro and, in clinical trials, a single dose treatment of 100 mg reduced HCV RNA level about $3.3\log_{10}$ without apparent toxicity.^{15,16} Subsequently, pharmaceutical companies and numerous research groups have focused on the development of a series of NS5A inhibitors.¹⁷⁻²¹ For instance, Merck reported the elbasvir (combination therapy with grazoprevir approved by Zepatier in 2016), Abbvie pharmaceutical research & development reported ombitasvir (combination therapy of paritaprevir and ritonavir approved by Viekira Pak in 2014), and ledipasvir (combination therapy with sofosbuvir approved by Harvoni in 2014) was developed by the Gilead Sciences. In addition to thesis efforts, currently known candidates in this series include GS-5885, ABT-267, PPI-461, AZD-7295, BMS-824393, ACH-2928, IDX-719, PPI-1301, and EDP-239.²² Daclatasvir (**1**) has a biphenyl core connected to an imidazole moiety, a proline moiety, and a capping group of amino acid derivatives. In 2012, Schinazi and co-workers reported new inhibitors containing a variety of extended biphenyl linkers with small

modifications at both ends of the inhibitors.²³⁻²⁵ Here, we report a new class of potent inhibitors based upon a benzidine prolinamide skeleton.

2. Result and Discussion

The symmetrical structure of the benzidine scaffold greatly simplified our synthetic route. Coupling of Boc-L-proline with benzidine resulted in excellent yield of an almost pure product, obviating the need for column chromatographic purification. After removal of the Boc group using trifluoroacetic acid (TFA) in CH₂Cl₂, a series of capping groups was added to the free amine using either peptide coupling (EDCI and Hünig's base in CH₂Cl₂) or reductive amination, to furnish the target compounds, **4-11** (Scheme I-1).^{26,27}



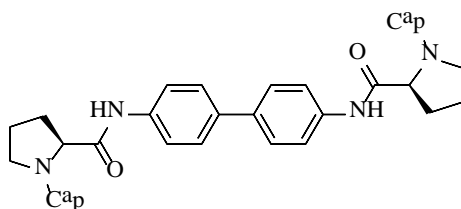
Scheme I-1. Synthesis of benzidine prolinamide skeleton^a

^aReagents and conditions: (a) N-Boc-L-Proline, EDC, DCM, 94%; (b) TFA, DCM; (c) Capping Group, EDC, DIPEA, DCM 22-49% (2 steps).

To determine the inhibitory activities (EC₅₀'s) of the compounds, dose-response experiments were performed using an infectious HCV cell culture system (HCVcc). JFH 5a-Rluc-ad34 is a derivative of JFH1 containing a Renilla luciferase reporter and cell culture adaptive mutations.²⁸ Huh 7.5.1 cells were inoculated with the HCVcc for 3 h and then cultivated for 3 d in the presence of the indicated compounds at serially diluted concentrations. After cell harvesting, EC₅₀'s were calculated by sigma plot analysis of the luciferase activities in the cells.

The assay data indicate that the inhibitory activity of these compounds is greatly dependent upon the structure of the flanking end groups (Table I-1).^{29,30} When both enantiomers of *N*-methyloxycarbonyl-protected valine were attached, a clear difference in inhibitory activity between the two epimers was observed, indicating the importance of the stereochemistry of the capping group. The inhibitory activity of the D-isomer (compound **4**) was 8 fold higher than that of the L-epimer (compound **5**, Table I-1, entries 1 and 2, respectively). Next, we identified the optimal capping group through a series of structure-activity relationship (SAR) studies. When phenylglycine derivatives were incorporated on both ends, extremely high inhibitory activities were observed, regardless of the *N*-protecting groups. The highest inhibition was observed for the compound containing an *N*-methyloxycarbonylphenylglycine group (compound **6**, Table I-1, entry 3), while *N,N*-dimethylamino- and *N,N*-diethylamino-protected phenylglycine derivatives also had inhibitory EC₅₀'s in the low nanomolar range. Compounds **6-8** were potent inhibitors of HCV proliferation, with EC₅₀'s of 260 pM, 2.3 nM, and 2.2 nM in infectious HCVcc, respectively, and none had detectable cytotoxic effects at 25 µM of concentration (Table I-1, entries 3-5, respectively). In contrast, compound **9** which contains a *N*-methyloxycarbonyl-L-alanine moiety, had no detectable inhibition at 1 µM. Inhibitors capped with *N*-methyloxycarbonyl-L-*tert*-leucine and *N*-2(R)-tetrahydrofurylcarbonyl groups inhibited HCV proliferation with EC₅₀'s of 24 and 400 nM inhibition, respectively (entries 7 and 8, Table I-1).

Table I-1. Structure-Activity-Relationships of inhibitors containing a benzidine prolinamide skeleton against HCV type 2a



Entry	Compound	Cap	EC ₅₀ (nM)	Cytotoxicity _y	SI (Cytotoxicity/EC ₅₀ ×1000)
1	4		15		
2	5		120		
3	6		0.26	>25μM	>96
4	7		2.3	>25μM	>11
5	8		2.2	>25μM	>11
6	9		>1000		
7	10		24		
8	11		400		

To assess the inhibitory activity of compounds on HCV replication, we measured EC₅₀'s using a HCV replicon containing a HCV non-structural protein, NS3-NS5B, and the Renilla luciferase reporter gene.^{31,32} Compound **6** showed the highest inhibition in the replicon assay (EC₅₀ = 28 pM), while compounds **7** (EC₅₀ = 0.43 nM) and **8** (EC₅₀ = 0.27 nM) also exhibited subnanomolar inhibition (Table I-2, entries 1-3).

Table I-2. Antiviral activity in an HCV genotype 1b replicon assay

Entry	Compound	HCV replicon (type 1b)	Cytotoxicity	SI (Cytotoxicity/EC ₅₀ ×1000)
1	6	0.028 nM	>25 μM	>893
2	7	0.43 nM	>25 μM	>58
3	8	0.27 nM	>25 μM	>93

Since compound **6** exhibited the highest inhibitory activity both in HCVcc infection (Table I-1, entry 3) and in the replicon system (Table I-2, entry 1), we next focused our attention on further evaluation of this compound.³³

First, to evaluate the potential cardiac toxicity of compound **6** through inhibition of the inward rectifying voltage gated potassium channel encoded by the hERG gene, we carried out a hERG assay.^{34,35} Compared to the astemizole control (EC₅₀ = 1.9 nM), compound **6** (EC₅₀ = 9.8 μM) was shown to bind poorly to the hERG membrane preparations, suggesting that compound **6** would have minimal cardiac toxicity (Table I-3).

Table I-3. hERG Ligand Binding Assay

Compound	% Inhibition (uM)
6	9.8
Control (Astemizole)	0.0019

Next, a rat plasma stability test^{36,37} of compound **6** (Table I-4) showed that more than 99% of the compound was intact after 4 h, indicating high in vivo stability (Table I-4).

Table I-4. Stability of compound **6** in rat plasma

Compound 6 (2 μ M)	0.5 h (%)	1 h (%)	4 h (%)
6	>99	>99	>99

Next, to evaluate potential drug-drug interactions of compound **6**, we carried out CYP450 screening (Table I-5).³⁸ A compound exhibiting greater than 50% inhibition of CYP450 activity at a concentration of 10 μ M is classified as a CYP450 enzyme inhibitor. CYP1A2 (18.12% inhibition) and CYP3A4 (23.87% inhibition) were weakly inhibited in the presence of 10 μ M compound **6**, while CYP2C9 and CYP2D6 retained maximal activity under the same conditions. We conclude that compound **6** does not significantly inhibit these four representative CYP enzymes.

Table I-5. CYP450 screening assay

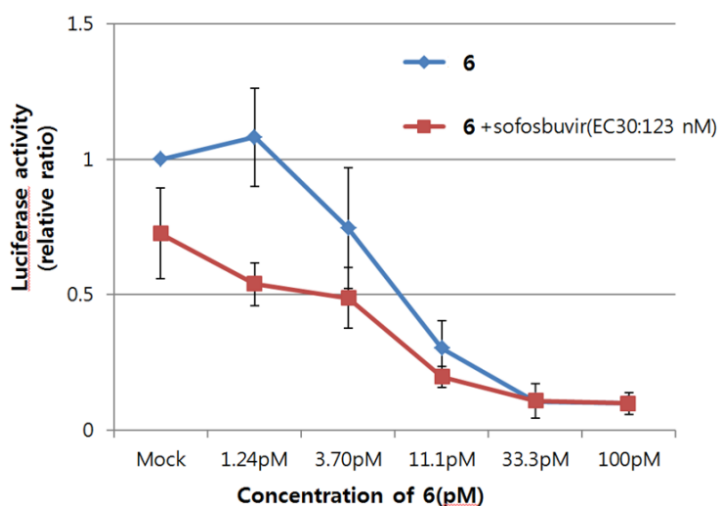
Compound	1A2	2C9	2D6	3A4
6^a	18.12	0	0	23.87
Inhibitor ^b	98.60	75.79	95.07	95.34

^aCYP inhibition (%) of Compound **6** at 10 μ M.

^b1A2: α -naphthoflavone, 2C9: sulfaphenazole, 2D6: quinidine, 3A4:ketoconazole

To determine whether compound **6** would have a synergistic or additive anti-HCV effect in combination with sofosbuvir therapy, we treated replicon with compound **6** in the presence of a 125 nM of concentrations of sofosbuvir^{39,40} and monitored the effect on HCV proliferation (Figure I-1). Our data show that compound **6** and sofosbuvir have a distinct additive effect on the proliferation of HCV, presumably due to the independent modes of action of compound **6** and sofosbuvir.

Figure I-1. Effect of co-treatment of compound **6** and sofosbuvir on HCV replicon system. All measurements were made in triplicate.



3. Conclusion

In summary, we have developed a series of inhibitors based on a new benzidine prolinamide core structure, several of which have extremely high anti-HCV activity. SAR studies using a variety of terminal capping groups showed particularly high inhibitory activities for inhibitors containing phenyl glycine capping groups, of which compound **6** was the most potent. Moreover, subsequent studies demonstrated that compound **6** has a desirable cardiac toxicity, rat plasma stability, and drug-drug interaction properties. Our data indicate that compound **6** is a potent, safe lead compound that warrants further study for its potential in anti-HCV therapy.

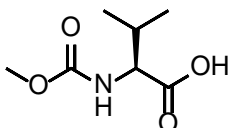
4. Experimental

General Information

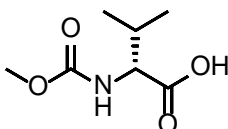
The ^1H and ^{13}C NMR-spectra were measured with a Bruker DPX-300 (300 MHz), an Agilent 400-MR DD2 Magnetic Resonance System (400 MHz) and a Varian/Oxford As-500 (500 MHz) spectrophotometer. Chemical shifts were measured as part per million (δ values) from tetramethylsilane as an internal standard at probe temperature in CDCl_3 or $\text{DMSO}-\text{D}_6$ for neutral compounds. Reactions that needed anhydrous conditions were carried out in flame-dried glassware under positive pressure of dry N_2 using standard Schlenk line techniques. Evaporation of solvents was performed at reduced pressure using a rotary evaporator. TLC was performed using silica gel 60F254 coated on aluminum sheet (E. Merck, Art.5554). Chromatogram was visualized by UV-lamp (Vilber Lournat, VL-4LC) and/or colorized with following solutions: (a) 20% ethanolic phosphomolybdic acid (PMA) (b) potassium permanganate solution (c) 2% ninhydrin ethanolic solution. Column chromatography was performed on silica gel (Merck. 7734 or 9385 Kiesel gel 60), and eluent was mentioned in each procedure. A Thermo-Finnigan LTQ-Orbitrap instrument (Thermo Scientific, USA) equipped with Dionex U 3000 HPLC system was used. Mass spectrometric analyses were performed using a ThermoFinnigan LTQ-Orbitrap ion trap mass spectrometer, with ESI interface. HPLC analyses were carried out on an HP1100 system Agilent (Santa Clara, CA, USA), composed of auto sampler, quaternary pump, photodiode array detector (DAD) and HP Chemstation software. The separation was carried out on a C18 Vydac 218TP54 column 250 x 4.6 mm i.d. (5 μm particle size) with 0.1% TFA in water(A), acetonitrile(B), as a mobile phase at a flow rate of 1 mL/min at 20 $^\circ\text{C}$. Method : 0% B(0 min), 100% B(10 min), 100% B(20 min), 0% B(22 min), 0% B(25 min). All materials were obtained from commercial supplier and used without further purification unless otherwise noted.

Preparation of compounds

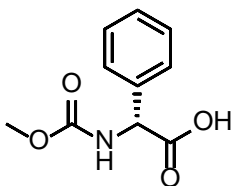
Synthesis of Capping groups



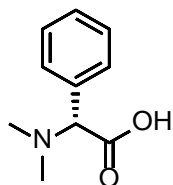
(S)-2-((methoxycarbonyl)amino)-3-methylbutanoic acid (Cap-1). Na_2CO_3 (1.83 g, 17.2 mmol) was added to aq NaOH (33 mL of 1 M/ H_2O , 33 mmol) solution of L-valine (3.900 g, 33.29 mmol) and the resulting solution was cooled with ice-water bath. Methyl chloroformate (2.8 mL, 36.1 mmol) was added dropwise, the cooling bath was removed and the reaction mixture was stirred at ambient temperature for 3.25 h. The reaction mixture was washed with ether (3x17 mL), and the aqueous phase was cooled with ice-water bath and acidified with conc HCl to a pH region of 1-2, and extracted with CH_2Cl_2 (3x17 mL). The organic phase was dried (MgSO_4), filtered, and concentrated in vacuo to afford Cap-1 as a white solid (5.00 g, 86%) ^1H NMR (DMSO-d_6 , $\delta=2.5$ ppm, 400 MHz): 12.51 (br s, 1H), 7.32 (d, 1H), 3.84 (t, 1H), 3.54 (s, 3H), 2.03 (m, 1H), 0.88 (d, $J=12$, 6H).



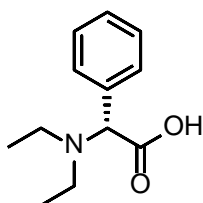
(R)-2-((methoxycarbonyl)amino)-3-methylbutanoic acid (Cap-2). Yield 760 mg (87%). ^1H NMR (DMSO-d_6 , $\delta=2.5$ ppm, 300 MHz): 12.54 (s, 1H), 7.32 (d, 1H), 3.84 (t, 1H), 3.54 (s, 3H), 2.03 (m, 1H), 0.87 (d, 6H).



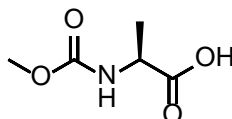
(R)-2-((methoxycarbonyl)amino)-2-phenylacetic acid (Cap-3). Na₂CO₃ (0.55 g, 5.2 mmol) was added to aq NaOH (10 mL of 1 M/H₂O, 10 mmol) solution of D-Phenylglycine (1.500 g, 10.0 mmol) and the resulting solution was cooled with ice-water bath. Methyl chloroformate (0.85 mL, 11.0 mmol) was added dropwise, the cooling bath was removed and the reaction mixture was stirred at ambient temperature for 3.25 h. The reaction mixture was washed with ether (3x18 mL), and the aqueous phase was cooled with ice-water bath and acidified with conc HCl to a pH region of 1-2, and extracted with CH₂Cl₂ (3x18mL). The organic phase was dried (MgSO₄), filtered, and concentrated in vacuo, and the resulting oil residue was treated with diethyl ether/hexanes (~5:4 ratio; 10 mL) to provide a precipitate. The precipitate was filtered and washed with diethyl ether/hexanes (~1:3 ratio) and dried in vacuo to provide Cap-3 as a fluffy white solid (1.4 g, 67%). ¹H NMR (DMSO-d₆, δ=2.5 ppm, 500 MHz): 12.79 (br s, 1H), 7.96 (d, J=12, 1H), 7.40-7.29 (m, 5H), 5.13 (d, J=12, 1H), 3.55 (s, 3H).



(R)-2-(dimethylamino)-2-phenylacetic acid (Cap-4). A suspension of 10% Pd/C (310 mg, 0.3 mmol) in methanol (1.5 mL) was added to a mixture of D-Phenylglycine (1.51 g, 10 mmol), formaldehyde (5 mL of 37% wt. in water), 1 N HCl (4.5 mL) and methanol (4.5 mL), and stirred under H₂ atmosphere (balloon) overnight. The reaction mixture was filtered through Celite, and the filtrate was concentrated in vacuo. The resulting crude material was recrystallized from isopropanol to provide an HCl salt of Cap-4 as a white needle (1.84 g, 89%). ¹H NMR (DMSO-d₆, δ=2.5 ppm, 500 MHz): 7.43-7.39 (m, 5H), 4.47 (s, 1H), 2.43 (s, 6H).

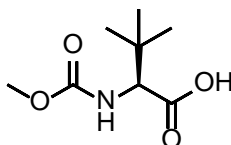


(R)-2-(diethylamino)-2-phenylacetic acid (Cap-5). NaBH₃CN (786 mg, 12.5 mmol) was added in portions over a few minutes to a cooled (ice/water) mixture of D-Phenylglycine (756 mg, 5.00 mmol) and methanol (13 mL), and the mixture was stirred for 5 min. To the mixture was added acetaldehyde (1.3 mL, 22.5 mmol) dropwise and stirring was continued at the same cooled temperature for 45 min and at ambient temperature for another ~6.5 h. The reaction mixture was cooled with ice-water bath, quenched with a dropwise addition of conc HCl until the pH of the mixture was 1.5-2.0. The reaction mixture was stirred overnight, filtered to remove the white suspension, and the filtrate was concentrated in vacuo. The crude material was recrystallized from ethanol to afford the HCl salt of Cap-5 as a shining white solid (625 mg, 60%). ¹H NMR (DMSO-d₆, δ=2.5 ppm, 500 MHz): 10.77 (br s, 1H), 7.72 (m, 2H), 7.51 (m, 3H), 5.33 (s, 1H), 3.17 (app br s, 2H), 3.01 (app br s, 2H), 1.20 (app br s, 6H).



(S)-2-((methoxycarbonyl)amino)propanoic acid (Cap-6). Na₂CO₃ (0.55 g, 5.2 mmol) was added to aq NaOH (10 mL of 1 M solution, 10 mmol) solution of L-alanine (0.890 g, 10.0 mmol) and the resulting solution was cooled with ice-water bath. To the mixture was added methyl chloroformate (0.85 mL, 11.0 mmol) dropwise, the cooling bath was removed and the reaction mixture was stirred at ambient temperature for 3.25 h. The reaction mixture was washed with ether (3x18 mL), and the aqueous phase was cooled with ice-water bath and acidified with conc HCl to a pH region of 1-2, and extracted with CH₂Cl₂ (3x18mL). The organic phase was dried (MgSO₄), filtered, and concentrated in

vacuo to afford Cap-6 as a colorless viscous oil (0.83 g, 56%). ¹H NMR (CDCl₃, δ=7.26 ppm, 500 MHz): 10.00 (br s, 1H), 5.49 (d, J=12, 1H), 4.38 (m, 1H), 3.69 (s, 3H), 1.45 (d, J=12, 3H).



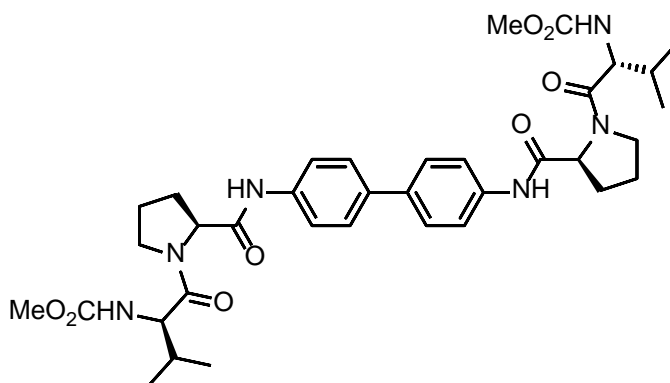
(*S*)-2-((methoxycarbonyl)amino)-3,3-dimethylbutanoic acid (**Cap-7**). Yield 670 mg (71%). ¹H NMR (CDCl₃, δ=7.26 ppm, 500 MHz): 9.57 (br s, 1H), 5.31 (d, 1H), 4.20 (d, 1H), 3.70 (s, 3H), 1.03 (s, 9H).

Synthesis of Biaryl Core

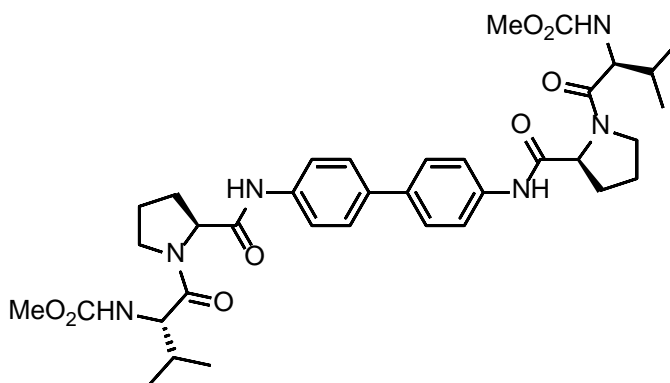


(*2S,2'S*)-*tert*-butyl 2,2'-(biphenyl-4,4'-diylbis(azanediyl))bis(oxomethylene)dipyrrolidine-1-carboxylate (**2**). A mixture of *N*-Boc-L-proline (8.00 g, 86.3 mmol), EDC (19.0 g, 99.0 mmol), and benzidine (7.00 g, 38.0 mmol) in CH₂Cl₂ (38 mL) was stirred at ambient temperature for 2 h. The resulting residue was partitioned between CH₂Cl₂ and H₂O. The organic layer was washed with 1 N aq HCl solution and brine, dried MgSO₄, filtered, and concentrated in vacuo. Without any purification, **2** was obtained as a brown solid (20.7 g, 94%). ¹H NMR (DMSO-*d*₆, δ=2.5 ppm, 300 MHz): 10.06 (s, 2H), 7.69-7.59 (dd, 8H), 4.24 (m, 2H), 3.39 (m, 4H), 2.21 (m, 2H), 1.85 (m, 6H), 1.41-1.28 (app br s, 18H). ¹³C NMR (DMSO-*d*₆, δ=39.52 ppm, 100 MHz): 171.5, 153.2, 138.2, 134.5, 126.4, 119.6, 78.5, 60.4, 46.6, 31.0, 28.1, 28.0, 23.4. LC/MS: Anal. Calcd. For [M+H]⁺ C₃₂H₄₂N₄O₆:579.3177; found 579.3152.

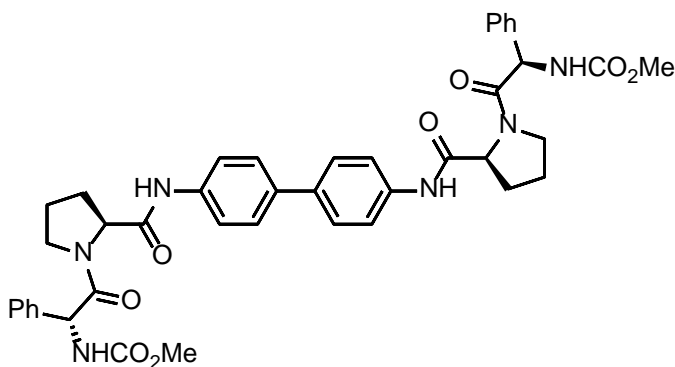
Synthesis of compound 4-11



dimethyl ((2*R*,2'*R*)-((2*S*,2'*S*)-2,2'-([1,1'-biphenyl]-4,4'-diylbis(azanediyl))bis(carbonyl))bis(pyrrolidine-2,1-diyl))bis(3-methyl-1-oxobutane-2,1-diyl)dicarbamate (**4**). A mixture of biphenyl **2** (138 mg, 0.238 mmol) in CF₃CO₂H (1 mL) and CH₂Cl₂ (1 mL) was stirred at room temperature for 5 h. The volatile component was removed in vacuo, EDC (119 mg, 0.620 mmol), **Cap-2** (100 mg, 0.572 mmol) was added in batches over 4 min to a solution of *i*-Pr₂NEt (208 μL, 1.192 mmol) in CH₂Cl₂ (1 mL) and the reaction mixture was stirred at room temperature for 75 min. The residue was partitioned between CH₂Cl₂ and H₂O. The organic layer was washed with H₂O and brine, dried over MgSO₄, filtered, and concentrated in vacuo. A silica gel mesh was prepared from the residue and submitted to flash chromatography (silica gel: EtOAc/hexane as eluent) to provide **4** as a white solid (69 mg, 42%). ¹H NMR (DMSO-*d*₆, δ=2.5 ppm, 400 MHz): 10.11 (s, 2H), 7.67-7.58 (dd, 8H), 7.32 (d, 2H), 4.48 (m, 2H), 4.05 (t, 2H), 3.83 (m, 2H), 3.64 (m, 2H), 3.54 (s, 6H), 2.18 (m, 2H), 1.94 (m, 8H), 0.96 (d, 6H), 0.90 (d, 6H). ¹³C NMR (DMSO-*d*₆, δ=39.52 ppm, 100 MHz): 170.4, 170.4, 156.8, 138.3, 134.3, 126.4, 119.4, 60.2, 58.0, 51.4 47.2, 29.9, 29.5, 24.7, 18.9, 18.6. LC/MS: Anal. Calcd. For [M+H]⁺ C₃₆H₄₈N₆O₈:693.3606; found 693.3577.

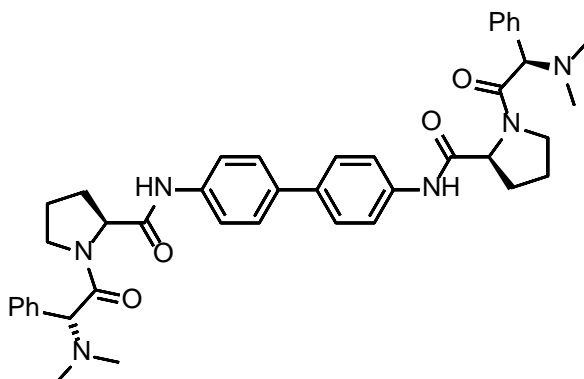


dimethyl ((2*S*,2'*S*)-((2*S*,2'*S*)-2,2'-([1,1'-biphenyl]-4,4'-diylbis(azanediyl))bis(carbonyl))bis(pyrrolidine-2,1-diyl))bis(3-methyl-1-oxobutane-2,1-diyl)dicarbamate (**5**). Yield 60 mg (36%). ¹H NMR (DMSO-*d*₆, δ=2.5 ppm, 400MHz): 10.07 (s, 2H), 7.63-7.54 (dd, 8H), 7.31 (d, 2H), 4.43 (m, 2H), 4.01 (t, 2H), 3.80 (m, 2H), 3.61 (m, 2H), 3.5 (s, 6H), 2.13 (m, 2H), 1.89 (m, 8H), 0.92 (d, 6H), 0.86 (d, 6H). ¹³C NMR (DMSO-*d*₆, δ=39.52 ppm, 100 MHz): 170.4, 170.4, 156.8, 138.3, 134.3, 126.4, 119.3, 60.2, 58.0, 51.4, 47.2, 29.9, 29.5, 24.7, 18.9, 18.6. LC/MS: Anal. Calcd. For [M+H]⁺ C₃₆H₄₈N₆O₈:693.3306; found 693.3572.

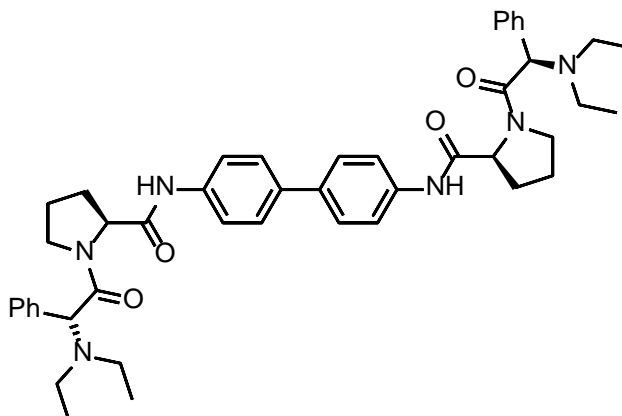


dimethyl ((1*R*,1'*R*)-((2*S*,2'*S*)-2,2'-([1,1'-biphenyl]-4,4'-diylbis(azanediyl))bis(carbonyl))bis(pyrrolidine-2,1-diyl))bis(2-oxo-1-phenylethane-2,1-diyl)dicarbamate (**6**). Yield 53 mg (46%). ¹H NMR (DMSO-*d*₆, δ=2.5 ppm, 400 MHz): 9.95 (s, 2H), 7.74-7.58 (m, 9H), 7.51-7.30 (m, 10H), 7.14 (app br s, 1H), 5.51 (d, 2H), 4.42 (app br d, 2H), 3.83 (app br s,

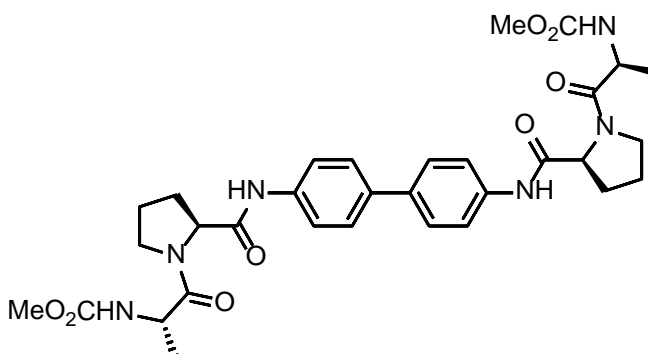
2H), 3.55 (s, 6H), 3.20 (app br d, 2H), 2.04-1.79 (m, 8H). ^{13}C NMR (DMSO- d_6 , δ =39.52 ppm, 100 MHz): 170.2, 168.4, 156.1, 138.1, 137.2, 134.4, 128.6, 128.0, 127.8, 126.4, 119.6, 60.7, 56.7, 51.6, 46.9, 29.3, 24.3. LC/MS: Anal. Calcd. For $[\text{M}+\text{H}]^+$ $\text{C}_{42}\text{H}_{44}\text{N}_6\text{O}_8$: 761.3293; found 761.3263.



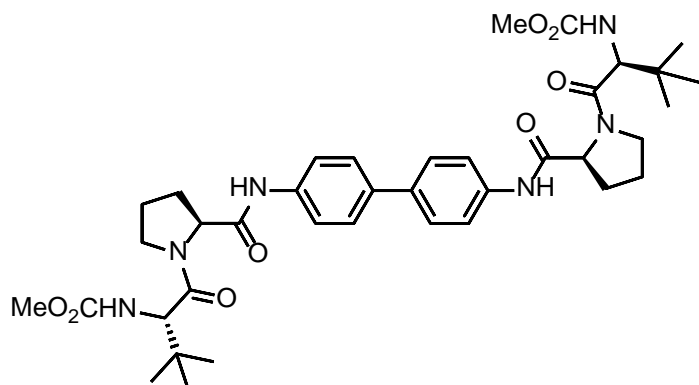
(*R,2S,2'S*)-*N,N'*-([1,1'-biphenyl]-4,4'-diyl)bis(1-((*R*)-2-(dimethylamino)-2-phenylacetyl)pyrrolidine-2-carboxamide) (7). Yield 40 mg (25%). ^1H NMR (DMSO- d_6 , δ =2.5 ppm, 400MHz): 10.09 (s, 2H), 7.68-7.60 (dd, 8H), 7.46-7.29 (m, 10H), 4.37 (m, 2H), 4.21 (s, 2H), 3.87 (m, 2H), 3.45 (m, 2H), 2.16 (s, 12H), 2.16-1.97 (m, 2H), 1.90-1.80 (m, 2H). ^{13}C NMR (DMSO- d_6 , δ =39.52 ppm, 100 MHz): 170.5, 169.1, 138.3, 134.3, 129.1, 129.0, 128.2, 127.9, 126.4, 119.4, 71.4, 60.6, 47.2, 42.9, 29.2, 24.5. LC/MS: Anal. Calcd. For $[\text{M}+\text{H}]^+$ $\text{C}_{42}\text{H}_{48}\text{N}_6\text{O}_4$: 701.3810; found 701.3774.



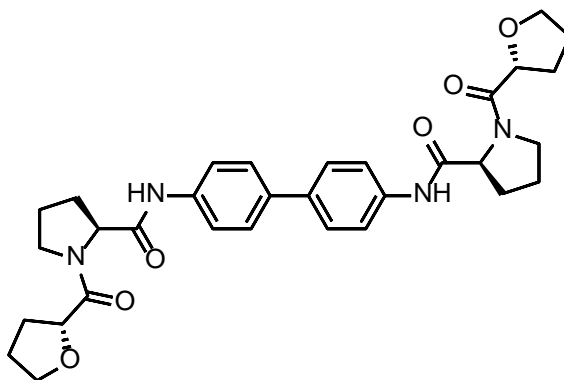
(R,2S,2'S)-N,N'-([1,1'-biphenyl]-4,4'-diyl)bis(1-((R)-2-(diethylamino)-2-phenylacetyl)pyrrolidine-2-carboxamide) (8). Yield 34 mg (22%). ¹H NMR (DMSO-*d*₆, δ=2.5 ppm, 400MHz): 10.08 (s, 2H), 7.68-7.60 (dd, 8H), 7.43-7.26 (m, 10H), 4.70 (s, 2H), 4.43 (m, 2H), 3.81 (m, 2H), 3.39 (q, 2H), 2.67-2.59 (m, 4H), 2.54-2.45 (m, 4H), 2.11-1.97 (m, 4H), 1.89-1.78 (m, 4H), 0.91 (t, 12H). ¹³C NMR (DMSO-*d*₆, δ=39.52 ppm, 100 MHz): 170.5, 169.8, 138.3, 137.5, 134.3, 129.1, 128.1, 127.5, 126.4, 119.4, 66.2, 60.5, 47.1, 43.2, 29.2, 24.6, 12.6. LC/MS: Anal. Calcd. For [M+H]⁺ C₄₆H₅₆N₆O₄:757.4436; found 757.4392.



dimethyl ((2S,2'S)-((2S,2'S)-2,2'-([1,1'-biphenyl]-4,4'-diylbis(azanediyl))bis(carbonyl))bis(pyrrolidine-2,1-diyl))bis(1-oxopropane-2,1-diyl))dicarbamate (9). Yield 69 mg (47%). ¹H NMR (DMSO-*d*₆, δ=2.5 ppm, 400MHz): 10.00 (s, 2H), 7.63-7.55 (dd, 8H), 7.32 (d, 2H), 4.43 (m, 2H), 4.30 (t, 2H), 3.65 (m, 2H), 3.58 (m, 2H), 3.49 (s, 6H), 2.14 (m, 2H), 1.96 (m, 6H), 1.18 (d, 6H). ¹³C NMR (DMSO-*d*₆, δ=39.52 ppm, 100 MHz): 171.3, 170.8, 156.7, 138.6, 134.7, 126.7, 119.8, 60.6, 51.7, 48.4, 47.1, 29.7, 25.1, 17.2. LC/MS: Anal. Calcd. For [M+H]⁺ C₃₂H₄₀N₆O₈:637.2980; found 637.2949.



dimethyl ((2*S*,2'*S*)-((2*S*,2'*S*)-2,2'-([1,1'-biphenyl]-4,4'-diylbis(azanediyl))bis(carbonyl))bis(pyrrolidine-2,1-diyl))bis(3,3-dimethyl-1-oxobutane-2,1-diyl)dicarbamate (**10**). Yield 38 mg (24%). ¹H NMR (DMSO-*d*₆, δ=2.5 ppm, 400MHz): 10.11 (s, 2H), 7.66-7.57 (dd, 8H), 7.09 (d, 2H), 4.48 (m, 2H), 4.23 (d, 2H), 3.79 (m, 2H), 3.63 (m, 2H), 3.54 (s, 6H), 2.18 (m, 2H), 2.00 (m, 2H), 1.89 (m, 4H), 0.98 (s, 18H). ¹³C NMR (DMSO-*d*₆, δ=39.52 ppm, 100 MHz): 170.4, 169.6, 156.9, 138.3, 134.3, 126.4, 119.3, 60.2, 59.1, 51.5, 47.9, 34.5, 29.5, 26.4, 24.8. LC/MS: Anal. Calcd. For [M+H]⁺ C₃₈H₅₂N₆O₈: 721.3919; found 721.3882.



(*R*,2*S*,2'*S*)-*N,N'*-([1,1'-biphenyl]-4,4'-diyl)bis(1-((*R*)-tetrahydrofuran-2-carbonyl)pyrrolidine-2-carboxamide) (**11**). Yield 101 mg (49%). ¹H NMR (DMSO-*d*₆, δ=2.5 ppm, 400MHz): 10.21 (s, 2H^{trans} or 2H^{cis}), 10.05 (s, 2H^{trans} or 2H^{cis}), 7.67-7.59 (dd, 8H), 4.79 (d, 2H^{trans} or 2H^{cis}), 4.58 (t, 2H^{trans} or 2H^{cis}), 4.42 (d, 2H^{trans} or 2H^{cis}), 4.30 (t, 2H^{trans} or 2H^{cis}), 3.83-3.68 (m, 5H^{trans}/5H^{cis}), 3.58-

3.37 (m, 3H^{trans}/3H^{cis}), 2.13-1.75 (m, 16H^{trans}/16H^{cis}). ¹³C NMR (DMSO-*d*₆, δ=39.52 ppm, 400 MHz): 170.78, 170.52, 170.29, 170.13, 138.2, 134.3, 126.50, 126.43, 126.38, 126.31, 119.77, 119.44, 76.22, 76.08, 68.38, 68.18, 60.37, 59.77, 46.99, 46.62, 32.1, 29.2, 28.2, 25.32, 25.05, 24.6, 21.8. LC/MS: Anal. Calcd. For [M+H]⁺ C₃₆H₃₈N₄O₆: 575.2864; found 575.2839.

**Chapter 2. New series of benzidine and
diaminofluorene prolinamide derivatives as
potent hepatitis C virus NS5A inhibitors**

1. Introduction

In 2010, a landmark NS5A inhibitor, daclatasvir (**1**), was reported to present excellent anti-HCV activity, especially in patients with HCV G-1 infection. This new class of inhibitor was approved Daklinza by the US FDA in 2015.^{15,41-44} The effective concentration (EC₅₀) value of daclatasvir was two-digit picomolar (pM) range in in vitro assay, and treatment with a single 100 mg dose in clinical trials reduced HCV RNA levels by an average of 3.3log₁₀ without apparent toxicity.⁴⁵ This result stimulated numerous research groups and pharmaceutical companies to focus on the development of new inhibitors targeting NS5A.^{17,19-22,46-50} Currently, there are many candidate compounds in this series: ABT-267, ACH-2928, ACH-3102, AZD-7295, BMS-346, BMS-665, BMS-824393, EDP-239, GS-5885, GSK-2336805, IDX-719, MK-4882, MK-8742, PPI-461, and PPI-1301 (Figure I-2).⁵¹⁻⁵⁸ Most recently, interferon-free multi-class drug combinations (daclatasvir and asunaprevier, Harvoni®, and Viekira Pak®) are viewed as the optimal therapy.⁵⁹ The structure of daclatasvir is characterized by a central biaryl core unit linked to an imidazole and proline moiety, and lastly, a methyl carbamate L-valine moiety as a capping group (Figure I-3).²³ In 2012, Schinazi et al. reported nascent NS5A inhibitors containing a part of biaryl core and some modifications on other parts through “Click” and C-C bond cross coupling reactions.^{24,25} We recently developed a new class of NS5A inhibitors represented by BMK-20113, which has benzidine (**i**) and L-proline (**ii**) connected as an amide functionality and a variety of capping groups (**iii**).⁶⁰ In this paper, we report improvements in antiviral potency through the introduction of new modifications to the backbone of BMK-

20113: L-proline to other proline isosteres (area **ii** in Figure I-3), and benzidine to substituted benzidine derivatives (area **i** in Figure I-3).

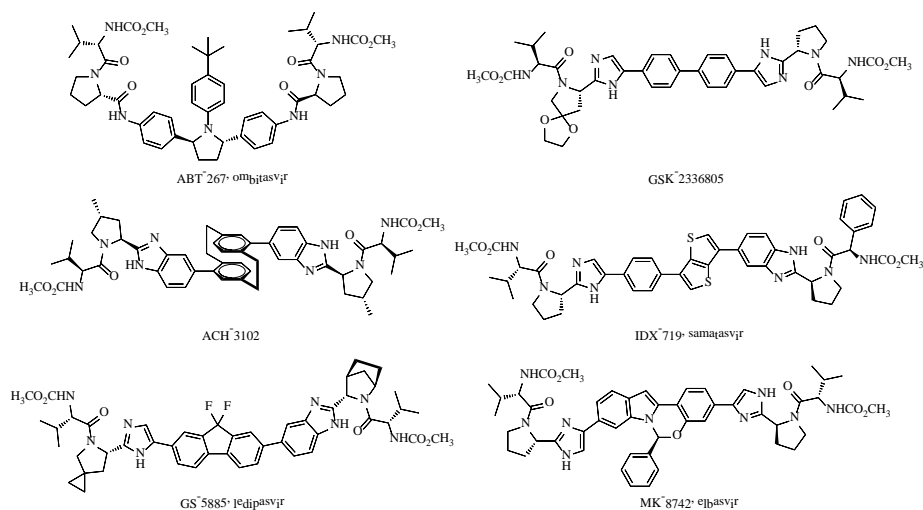


Figure I-2. Structure of NS5A inhibitors

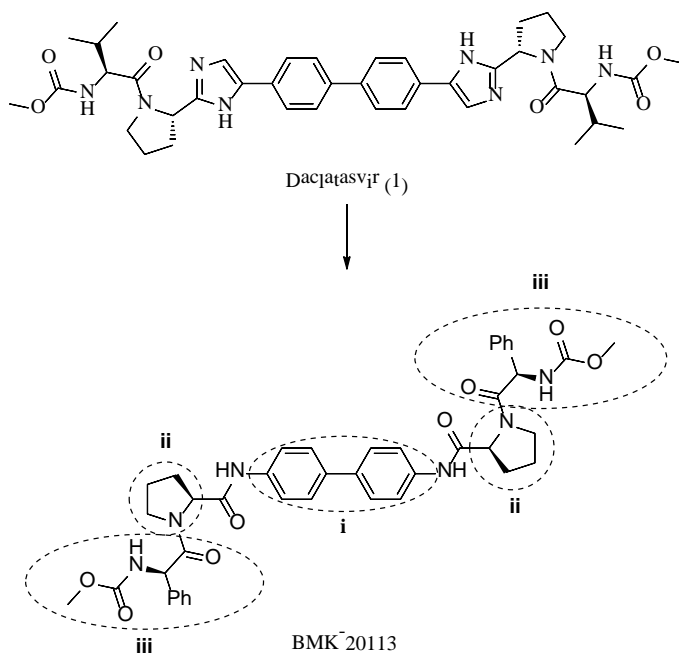
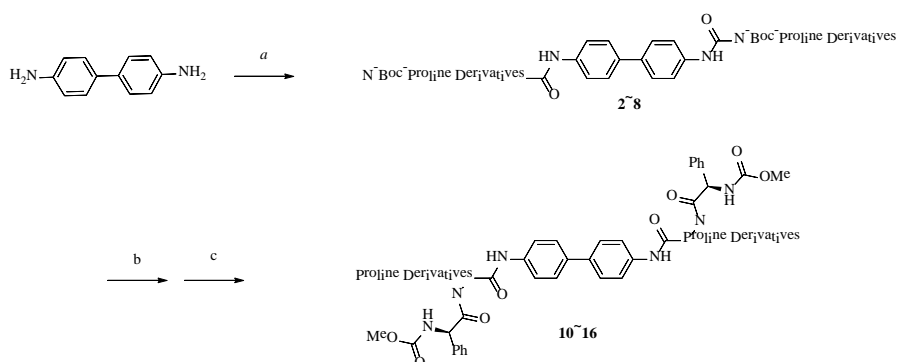


Figure I-3. Our strategy for producing HCV inhibitors

2. Result and Discussion

The symmetry in the benzidine-proline scaffold greatly streamlined our strategy of synthesizing BMK-20113. Initially, we wanted to evaluate the antiviral activity of the proline variation; therefore, L-proline isosteres were employed, such as D-proline, 4-oxo-L-proline, L-thioprolin, L-pipecolic acid, D-pipecolic acid, and α -methyl-L-proline, by using the standard peptide coupling protocol of EDCI in DCM. After purification of intermediates **2-8** through chromatographic columns, the Boc protected secondary amine site was removed with diluted trifluoroacetic acid (TFA) in DCM.⁶¹ Then methyl carbamate phenylglycine **9** was coupled with the free amine with the aid of EDCI and DIPEA in DCM. In cases where solubility was a persistent problem, we used DMF as a solvent.^{26,27} The targeted benzidine proline derivatives **10-16** were then prepared in low to reasonable yields (13-57%) (Scheme I-2).

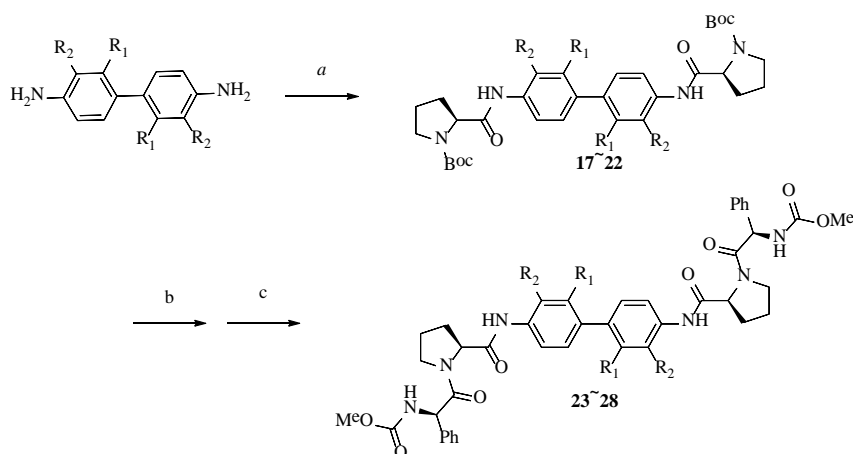


Proline Derivatives		
2	10	L-Proline
3	11	D-Proline
4	12	4-Oxo-L-proline
5	13	L-Thioprolin
6	14	L-Pipecolic acid
7	15	D-Pipecolic acid
8	16	α -Methyl-L-proline

Scheme I-2. Synthesis of benzidine and proline derivatives from an amide skeleton^a

^aReagents and conditions: (a) *N*-Boc-proline derivatives, EDCI, DCM, 31-99%; (b) TFA, DCM; (c) **9** (Capping Group), EDCI, DIPEA, DCM or DMF, 13-57% (2 steps).

Next, structure-activity relationship studies centered on the benzidine core by employing various substituted benzidine compounds were carried out using *o*- or *m*-substituted benzidine derivatives (*o*-methyl, *m*-methyl, *m*-trifluoromethyl, *m*-fluoro, *m*-chloro, and *m*-bromo). After a coupling reaction, almost pure *N*-Boc-protected prolinamide products **17-22** were obtained in excellent yields (92-97%). Using the same method described above, capping groups were incorporated and the final products **23-28** were obtained in low to good yields (32-73%) (Scheme I-3).



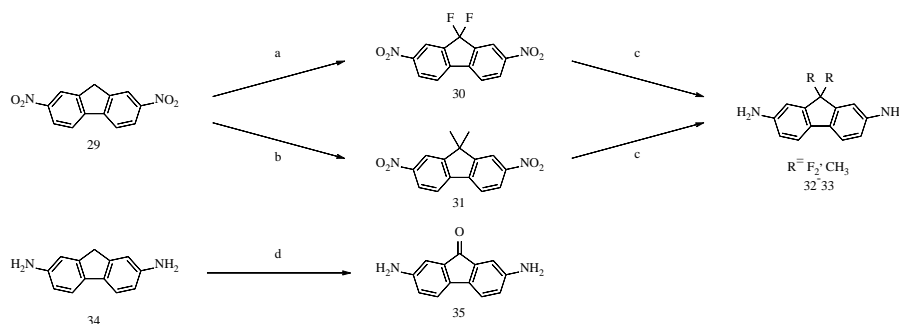
		R ₁	R ₂
17	23	H	CH ₃
18	24	CH ₃	H
19	25	CF ₃	H
20	26	F	H
21	27	Cl	H
22	28	Br	H

Scheme I-3. Synthesis of benzidine derivatives and prolinamide skeleton^a

^aReagents and conditions: (a) N-Boc-L-Proline, EDCI, DCM, 92-97%; (b) TFA, DCM; (c) **9** (capping group), EDCI, DIPEA, DCM, 32-73% (2 steps).

For the construction of the fluorene derivative core structures, we first needed to synthesize 2,7-diaminofluorene derivatives (Scheme I-4). After the treatment of 2,7-dinitrofluorene with 1.00 M LiHMDS followed by *N*-fluorobenzenesulfonimide (NFSI) in THF, we obtained 9,9-difluoro-2,7-dinitro-9*H*-fluorene **30** in 86% yield. Dimethyl derivative was synthesized likewise, treating 2,7-dinitrofluorene with NaOt-Bu followed by iodomethane in DMF to furnish the desired 9,9-dimethyl-2,7-dinitro-9*H*-fluorene **31** with an 80% yield.⁶² The nitro groups of both **30** and **31** were efficiently reduced to amino functionality per our recent report on commercially available Fe₃O₄

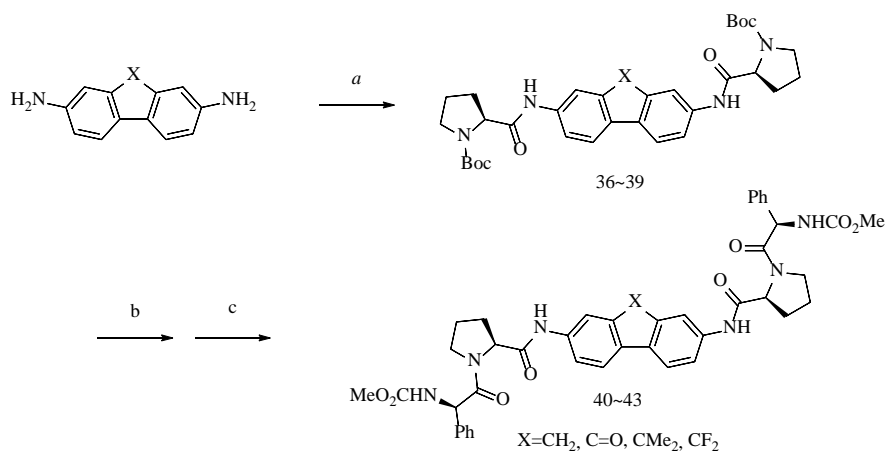
nanoparticles as a heterogeneous catalyst for nitro group reduction in combination with hydrazine monohydrate.⁶³ Extremely high yields (99%) of the desired diamino compounds **32** and **33** were obtained. Moreover, a reasonable yield (76%) of the diamino ketone compound **35** was obtained by oxidizing the 9*H*-fluorene-2,7-diamine in the presence of a strong base (Cs₂CO₃) in DMSO in open air.⁶⁴



Scheme I-4. Synthesis of fluorene-2,7-diamine derivatives^a

^aReagents and conditions: (a) *N*-fluorobenzenesulfonimide, LiHMDS in THF (1.00 M solution), THF, 86%; (b) iodomethane, NaO*t*-Bu, DMF, 80%; (c) Fe₃O₄, NH₂NH₂·H₂O, DMF, 99%; (d) Cs₂CO₃, DMSO, 76%.

After preparation of various 2,7-diaminofluorene derivatives, inhibitors containing L-proline and the capping group were prepared using the method described in Scheme I-2. *N*-Boc-protected fluorine prolinamides **36-39** were thus obtained in high yields (91-97%), obviating column chromatographic purification. Deprotected amines and coupling of the (*R*)-phenylglycine derivative gave us the desired fluorene derivatives **40-43** in moderate yields (50-66%) (Scheme I-5).



Scheme I-5. Synthesis of fluorine-containing prolinamide derivatives^a

^aReagents and conditions: (a) *N*-Boc-L-Proline, EDCI, DCM, 91-97%; (b) TFA, DCM; (c) **3** (capping group), EDCI, DIPEA, DCM 50-66% (2 steps).

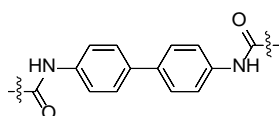


Table I-6. Structure-activity relationships of inhibitors containing various proline isosteres against HCV type 2a and type 1b.

Entry	Compounds	R	Proline	HCVCC EC ₅₀ (type 2a) (nM)	Replicon EC ₅₀ (type 1b) (nM)	Cytotoxicity (μM)
1	10		L-proline	0.26	0.028	>25
2	11		D-proline	1,770	83	>25
3	12		4-oxo-L-proline	0.26	0.044	>25
4	13		L-thioproline	15.5	0.027	>25
5	14		L-pipecolic acid	180	2.1	>25
6	15		D-pipecolic acid	419	370	>25
7	16		α-methyl-L-proline	3.3	2.2	>25

To determine the inhibitory activities (EC_{50} values) of each compounds, we used the HCV cell culture system (HCVcc) and HCV replicon system.^{32,65,66} To determine EC_{50} values in the HCVcc system (genotype 2a), we used a modified JFH1 clone (JFH 5a-Rluc-ad34) containing the *Renilla* luciferase gene (Rluc) in the NS5A region and cell culture adaptive mutations in the E2 and p7 region.²⁸ Huh7.5.1 cells were infected with JFH5a-Rluc-ad34 for 4 h. After infection, Huh7.5.1 cells were incubated with compounds of interest at various concentrations for 3 d. Then, the cells were harvested and luciferase activities were measured. We determined EC_{50} values using the HCV replicon system to evaluate the inhibitory activities of the synthesized compounds on HCV replication. HCV replicon systems (genotype 1b) containing HCV NS3-5B and the *Renilla* luciferase gene allow for productive viral RNA replication in cell culture systems. HCV replicon-containing cells were cultivated in the presence of serially diluted compounds for 3 d. Cells were harvested after treatment with chemicals for 3 d, and luciferase activities were measured. Luciferase activities were normalized to those obtained from mock-treated cells and EC_{50} values were calculated using a Sigma Plot analysis based on luciferase activities in the cells. The antiviral activities (EC_{50}) of these compounds against the HCV GT-2a and GT-1b are listed in Tables I-6, I-7, and I-8.

The SAR data indicates that the inhibitory activities of these compounds are significantly dependent upon the structural feature of the proline derivatives (Table I-6). The EC_{50} 's of our previously reported inhibitor containing L-proline, namely BMK-20113 (entry 1, compound **10**), against GT-2a and GT-1b were reported to be 260 and 28 pM, respectively. The inhibitory activities of the D-isomer **11** were 6,500-fold and 2,900-fold lower than those of the L-epimer, respectively, against the GT-2a and GT-1b genes (Table I-6, entry 2). Installation of a ketone at the 4-position of L-proline **12** resulted in a similar GT-2a inhibitory activity (EC_{50} : 0.26 nM), and a slightly decreased GT-1b inhibitory activity (EC_{50} : 0.044 nM) compared to those of the L-proline derivatives (Table I-6, entry 3). When L-thiopline was incorporated into the

benzidine **13**, the activity was slightly decreased in GT-2a, but there was a similar potency in GT-1b (EC₅₀ of GT-2a and GT-1b: 15.5 nM and 0.027 nM, respectively; Table I-6, entry 4). The inhibitor containing a six-membered L-pipecolic acid moiety **14** showed lower activity than its five-membered ring counterpart (Table I-6, entry 5). The opposite stereoisomeric D-pipecolic acid derivative **15** exhibited an even more pronounced decrease in inhibitory activities (EC₅₀ values all in the nanomolar range; Table I-6, entry 6). Lastly, the antiviral activities of the α -methyl substituted L-proline derivative **16** were lower than those of BMK-20113 (EC₅₀ of GT-2a and GT-1b: 3.3 nM and 2.2 nM, respectively; Table I-6, entry 7).

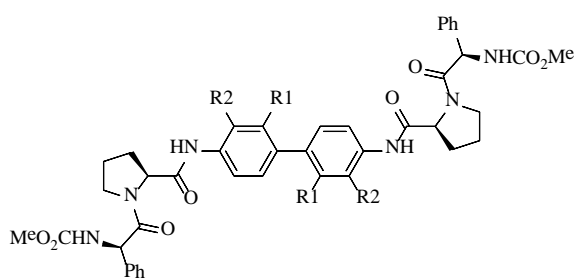


Table I-7. Structure-activity relationships of inhibitors containing substituted benzidine derivatives against HCV type 2a and type 1b.

Entry	Compound	R ₁	R ₂	HCVCC EC ₅₀ (type 2a)(nM)	Replicon EC ₅₀ (type 1b) (nM)	Cytotoxicity (μ M)
1	10	H	H	0.26	0.028	>25
2	23	H	CH ₃	193	7.4	>25
3	24	CF ₃	H	0.025	0.0025	>25
4	25	CH ₃	H	0.32	0.035	>25
5	26	F	H	0.16	0.005	>25
6	27	Cl	H	0.01	0.007	>25
7	28	Br	H	0.01	0.007	>25

Next, after fixing the L-proline and capping groups at both ends, we investigated the structure-activity relationship (SAR) studies of various

benzidine-containing derivatives by varying the middle biaryl portion (area **i** in Figure I-3). We first tested the *o*-methyl substituted benzidine derivative **23** for inhibitory effects and observed that low activities against the HCV (EC₅₀ of GT-2a and GT-1b: 193 nM and 7.4 nM, respectively; Table I-7, entry 2). However, a series of *m*-substituted benzidine derivatives **24-28** exhibited more enhanced inhibitory activities against HCV. In detail, the EC₅₀ of CF₃-substituted compound **24** in GT-2a and GT-1b were 25 and 2.5 pM, respectively (Table I-7, entry 3), and the values for CH₃-substituted compound **25** were 320 and 35 pM, respectively (Table I-7, entry 4). After noticing the strong inhibitory effect of the meta-substituted compound, we decided to explore a heteroatom substitution in the *m*-position of the benzidine core.⁶⁷⁻⁷⁰ All three inhibitors containing *m*-fluoro-, *m*-chloro- and *m*-bromo-substituted benzidine cores (compounds **26**, **27**, and **28**, respectively) exhibited powerful antiviral activities. EC₅₀ values against GT-2a and GT-1b were 160 and 5 pM, respectively, for compound **26** (Table 2, entry 5) and 10 and 7 pM for compounds **27** and **28** (entries 6 and 7, respectively).

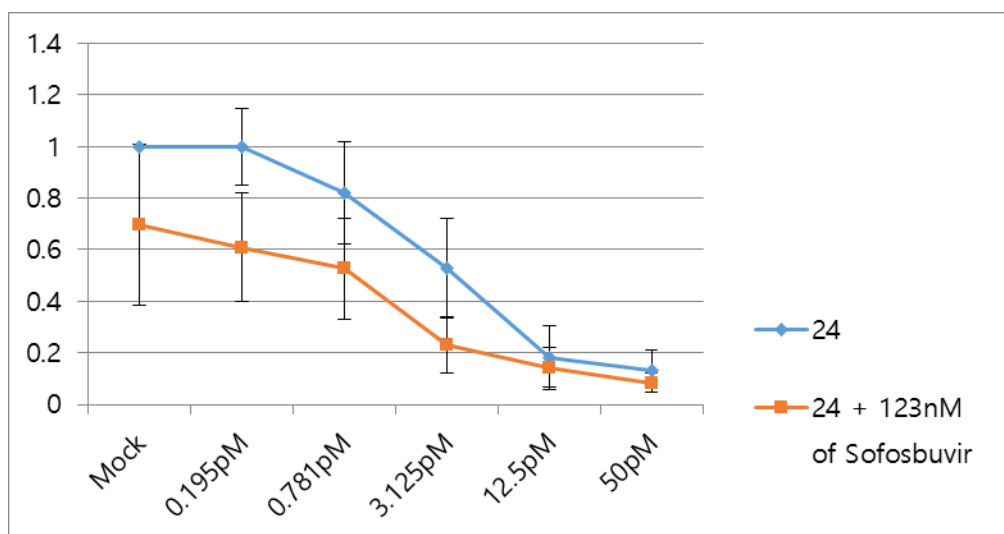


Figure I-4. Effect of compound **24** in combination with EC₃₀ of NS5B polymerase inhibitor (sofosbuvir) on the HCV GT-1b replicon system. Measurements were carried out in triplicate.

To see whether compound **24** has an additive or synergistic anti-viral effect in combination with an NS5B polymerase inhibitor (sofosbuvir), one of the top 10 blockbuster drugs in 2014,^{6,71-74} we treated NK/R2AN replicon cells with serially diluted compound **24** in the presence of an EC₃₀ concentration (123 nM) of sofosbuvir, and the luciferase activities in the cells were measured. Our data demonstrated that the combination therapy of compound **24** and sofosbuvir has a remarkably positive effect against HCV replicon cells, probably due to the independent mechanisms of action of the dual treatment (Figure I-4).⁷⁵⁻⁷⁸

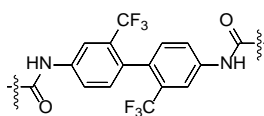


Table I-8. Kinetic resolution of compound **24**

Entry	Compound 24	HCVCC EC ₅₀ (type 2a) (pM)	Replicon EC ₅₀ (type 1b) (pM)	Cytotoxicity (μM)
1	Isomer 1	332	27.9	>25
2	Isomer 2	24.6	2.4	>25

Since compound **24** contains a core structure that can exist as atropisomers, we were curious about the potentially different inhibitory activities of each isomer. The separation of racemic 2,2'-bis(trifluoromethyl)benzidine was successfully performed through the use of a chiral preparative column on supercritical fluid chromatography (SFC).⁷⁹ Then, each isomer of compound **24** was synthesized using each isomer from the separation following the method described in Scheme I-3. Its effect on HCV proliferation was measured. It was found that isomer **1** of compound **24** showed a 13-fold less potent anti-viral activity than isomer **2**, which exhibited a similar activity to that of racemic **24** (Table I-8, entries 1-2, and Table I-7, entry 3, respectively). Therefore, we concluded that the isomer **2** of **24** is the active inhibitor of HCV.

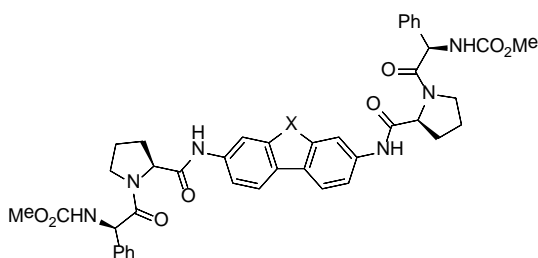


Table I-9. Structure-activity relationship studies of inhibitors containing a fluorene skeleton against HCV type 2a and type 1b.

Entry	Compound	X	HCVCC EC ₅₀ (type 2a) (nM)	Replicon EC ₅₀ (type 1b) (nM)	Cytotoxic ity (μM)
1	40	CH ₂	5.6	0.009	>25
2	41	C=O	4.3	0.004	>25
3	42	CMe ₂	0.020	0.004	>25
4	43	CF ₂	0.059	0.003	>25

When we tested the anti-viral activities of compounds **23-28**, meta-substitution of the benzidine prolinamides made the inhibitors highly potent HCV inhibitors. Therefore, we envisioned that the activity of *m,m*-connected benzidine, i.e., fluorene derivatives would exhibit high potency in the antiviral assays. Based on the positive results of previously reported NS5A inhibitors containing a fluorenyl core structure,⁵⁷ we synthesized and investigated inhibitors with a fluorenyl core. We were extremely pleased to observe that these inhibitors exhibited exceptionally high potencies, particularly in the replicon (GT-1b) assay (Table I-9, entries 1-4). Inhibitory activities (EC₅₀) of compound **40** containing the parent fluorene were 5.6 and 9 pM against GT-2a and GT-1b, respectively (Table I-9, entry 1). The fluorenone-containing inhibitor **41** exhibited a similar potency to compound **40**; EC₅₀ of GT-2a and GT-1b were 4.3 and 4 pM, respectively (Table I-9, entry 2). Furthermore, substituents at the methylene position of the fluorene core showed a dramatic increase in anti-viral activity against the GT-2a gene.⁸⁰ The inhibitory activity of compound **42** with a dimethyl-substituted fluorene moiety was 2,800-fold higher against the GT-2a gene than that of compound **40** containing the parent

fluorene (EC₅₀ of GT-2a and GT-1b: 20 and 4 pM, respectively; Table I-9, entry 3). Replacement of the dimethyl with difluorine **43** showed a similar effect (EC₅₀ of GT-2a and GT-1b: 59 and 3 pM, respectively; Table I-9, entry 4).⁸¹ All of the inhibitors listed in Table I-6, Table I-7, Table I-8, and Table I-9 were not cytotoxic at 25 μ M.

Table I-10. Result of hERG ligand binding assay^a

Entry	Compound	Inhibition % (10 μ M)
1	24	7.98 \pm 4.49
2	26	<1
3	27	5.80 \pm 3.22
4	42	25.7 \pm 4.90
5	43	39.1 \pm 2.93
6	Control (astemizole)	99.9
^a Fluorescence polarization assay		

Since the compounds **24**, **26**, **27**, **41**, and **43** exhibited highly inhibitory activities both in the HCV GT-2a and the replicon (GT-1b) system (Table I-7, entries 3, 6, 7, and Table I-9, entries 3, 4, respectively), we next focused on further evaluation of these selected compounds.⁸² First, to evaluate any probable cardiac toxicity, we performed a hERG ligand binding assay, examining inhibition of the inner rectifying voltage-gated fluorescence polarization potassium ion channel which is encoded by hERG gene.^{34,83} Compared to astemizole, which was used as a control (99.9% inhibition at 10 μ M), the values of compounds **24**, **26**, **27**, **42**, and **43** (7.98%, 1%, 5.80%, 25.7%, 39.1% inhibition at 10 μ M, respectively) suggested that these inhibitors bound poorly to the hERG membrane preparations, meaning minimal cardiac toxicity (Table I-10).

Table I-11. Stability in rat plasma (% remaining)

Entry	Compound	0.5 h (%)	1 h (%)	2 h (%)
1	24	93	99	99
2	26	65	61	63
3	27	72	75	70

Next, when the compounds were tested against rat plasma, our data showed a high *in vitro* stability for compound **24**, which was unscathed after 2 hours (99% of the compound remained; Table I-11, entry 1), whereas after incubating for 30 min, compounds **26** and **27** had degraded slightly (Table I-11, entries 2 and 3). Consequently, it was necessary to carry out additional stability tests.

Table I-12. Human liver microsomal stability (% remaining)

Entry	Compound	0.5 h (%)
1	24	79
2	26	97
3	27	96
4	42	95
5	43	92

In the human liver microsomal stability test, compound **24** was 21% digested in the plasma after 0.5 h (Table I-12, entry 1). Compounds **26**, **27**, **42**, and **43** had lower levels of degradation after 0.5 h (Table I-12, entries 2, 3, 4, and 5, respectively). These results indicate that these promising compounds had high microsomal stability in the human liver.^{37,84}

Table I-13. EC₅₀ of compounds (μM) against various subtypes of CYP₄₅₀^a

Entry	Compound	1A2	2C9	2D6	2C19	3A4
1	24	78.8	0.660	>100	4.64	4.64
2	26	>100	0.0877	4.94	0.724	2.46
3	27	23.9	0.116	41.2	1.04	3.99
5	42	>100	0.269	>100	2.94	1.03
4	43	>100	0.277	>100	13.9	0.976

^a Standard inhibitors for each CYP₄₅₀ subzymes: 1A2: α-naphthoflavone, 2C9: sulfaphenazole, 2D6: quinidine, 2C19: miconazole 3A4: ketoconazole.

Next, we outlined CYP₄₅₀ inhibitory profiles to evaluate any drug-drug interactions possible with the selected compounds **24**, **26**, **27**, **42**, and **43**. In general, high EC₅₀ values for the CYP₄₅₀ enzyme inhibitor indicate decreased liability for drug-drug interactions.^{38,85} Our selected compounds exhibited low inhibition profiles for various CYP₄₅₀ isoforms. CYP1A2, CYP2D6, CYP2C19, and CYP3A4 were rather weakly inhibited in the presence of compounds **24**, **26**, **27**, **42**, and **43**, while the inhibition was higher for CYP2C9 (0.14, 0.0877, 0.116, 0.269, and 0.277 μM respectively; Table I-13). However, there should still be a large safety margin when we compare these inhibitions to their anti-viral activity.⁸⁶ In summary, compounds **24**, **26**, **27**, **42**, and **43** do not significantly inhibit these five representative CYP enzymes (Table I-13).⁸⁷

Table I-14. Pharmacokinetics features of selected inhibitors in rats^a

Entry	Compound	Administration route	Dose (mg/kg)	C_{\max} ($\mu\text{mol/mL}$)	$t_{1/2}$ (h)	F (%)
1	24	p.o.	10	0.44 \pm 0.14	3.80 \pm 0.11	11.7
2	26		10	0.11 \pm 0.07	2.34 \pm 0.37	3.12
3	27		10	0.17 \pm 0.07	6.37 \pm 3.39	4.99
5	42		10	0.98 \pm 0.02	4.45 \pm 4.02	13.8
4	43		10	0.39 \pm 0.20	1.68 \pm 0.43	7.6
6	24	iv	5	13.76 \pm 4.1	2.90 \pm 0.62	
7	26		5	16.63 \pm 2.57	0.88 \pm 0.34	
8	27		5	15.88 \pm 1.62	1.55 \pm 0.25	
10	42		5	13.26 \pm 1.13	1.62 \pm 0.78	
9	43		5	18.64 \pm 19.4	0.90 \pm 0.02	

^a Vehicle : 5% DMSO/10% Solutol/85% HPBCD (20%, w/v), n = 3

Studies on the pharmacokinetics (PK) of 5 selected compounds were carried out in rats, with the vehicles consisting of 5% DMSO, 10% solutol, and 85% (2-hydroxypropyl)- β -cyclodextrin (HPBCD) (Table I-14). Despite high potencies in *in vitro* studies of HCV inhibition, the selected compounds provoked some concern due to the symmetrical natures of their structures and their high molecular weights, which might lead to undesirable PK properties.^{33,88-93} Our data showed that the highest maximum concentration in plasma (C_{\max}) was obtained with compound **42** (0.98 $\mu\text{mol/mL}$) through oral administration, and compound **43** (18.64 $\mu\text{mol/mL}$) through intravenous administration (Table I-14, entries 5 and 9, respectively). The half-lives ($t_{1/2}$) of these two compounds upon p.o. administration were 1.7 to 6.4 h, and in IV administration were 0.9 to 2.9 h, respectively. When we checked the oral bioavailability (F%), their low solubility and high lipophilicity contributed to a moderate oral absorption and bioavailability.^{94,95}

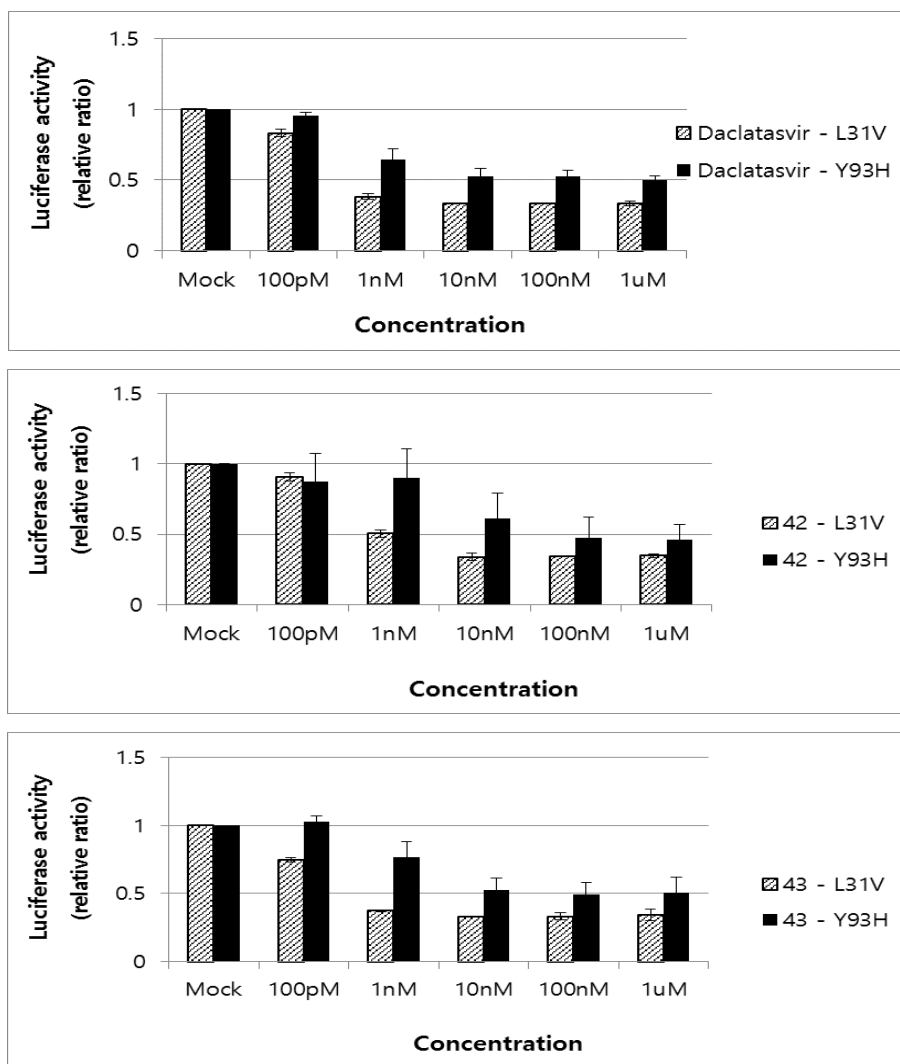


Figure I-5. Resistance profiles of inhibitors daclatasvir, **42**, and **43**. Measurements were carried out in triplicate.

Then, we tested some of our selected inhibitors (**42** and **43**) against daclatasvir resistant mutants (L31V and Y93H) as described in Materials and Method.⁵⁵ *In vitro* transcribed resistant mutant RNAs (L31V and Y93H) were individually transfected to Huh7.5.1 cells.^{96,97} After 4 h after transfection, the culture media were replaced with DMEM media containing serially diluted compounds. By

comparing the luciferase activities of **42** and **43** with those of daclatasvir, we concluded that **43** had a higher activity than **42** and a similar anti-viral potency to daclatasvir, to single mutant viruses. Therefore, we concluded that **43** could be a solution to the resistance problems of current HCV drugs (Figure I-5).

Table I-15. Cytotoxicity of **43** in eukaryotic cells^a

Compound	IC ₅₀ (μM)				
	VERO	HFL-1	L929	NIH 3T3	CHO-K1
43	>100	>100	>100	>100	>100

^a VERO: African green monkey kidney cell line; HFL-1: human embryonic lung cell line; L929: NCTC clone 929, mouse fibroblast cell line; NIH 3T3: mouse embryonic fibroblast cell line; CHO-K1: Chinese hamster ovary cell line.

Then, we tested the cytotoxicity of compound **43** against some eukaryotic cells.⁹⁸ The cell counting kit-8 assay method was used to measure the survival rate of the cells by using WST-8 tetrazolium salt. Hydrophilic WST-8 turns into orange formazan dye by dehydrogenase in cell lines. The number of living cells is determined by the activated dehydrogenase, which indicates the eukaryotic cell survival rate. At the maximal concentration (100 μM) used in the experiment, compound **43** showed less than 50% inhibition (the limit) in monkey kidney, human embryonic lung, mouse fibroblast, and hamster ovary cell line (Table I-15). Thus, we concluded that **43** is nontoxic and safe in the tested eukaryotic cell lines.

Table I-16. Bacterial reverse mutation assay of **43**^a

Tester strain	Compound	Dose (µg/plate)	Revertant colonies/plate (Mean ± SD) [Factor] ^b	
			Without S-9 mix	With S-9 mix
TA-98	Vehicle control	0	18 ± 2	28 ± 3
	43	200	23 ± 5[1.3]	30 ± 2[1.1]
TA-100	Vehicle control	0	117 ± 10	126 ± 19
	43	200	106 ± 3[0.9]	115 ± 8[0.9]
	Positive control	Dose (µg/plate)	Without S-9 mix	With S-9 mix
TA-98	2-Nitrofluorene	1	187 ± 14[10.2]	ND
	Benzo[a]pyrene	2	ND	171 ± 10[6.1]
TA-100	Sodium azide	1	728 ± 15[6.2]	ND
	Benzo[a]pyrene	2	ND	521 ± 28[4.1]

^a (Mean ± SD, n = 3)^b No. of revertant colonies in the treated plate/No. of revertant colonies in the vehicle control plate

ND : Non Determined

Next, we investigated the possibility that compound **43** might have genetic toxicity using the Ames test.^{99,100} For this purpose, we used *Salmonella typhimurium* strains TA-98 and TA-100 that require several amino acids for growth to test whether compound **43** functions as a mutagen. Growth of TA-98 and TA-100 strains in the presence of the compound of interest in the media lacking histidine indicates that the compound is a potential mutagen inducing substitution, addition, and/or deletion of DNA. The result is considered to be positive when the number of colonies on the compound-treated plate increases double or more of those on the vehicle control plate. When we tested 200 µg/plate of **43**, the number of revertant colonies on the compound-treated plate was not increased compared with that on the vehicle-treated plate. And the number was much lower than those on 4 positive control compound-treated plates (Table I-16). Therefore, compound **43** is considered to be non-genotoxic.

3. Conclusion

In conclusion, we developed a series of extremely potent HCV NS5A inhibitors using new benzidine and fluorene prolinamide derivatives as core structures. Several of them have highly potencies that produce inhibition even at the single digit pM level. Through the SAR studies using a variety of benzidine, proline, and fluorene derivatives with a phenyl glycine capping group, we were able to identify inhibitors possessing excessively high inhibitory activities. Among the new inhibitors, compounds **24**, **26**, **27**, **42**, and **43** were the most potent. A synergistic effect with the NS5B polymerase inhibitor was seen with compound **24**. Moreover, subsequent studies demonstrated that these compounds have a desirable low cardiac toxicity, high human microsomal stability, and limited drug-drug interactions. Compound **43** was revealed to be non-toxic for eukaryotic cells and genetically non-toxic by the Ames test. The results of this study suggest that compound **43** is a highly potent and safe lead warranting further study as a potential HCV drug candidate. Further research on other pharmacological properties of the selected inhibitors and new structure of the HCV NS5A inhibitors is currently under progress at our laboratories.

4. Experimental

General Information

The ^1H and ^{13}C NMR-spectra were measured with an Agilent 400-MR DD2 Magnetic Resonance System (400 MHz) and a Varian/Oxford As-500 (500 MHz) Spectrophotometer. The signals were reported as s (singlet), d (doublet), t (triplet), q (quartet), m (multiplet), or br s (broad singlet) and chemical shifts were measured as parts per million (δ values) from tetramethylsilane as an internal standard at probe temperature in CDCl_3 or DMSO-D_6 for neutral compounds. Reactions that needed anhydrous conditions were carried out in flame-dried glassware under a positive pressure of dry N_2 using standard Schlenk line techniques. Evaporation of solvents was performed at reduced pressure using a rotary evaporator. TLC was performed using silica gel 60F254 coated on an aluminum sheet (E. Merck, Art.5554). Chromatogram was visualized by UV-lamp (Vilber Lournat, VL-4LC) and/or colorized with following solutions: (a) 20% ethanolic phosphomolybdic acid (PMA), (b) potassium permanganate solution, and (c) 2% ninhydrin ethanolic solution. Column chromatography was performed on silica gel (Merck. 7734 or 9385 Kiesel gel 60), and the eluent was mentioned in each procedure. High resolution mass spectra (HRMS) were recorded on a ThermoFinnigan LCQTM Classic, Quadrupole Ion-Trap Mass Spectrometer. HPLC analyses were carried out on an Agilent HP1100 system (Santa Clara, CA, USA), composed of an auto sampler, quaternary pump, photodiode array detector (DAD), and HP Chemstation software. The separation was carried out on a C18 Vydac 218TP54 column 250 x 4.6 mm i.d. (5 μm particle size) with 0.1% TFA in water (A), acetonitrile (B), as a mobile phase at a flow rate of 1 mL/min at 20 °C. Method: 100% A and 0% B (0 min), 0% A and 100% B (10 min), 0% A and 100% B (20 min), 100% A and 0% B (22 min), 100% A and 0% B (25 min). All materials

were purchased from a commercial supplier and used without further purification unless otherwise noted.

Preparation of compounds

(R)-2-((Methoxycarbonyl)amino)-2-phenylacetic acid (9). Na₂CO₃ (0.55 g, 5.2 mmol) was added to an aq NaOH (10 mL of 1 M/H₂O, 10 mmol) solution of D-phenylglycine (1.500 g, 10.0 mmol) and the resulting solution was cooled in an ice-water bath. Methyl chloroformate (0.85 mL, 11.0 mmol) was added dropwise, then the cooling bath was removed and the reaction mixture was stirred at ambient temperature for 3.25 h. The reaction mixture was washed with ether (3 x 18 mL), and the aqueous phase was cooled in an ice-water bath and acidified with conc. HCl to a pH range of 1-2, and extracted with CH₂Cl₂ (3 x 18 mL). The organic phase was dried (MgSO₄), filtered, and concentrated in vacuo, and the resulting oil residue was treated with diethyl ether/hexanes (~5:4 ratio; 10 mL) to provide a precipitate. The precipitate was filtered and washed with diethyl ether/hexanes (~1:3 ratio) and dried in vacuo to provide **9** as a fluffy white solid (1.4 g, 67%). ¹H NMR (DMSO-*d*₆, δ = 2.5 ppm, 500 MHz): 12.79 (br s, 1H), 7.96 (d, *J* = 12, 1H), 7.40-7.29 (m, 5H), 5.13 (d, *J* = 12, 1H), 3.55 (s, 3H).

(2R,2'R)-Di-tert-butyl 2,2'-((([1,1'-biphenyl]-4,4'-diylbis(azanediyl))bis(carbonyl))bis(pyrrolidine-1-carboxylate) (3). A mixture of *N*-Boc-D-proline (771 mg, 3.6 mmol), EDCI (812 mg, 4.2 mmol), and benzidine (300 mg, 1.63 mmol) in CH₂Cl₂ (4 mL) was stirred at ambient temperature for 2 h. The resulting residue was divided between CH₂Cl₂ and H₂O. The organic soluble layer was washed with 1 N aq HCl solution and brine, dried over MgSO₄, filtered, and concentrated in vacuo. Without any purification, **17** was obtained as a solid (930 mg, 99%). ¹H NMR (DMSO-*d*₆, δ = 2.5 ppm, 400 MHz): 10.08 (s, 2H), 7.69-7.59 (dd, 8H), 4.29-4.20 (m, 2H), 3.44-3.35 (m, 4H), 2.21 (m, 2H), 1.90-1.78 (m, 6H), 1.40-1.28 (app br s, 18H). ¹³C NMR

(DMSO- d_6 , δ = 39.52 ppm, 100 MHz): 171.5, 153.2, 138.2, 134.4, 126.4, 119.6, 78.5, 60.4, 46.6, 31.0, 28.2, 28.0, 23.4. HRMS: Anal. calcd. for $[M+H]^+$ $C_{32}H_{42}N_4O_6$: 579.3177; found 579.3167.

(5*S*,5'*S*)-Di-*tert*-butyl **5,5'-([1,1'-biphenyl]-4,4'-diylbis(azanediyl))bis(carbonyl))bis(3-oxopyrrolidine-1-carboxylate)** (**4**).

Yield 320 mg (87%). 1H NMR (DMSO- d_6 , δ = 2.5 ppm, 400 MHz): 10.36 (d, 2H), 7.65 (m, 8H), 4.78-6.49 (m, 2H), 3.89-3.76 (m, 4H), 3.11 (m, 2H), 2.57 (m, 2H), 1.42-1.33 (app br s, 18H). ^{13}C NMR (DMSO- d_6 , δ = 39.52 ppm, 100 MHz): 209.5, 208.9, 171.0, 170.7, 153.8, 153.4, 137.8, 134.8, 126.64, 126.58, 119.7, 79.9, 79.8, 57.8, 57.0, 53.1, 41.5, 41.2, 28.1, 28.0. HRMS: Anal. calcd. for $[M+H]^+$ $C_{32}H_{38}N_4O_8$: 607.2762; found 607.2756.

(4*R*,4'*R*)-Di-*tert*-butyl **4,4'-([1,1'-biphenyl]-4,4'-diylbis(azanediyl))bis(carbonyl))bis(thiazolidine-3-carboxylate)** (**5**).

Yield 2.5 g (64%). 1H NMR (DMSO- d_6 , δ = 2.5 ppm, 400 MHz): 10.15 (s, 2H), 7.68-7.61 (dd, 8H), 4.72 (app br s, 1H), 4.63 (d, 2H), 4.55 (app br s, 1H), 4.45 (d, 2H), 3.46 (m, 2H), 3.15 (m, 2H), 1.94-1.81 (m, 6H), 1.43-1.32 (app br s, 18H). ^{13}C NMR (DMSO- d_6 , δ = 39.52 ppm, 100 MHz): 169.0, 152.6, 137.9, 134.7, 126.5, 119.8, 80.0, 63.0, 50.0, 35.2, 27.9. HRMS: Anal. calcd. for $[M+H]^+$ $C_{30}H_{38}N_4O_6S_2$: 615.2306; found 615.2278.

(2*S*,2'*S*)-Di-*tert*-butyl **2,2'-([1,1'-biphenyl]-4,4'-diylbis(azanediyl))bis(carbonyl))bis(piperidine-1-carboxylate)** (**6**).

A mixture of *N*-Boc-L-pipecolic acid (400 mg, 1.75 mmol), EDC (363 mg, 1.9 mmol), and benzidine (134 mg, 0.73 mmol) in CH_2Cl_2 (7 mL) was stirred at ambient temperature for 2 h. The resulting residue was partitioned between CH_2Cl_2 and H_2O . The organic layer was washed with 1.0 N aq HCl solution and brine, dried over $MgSO_4$, filtered, and concentrated in vacuo. A silica gel mesh was prepared from the residue and submitted to flash chromatography (silica gel: EtOAc/hexane as eluent) to provide **20** as a solid (186 mg, 42%). 1H NMR

(DMSO-*d*₆, δ = 2.5 ppm, 400 MHz): 9.99 (s, 2H), 7.67-7.58 (dd, 8H), 4.70 (m, 2H), 3.82 (d, 2H), 3.34 (m, 2H), 2.08 (app br s, 2H), 1.72-1.58 (m, 6H), 1.37 (app br s, 22H). ¹³C NMR (DMSO-*d*₆, δ = 39.52 ppm, 100 MHz): 170.8, 155.3, 138.1, 134.5, 126.4, 119.7, 78.9, 55.2, 53.9, 42.0, 28.0, 27.5, 24.2, 19.3. HRMS: Anal. calcd. for [M+H]⁺ C₃₄H₄₆N₄O₆: 607.3490; found 607.3491.

(2*R*,2'*R*)-Di-*tert*-butyl 2,2'-((*[1,1'*-biphenyl]-4,4'-diylbis(azanediyl))bis(carbonyl))bis(piperidine-1-carboxylate) (7). Yield 190 mg (35%). ¹H NMR (DMSO-*d*₆, δ = 2.5 ppm, 400 MHz): 10.00 (s, 2H), 7.67-7.58 (dd, 8H), 4.69 (m, 2H), 3.81 (d, 2H), 3.26 (m, 2H), 2.07 (app br s, 6H), 1.64-1.58 (m, 6H), 1.37 (app br s, 22H). ¹³C NMR (DMSO-*d*₆, δ = 39.52 ppm, 100 MHz): 170.8, 155.3, 138.1, 134.5, 126.4, 119.7, 78.9, 55.2, 53.9, 42.0, 28.0, 27.5, 24.2, 19.6. HRMS: Anal. calcd. for [M+H]⁺ C₃₄H₄₆N₄O₆: 607.3490; found 607.3489.

(2*S*,2'*S*)-Di-*tert*-butyl 2,2'-((*[1,1'*-biphenyl]-4,4'-diylbis(azanediyl))bis(carbonyl))bis(2-methylpyrrolidine-1-carboxylate) (8). Yield 86 mg (31%). ¹H NMR (DMSO-*d*₆, δ = 2.5 ppm, 400 MHz): 9.37 (app br s, 2H), 7.74-7.62 (m, 8H), 3.67 (m, 2H), 3.41 (m, 2H), 2.15 (m, 2H), 1.90 (m, 6H), 1.51-1.26 (m, 24H). ¹³C NMR (DMSO-*d*₆, δ = 39.52 ppm, 100 MHz): 173.0, 172.5, 153.0, 152.6, 138.4, 134.3, 126.1, 120.8, 120.6, 78.7, 78.6, 66.2, 65.9, 47.5, 47.1, 28.2, 28.0, 22.6, 22.1, 21.1. HRMS: Anal. calcd. for [M+H]⁺ C₃₄H₄₆N₄O₆: 607.3490; found 607.3490.

Dimethyl ((1*R*,1'*R*)-((2*R*,2'*R*)-2,2'-((*[1,1'*-biphenyl]-4,4'-diylbis(azanediyl))bis(carbonyl))bis(pyrrolidine-2,1-diyl))bis(2-oxo-1-phenylethane-2,1-diyl))dicarbamate (11). Compound **17** (300 mg, 0.52 mmol) in CF₃CO₂H (2 mL) and CH₂Cl₂ (2 mL) was stirred at room temperature for 4 h. The volatile component was removed in vacuo, EDCI (258 mg, 0.620 mmol) and **9** (260 mg, 1.24 mmol) were added in batches over 4 min to a solution of *i*-Pr₂NEt (455 μ L, 2.6 mmol) in CH₂Cl₂ (3 mL) and the reaction mixture was

stirred at room temperature for 75 min. The residue was partitioned between CH₂Cl₂ and H₂O. The organic layer was washed with H₂O and brine, dried over MgSO₄, filtered, and concentrated in vacuo. A silica gel mesh was prepared from the residue and submitted to flash chromatography (silica gel: EtOAc/hexane as eluent) to provide **23** as a white solid (171 mg, 57%). ¹H NMR (DMSO-*d*₆, δ = 2.5 ppm, 400 MHz): 10.14 (s, 2H), 7.68-7.60 (m, 9H), 7.46-7.30 (m, 11H), 5.49 (d, 2H), 4.53 (m, 2H), 3.68 (m, 2H), 3.54 (s, 6H), 3.12 (m, 2H), 2.00-2.13 (m, 2H), 1.89-1.82 (m, 6H). ¹³C NMR (DMSO-*d*₆, δ = 39.52 ppm, 100 MHz): 170.2, 168.1, 156.4, 138.2, 136.9, 134.4, 128.4, 128.4, 127.8, 126.4, 119.4, 60.6, 56.6, 51.6, 46.9, 29.4, 24.7. HRMS: Anal. calcd. for [M+H]⁺ C₄₂H₄₄N₆O₈: 761.3293; found 761.3281.

Dimethyl ((1*R*,1'*R*)-((5*S*,5'*S*)-5,5'-([1,1'-biphenyl]-4,4'-diylbis(azanediyl))bis(carbonyl))bis(3-oxopyrrolidine-5,1-diyl))bis(2-oxo-1-phenylethane-2,1-diyl))dicarbamate (**12**). Yield 48 mg (23%). ¹H NMR (DMSO-*d*₆, δ = 2.5 ppm, 400 MHz): 10.38 (s, 2H), 7.92 (d, 2H), 7.70-7.10 (m, 18H), 5.46 (d, 2H), 4.94 (d, 2H), 4.25 (d, 2H) 3.89 (d, 2H), 3.54 (s, 6H), 3.06 (m, 2H), 2.54 (m, 2H). ¹³C NMR (DMSO-*d*₆, δ = 39.52 ppm, 100 MHz): 208.5, 170.1, 169.4, 156.1, 137.8, 136.8, 134.7, 128.6, 128.2, 128.1, 126.5, 119.7, 57.4, 56.9, 53.1, 51.7, 40.4. HRMS: Anal. calcd. for [M+H]⁺ C₄₂H₄₀N₆O₁₀: 789.2879; found 789.2877.

Dimethyl ((1*R*,1'*R*)-((4*R*,4'*R*)-4,4'-([1,1'-biphenyl]-4,4'-diylbis(azanediyl))bis(carbonyl))bis(thiazolidine-4,3-diyl))bis(2-oxo-1-phenylethane-2,1-diyl))dicarbamate (**13**). Yield 25 mg (14%). ¹H NMR (DMSO-*d*₆, δ = 2.5 ppm, 400 MHz): 9.89 (s, 2H), 7.93 (d, 2H), 7.73-7.59 (m, 8H), 7.46-7.13 (m, 10H), 5.64 (d, 2H), 4.87 (m, 4H), 4.53 (d, 2H), 3.58 (s, 6H), 3.36 (m, 2H), 3.19 (m, 2H). ¹³C NMR (DMSO-*d*₆, δ = 39.52 ppm, 100 MHz): 168.3, 167.9, 156.4, 137.8, 136.3, 134.7, 128.7, 128.3, 128.1, 126.4, 119.8, 63.2, 56.8, 51.8, 49.0, 33.1. HRMS: Anal. calcd. for [M+H]⁺ C₄₀H₄₀N₆O₈S₂: 797.2422; found 797.2422.

Dimethyl ((1*R*,1'*R*)-((2*S*,2'*S*)-2,2'-([1,1'-biphenyl]-4,4'-diylbis(azanediyl))bis(carbonyl))bis(piperidine-2,1-diyl))bis(2-oxo-1-phenylethane-2,1-diyl))dicarbamate (14). Compound **20** (73 mg, 0.12 mmol) in CF₃CO₂H (1 mL) and CH₂Cl₂ (1 mL) was stirred at room temperature for 5 h. The volatile component was removed in vacuo, EDCI (60 mg, 0.31 mmol) and compound **9** (60 mg, 0.29 mmol) were added in batches over 4 min to a solution of *i*-Pr₂NEt (105 μL, 0.60 mmol) in DMF (1 mL) and the reaction mixture was stirred at room temperature for 75 min. The residue was partitioned between CH₂Cl₂ and H₂O. The organic soluble layer was washed with H₂O and brine, dried over MgSO₄, filtered, and concentrated in vacuo. A silica gel mesh was prepared from the residue and submitted to flash chromatography (silica gel: EtOAc/hexane as eluent) to provide **26** as a solid (12 mg, 13%). ¹H NMR (DMSO-*d*₆, δ = 2.5 ppm, 400 MHz): 9.99-9.84 (s, 2H), 7.85-7.30 (m, 20H), 5.73-5.64 (m, 2H), 5.17/4.85 (m, 2H), 4.45/3.77 (m, 2H), 3.55 (app br s, 6H), 3.18/2.83 (m, 2H), 2.15 (m, 2H), 1.76 (m, 2H), 1.63-1.24 (m, 8H). ¹³C NMR (DMSO-*d*₆, δ = 39.52 ppm, 100 MHz): 170.0, 169.3, 168.5, 156.2, 138.0, 137.2, 134.5, 128.6, 128.4, 128.2, 127.7, 126.5, 120.2, 119.7, 67.0, 55.5, 52.8, 51.6, 43.2, 27.5, 25.1, 24.6, 19.7. HRMS: Anal. calcd. for [M+H]⁺ C₄₄H₄₈N₆O₈: 789.3606; found 789.3605.

Dimethyl ((1*R*,1'*R*)-((2*R*,2'*R*)-2,2'-([1,1'-biphenyl]-4,4'-diylbis(azanediyl))bis(carbonyl))bis(piperidine-2,1-diyl))bis(2-oxo-1-phenylethane-2,1-diyl))dicarbamate (15). Yield 23 mg (15%). ¹H NMR (DMSO-*d*₆, δ = 2.5 ppm, 400 MHz): 9.98-9.84 (s, 2H), 7.84-7.28 (m, 20H), 5.72-5.64 (m, 2H), 5.16/4.85 (m, 2H), 4.45/3.75 (m, 2H), 3.55 (app br s, 6H), 3.17/2.83 (m, 2H), 2.15 (m, 2H), 1.76 (m, 2H), 1.63-1.23 (m, 8H). ¹³C NMR (DMSO-*d*₆, δ = 39.52 ppm, 100 MHz): 170.0, 169.3, 168.5, 156.2, 138.0, 137.2, 134.5, 128.6, 128.4, 128.2, 127.7, 126.5, 120.2, 119.7, 67.0, 55.5, 52.8, 51.6, 43.2, 27.5, 25.1, 24.6, 19.7. HRMS: Anal. calcd. for [M+H]⁺ C₄₄H₄₈N₆O₈: 789.3606; found 789.3605.

Dimethyl ((1*R*,1'*R*)-((2*S*,2'*S*)-2,2'-([1,1'-biphenyl]-4,4'-diylbis(azanediyl))bis(carbonyl))bis(2-methylpyrrolidine-2,1-diyl))bis(2-oxo-1-phenylethane-2,1-diyl))dicarbamate (16). Yield 77 mg (41%). ¹H NMR (DMSO-*d*₆, δ = 2.5 ppm, 400 MHz): 9.03 (s, 1H), 8.89 (s, 1H), 7.77-7.57 (m, 10H), 7.40-7.32 (m, 10H), 5.46 (m, 2H), 3.99 (m, 1H), 3.76 (m, 1H), 3.56 (s, 3H), 3.54 (s, 3H), 3.48 (m, 1H), 3.21 (m, 1H), 2.18-2.08 (m, 2H), 1.91-1.80 (m, 6H), 1.55 (s, 3H), 1.43 (s, 3H). ¹³C NMR (DMSO-*d*₆, δ = 39.52 ppm, 100 MHz): 171.8, 171.7, 168.2, 167.7, 156.4, 156.2, 138.2, 138.0, 137.2, 136.5, 134.7, 134.3, 128.7, 128.4, 128.22, 128.17, 127.70, 127.68, 126.09, 126.05, 120.9, 120.3, 67.6, 67.5, 57.2, 57.0, 51.7, 51.6, 47.7, 47.5, 23.5, 23.1, 20.6, 20.5. HRMS: Anal. calcd. for [M+H]⁺ C₄₄H₄₈N₆O₈: 789.3606; found 789.3600.

(2*S*,2'*S*)-Di-*tert*-butyl 2,2'-(((3,3'-dimethyl-[1,1'-biphenyl]-4,4'-diyl))bis(azanediyl))bis(carbonyl))bis(pyrrolidine-1-carboxylate) (17). A mixture of *N*-Boc-L-proline (9.47 g, 44.0 mmol), EDC (9.97 g, 52.0 mmol), and *ortho*-tolidine (4.25 g, 20.0 mmol) in CH₂Cl₂ (30 mL) was stirred at ambient temperature for 2 h. The resulting residue was partitioned between CH₂Cl₂ and H₂O. The organic layer was washed with 1.0 N aq HCl solution and brine, dried over MgSO₄, filtered, and concentrated in vacuo. Without any purification, **3** was obtained as a solid (11.3 g, 93%). ¹H NMR (DMSO-*d*₆, δ = 2.5 ppm, 400 MHz): 9.35 (d, 2H), 7.51 (s, 2H), 7.48-7.42 (m, 4H), 4.34 (m, 2H), 3.45 (m, 2H), 3.55 (m, 2H), 2.17 (s, 6H), 2.16 (m, 2H), 1.94-1.81 (m, 6H), 1.42-1.37 (app br s, 18H). ¹³C NMR (DMSO-*d*₆, δ = 39.52 ppm, 100 MHz): 171.4, 153.3, 138.5, 135.4, 132.2, 128.3, 125.3, 124.0, 78.5, 59.9, 46.6, 31.4, 28.1, 23.3, 17.9. HRMS: Anal. calcd. for [M+H]⁺ C₃₄H₄₆N₄O₆: 607.3490; found 607.3480.

(2*S*,2'*S*)-Di-*tert*-butyl 2,2'-(((2,2'-bis(trifluoromethyl)-[1,1'-biphenyl]-4,4'-diyl))bis(azanediyl))bis(carbonyl))bis(pyrrolidine-1-carboxylate) (18). Yield 4.3 g (96%). ¹H NMR (DMSO-*d*₆, δ = 2.5 ppm, 400 MHz): 10.44 (d, 2H), 8.21 (s, 1H), 8.14(s, 1H), 7.92-7.82 (dd, 2H), 7.33(m, 2H), 4.26 (m, 2H), 3.50-3.38

(m, 4H), 2.22 (m, 2H), 1.94-1.80 (m, 6H), 1.42 (s, 9H), 1.30 (s, 9H). ¹³C NMR (DMSO-*d*₆, δ = 39.52 ppm, 100 MHz): 171.9, 171.6, 153.8, 153.2, 139.0, 132.0, 131.0, 128.19, 128.15, 127.9, 124.9, 122.1, 121.2, 121.0, 116.34, 116.28, 116.2, 116.1, 78.7, 78.6, 60.5, 60.1, 54.1, 46.6, 46.4, 31.0, 29.9, 27.8, 27.7, 24.0, 23.3. ¹⁹F NMR (DMSO-*d*₆, 377 MHz): δ -57.37. HRMS: Anal. calcd. for [M+H]⁺ C₃₄H₄₀F₆N₄O₆: 715.2925; found 715.2919.

(2*S*,2'*S*)-Di-*tert*-butyl 2,2'-(((2,2'-dimethyl-[1,1'-biphenyl]-4,4'-diyl)bis(azanediyl))bis(carbonyl))bis(pyrrolidine-1-carboxylate) (19). Yield 2.75 g (96%). ¹H NMR (DMSO-*d*₆, δ = 2.5 ppm, 400 MHz): 9.97 (s, 2H), 7.57-7.41 (m, 4H), 6.97 (app br s, 2H), 4.26 (m, 2H), 3.42-3.35 (m, 4H), 2.21 (m, 2H), 1.97 (s, 6H), 1.89-1.78 (m, 6H), 1.40-1.31 (app br s, 18H). ¹³C NMR (DMSO-*d*₆, δ = 39.52 ppm, 100 MHz): 171.4, 171.0, 153.6, 153.2, 138.0, 138.0, 135.69, 135.65, 129.52, 120.48, 120.47, 120.4, 120.3, 116.7, 116.5, 78.6, 78.4, 60.3, 60.0, 46.7, 46.5, 31.3, 31.1, 30.2, 28.1, 28.0, 23.9, 23.3, 19.7. HRMS: Anal. calcd. for [M+H]⁺ C₃₄H₄₆N₄O₆: 607.3490; found 607.3489.

(2*S*,2'*S*)-Di-*tert*-butyl 2,2'-(((2,2'-difluoro-[1,1'-biphenyl]-4,4'-diyl)bis(azanediyl))bis(carbonyl))bis(pyrrolidine-1-carboxylate) (20). Yield 2.6 g (93%). ¹H NMR (DMSO-*d*₆, δ = 2.5 ppm, 400 MHz): 10.33 (s, 2H), 7.72-7.68 (m, 2H), 7.46-7.36 (m, 4H), 4.28-4.19 (m, 2H), 3.45-3.32 (m, 4H), 2.22 (m, 2H), 1.99-1.79 (m, 6H), 1.40-1.29 (app br s, 18H). ¹³C NMR (DMSO-*d*₆, δ = 39.52 ppm, 100 MHz): 172.0, 171.6, 160.1, 157.7, 153.6, 153.1, 140.5, 140.4, 131.58, 131.55, 117.0, 116.9, 115.1, 115.0, 106.2, 106.0, 78.74, 78.57, 60.4, 60.1, 46.7, 46.6, 31.0, 30.2, 28.1, 28.0, 24.0, 23.4. ¹⁹F NMR (DMSO-*d*₆, 377 MHz): δ -113.53. HRMS: Anal. calcd. for [M+H]⁺ C₃₂H₄₀F₂N₄O₆: 647.2398; found 647.2887.

(2*S*,2'*S*)-Di-*tert*-butyl 2,2'-(((2,2'-dichloro-[1,1'-biphenyl]-4,4'-diyl)bis(azanediyl))bis(carbonyl))bis(pyrrolidine-1-carboxylate) (21). Yield 2.8 g (95%). ¹H NMR (DMSO-*d*₆, δ = 2.5 ppm, 400 MHz): 10.31 (app br s, 2H),

7.97-7.87 (m, 2H), 7.63-7.52 (m, 2H), 7.29-7.25 (m, 2H), 4.29-4.20 (m, 2H), 3.47-3.41 (m, 2H), 3.38-3.32 (m, 2H), 2.25-2.19 (m, 2H), 1.92-1.82 (m, 6H), 1.41-1.31 (app br s, 18H). ^{13}C NMR (DMSO- d_6 , δ = 39.52 ppm, 100 MHz): 171.9, 171.5, 153.6, 153.1, 139.9, 132.5, 132.0, 131.6, 119.2, 117.6, 78.7, 78.5, 60.4, 60.1, 46.7, 46.5, 31.3, 31.0, 30.1, 28.1, 28.0, 23.9, 23.3. HRMS: Anal. calcd. for $[\text{M}+\text{H}]^+$ $\text{C}_{32}\text{H}_{40}\text{Cl}_2\text{N}_4\text{O}_6$: 647.2398; found 647.2394.

(2*S*,2'*S*)-Di-*tert*-butyl 2,2'-(((2,2'-dibromo-[1,1'-biphenyl]-4,4'-diyl)bis(azanediyl))bis(carbonyl))bis(pyrrolidine-1-carboxylate) (22). Yield 990 mg (92%). ^1H NMR (DMSO- d_6 , δ = 2.5 ppm, 400 MHz): 10.26 (s, 2H), 8.12-8.01 (m, 2H), 7.66-7.55 (m, 2H), 7.23 (app br s, 2H), 4.26-4.20 (m, 2H), 3.39-3.35 (m, 4H), 2.22 (m, 2H), 1.89-1.81 (m, 6H), 1.40-1.30 (app br s, 18H). ^{13}C NMR (DMSO- d_6 , δ = 39.52 ppm, 100 MHz): 172.0, 171.6, 153.7, 153.1, 139.9, 135.9, 131.4, 123.0, 122.3, 122.2, 118.2, 118.1, 78.8, 78.6, 60.5, 60.2, 46.8, 46.6, 31.0, 30.2, 28.2, 28.0, 24.0, 23.4. HRMS: Anal. calcd. for $[\text{M}+\text{H}]^+$ $\text{C}_{32}\text{H}_{40}\text{Br}_2\text{N}_4\text{O}_6$: 735.1387; found 735.1373.

Dimethyl ((1*R*,1'*R*)-((2*S*,2'*S*)-2,2'-(((3,3'-dimethyl-[1,1'-biphenyl]-4,4'-diyl)bis(azanediyl))bis(carbonyl))bis(pyrrolidine-2,1-diyl))bis(2-oxo-1-phenylethane-2,1-diyl))dicarbamate (23). Compound **3** (144 mg, 0.238 mmol) in $\text{CF}_3\text{CO}_2\text{H}$ (1 mL) and CH_2Cl_2 (1 mL) was stirred at room temperature for 5 h. The volatile component was removed in vacuo, EDCI (119 mg, 0.620 mmol), and **9** (100 mg, 0.572 mmol) were added in batches over 4 min to a solution of *i*-Pr₂NEt (208 μL , 1.192 mmol) in CH_2Cl_2 (1 mL). The reaction mixture was stirred at room temperature for 75 min. The residue was divided between CH_2Cl_2 and H_2O . The organic layer was washed with H_2O and brine, dried over MgSO_4 , filtered, and concentrated in vacuo. A silica gel mesh was prepared from the residue and submitted to flash chromatography (silica gel: EtOAc/hexane as eluent) to provide **11** as a white solid (77 mg, 41%). ^1H NMR (DMSO- d_6 , δ = 2.5 ppm, 400 MHz): 9.31 (s, 2H), 7.74 (d, 2H), 7.54-7.23 (m, 16H), 5.52 (d, 2H), 4.52 (m, 2H), 3.85 (m, 2H), 3.52 (s, 6H), 3.18 (m, 2H), 2.28

(s, 6H), 2.00-1.82 (m, 8H). ^{13}C NMR (DMSO- d_6 , δ = 39.52 ppm, 100 MHz): 170.1, 168.8, 156.1, 137.1, 136.5, 135.4, 132.2, 128.6, 128.2, 128.1, 128.0, 125.2, 123.9, 60.6, 56.8, 51.6, 46.9, 29.1, 24.3, 17.9. HRMS: Anal. calcd. for $[\text{M}+\text{H}]^+$ $\text{C}_{44}\text{H}_{48}\text{N}_6\text{O}_8$: 789.3606; found 789.3597.

Dimethyl ((1*R*,1'*R*)-((2*S*,2'*S*)-2,2'-(((2,2'-bis(trifluoromethyl)-[1,1'-biphenyl]-4,4'-diyl)bis(azanediyl))bis(carbonyl))bis(pyrrolidine-2,1-diyl))bis(2-oxo-1-phenylethane-2,1-diyl))dicarbamate (24). Yield 145 mg (32%). ^1H NMR (DMSO- d_6 , δ = 2.5 ppm, 400 MHz): 10.29 (s, 2H), 8.21 (d, 2H), 7.83 (m, 2H), 7.75 (d, 2H), 7.43-7.05 (m, 12H), 5.51 (d, 2H), 4.41 (m, 2H), 3.85 (app br s, 2H), 3.54 (s, 6H), 3.20 (app br d, 2H), 2.06-1.82 (m, 8H). ^{13}C NMR (DMSO- d_6 , δ = 39.52 ppm, 100 MHz): 171.26, 168.75, 156.42, 139.30, 137.16, 132.79, 131.36, 128.89, 128.35, 128.25, 125.07, 122.88, 121.81, 116.37, 61.05, 56.97, 51.87, 47.22, 29.45, 24.51. ^{19}F NMR (DMSO- d_6 , 377 MHz): δ -57.28. HRMS: Anal. calcd. for $[\text{M}+\text{H}]^+$ $\text{C}_{44}\text{H}_{42}\text{F}_6\text{N}_6\text{O}_8$: 897.3041; found 897.3046.

Dimethyl ((1*R*,1'*R*)-((2*S*,2'*S*)-2,2'-(((2,2'-dimethyl-[1,1'-biphenyl]-4,4'-diyl)bis(azanediyl))bis(carbonyl))bis(pyrrolidine-2,1-diyl))bis(2-oxo-1-phenylethane-2,1-diyl))dicarbamate (25). Yield 292 mg (73%). ^1H NMR (DMSO- d_6 , δ = 2.5 ppm, 400 MHz): 9.84 (s, 2H), 7.73 (d, 2H), 7.59 (s, 2H), 7.48-7.14 (m, 12H), 6.87 (d, 2H), 5.51 (d, 2H), 4.42 (m, 2H), 3.84 (m, 2H), 3.55 (s, 6H), 3.20 (m, 2H), 1.98 (s, 6H), 1.97-1.78 (m, 8H). ^{13}C NMR (DMSO- d_6 , δ = 39.52 ppm, 100 MHz): 170.2, 168.4, 156.1, 137.9, 137.1, 135.8, 135.8, 129.58, 128.62, 128.1, 127.9, 120.5, 116.7, 60.7, 56.8, 51.7, 47.0, 29.4, 24.3, 19.8. HRMS: Anal. calcd. for $[\text{M}+\text{H}]^+$ $\text{C}_{44}\text{H}_{48}\text{N}_6\text{O}_8$: 789.3606; found 789.3605.

Dimethyl ((1*R*,1'*R*)-((2*S*,2'*S*)-2,2'-(((2,2'-difluoro-[1,1'-biphenyl]-4,4'-diyl)bis(azanediyl))bis(carbonyl))bis(pyrrolidine-2,1-diyl))bis(2-oxo-1-phenylethane-2,1-diyl))dicarbamate (26). Yield 134 mg (40%). ^1H NMR (DMSO- d_6 , δ = 2.5 ppm, 400 MHz): 10.43 (s, 2H), 7.74-7.71 (m, 3H), 7.46-

7.11 (m, 15H), 5.51 (d, 2H), 4.43 (m, 2H), 3.83 (m, 2H), 3.54 (s, 6H), 3.19 (m, 2H), 2.05-1.77 (m, 8H). ^{13}C NMR (DMSO- d_6 , δ = 39.52 ppm, 100 MHz): 170.8, 168.4, 160.0, 158.0, 156.1, 140.5, 137.2, 131.6, 128.6, 128.5, 128.1, 127.9, 127.6, 117.1, 115.1, 106.3, 106.1, 60.8, 56.7, 51.7, 47.0, 29.3, 24.3. ^{19}F NMR (DMSO- d_6 , 377 MHz): δ -73.45. HRMS: Anal. calcd. For $[\text{M}+\text{H}]^+$ $\text{C}_{42}\text{H}_{42}\text{F}_2\text{N}_6\text{O}_8$: 797.3105; found 797.3112.

Dimethyl ((1*R*,1'*R*)-((2*S*,2'*S*)-2,2'-(((2,2'-dichloro-[1,1'-biphenyl]-4,4'-diyl)bis(azanediyl))bis(carbonyl))bis(pyrrolidine-2,1-diyl))bis(2-oxo-1-phenylethane-2,1-diyl))dicarbamate (27). Yield 146 mg (44%). ^1H NMR (DMSO- d_6 , δ = 2.5 ppm, 400 MHz): 10.14 (s, 2H), 7.97-7.91 (m, 2H), 7.75 (d, 2H), 7.65-7.55 (m, 2H), 7.43-7.12 (m, 12H), 5.51 (d, 2H), 4.39 (m, 2H), 3.84 (m, 2H), 3.55 (s, 6H), 3.20 (m, 2H), 2.06-1.79 (m, 8H). ^{13}C NMR (DMSO- d_6 , δ = 39.52 ppm, 100 MHz): 170.8, 168.5, 156.2, 139.9, 137.1, 132.6, 132.1, 131.7, 128.6, 128.1, 127.9, 119.3, 117.7, 60.8, 56.73, 51.68, 47.0, 29.3, 24.3. HRMS: Anal. calcd. for $[\text{M}+\text{H}]^+$ $\text{C}_{42}\text{H}_{42}\text{Cl}_2\text{N}_6\text{O}_8$: 829.2514; found 829.2518.

Dimethyl ((1*R*,1'*R*)-((2*S*,2'*S*)-2,2'-(((2,2'-dibromo-[1,1'-biphenyl]-4,4'-diyl)bis(azanediyl))bis(carbonyl))bis(pyrrolidine-2,1-diyl))bis(2-oxo-1-phenylethane-2,1-diyl))dicarbamate (28). Yield 110 mg (42%). ^1H NMR (DMSO- d_6 , δ = 2.5 ppm, 400 MHz): 10.13 (s, 2H), 8.32-8.12 (m, 2H), 7.92-7.61 (m, 4H), 7.41-7.13 (m, 12H), 5.51 (d, 2H), 4.39 (m, 2H), 3.84 (m, 2H), 3.55 (s, 6H), 3.52 (m, 2H), 3.19 (m, 2H), 2.05-1.81 (m, 8H). ^{13}C NMR (DMSO- d_6 , δ = 39.52 ppm, 100 MHz): 170.7, 168.5, 156.2, 139.8, 137.1, 135.9, 131.3, 128.6, 128.1, 127.9, 123.0, 122.3, 118.1, 60.8, 56.7, 51.7, 47.0, 29.3, 24.3. HRMS: Anal. calcd. for $[\text{M}+\text{H}]^+$ $\text{C}_{42}\text{H}_{42}\text{Br}_2\text{N}_6\text{O}_8$: 917.1504; found 917.1521.

9,9-Difluoro-2,7-dinitro-9H-fluorene (30). 2,7-Nitro-9H-fluorene (100 mg, 0.39 mmol) and *N*-fluorobenzenesulfonimide (NFSI) (369 mg, 1.17 mmol) were dissolved in DMF and cooled to -20°C. LiHMDS (1.0 M in THF, 1.17 mL, 1.17 mmol) was added dropwise over 5 min. After an additional 2 h at 0°C,

TLC indicated the completion of the reaction, and the excess base was quenched by addition of MeOH. The suspension was filtered over Celite and concentrated in vacuo. A silica gel mesh was prepared from the residue and submitted to flash chromatography (silica gel: CH₂Cl₂/hexane as eluent) to provide **30** as a yellow solid (98 mg, 86%). ¹H NMR (DMSO-*d*₆, δ = 2.5 ppm, 400 MHz): 8.63 (d, 2H), 8.53 (d, 1H), 8.56 (d, 1H), 8.36 (s, 1H), 8.34 (s, 1H). ¹³C NMR (DMSO-*d*₆, δ = 39.52 ppm, 100 MHz): 149.1, 142.5, 138.5, 129.2, 144.3, 120.8, 119.6. ¹⁹F NMR (DMSO-*d*₆, 377 MHz,): δ -110.3.

9,9-Dimethyl-2,7-dinitro-9H-fluorene (31). A mixture of 2,7-nitro-9H-fluorene (100 mg, 0.39 mmol) and NaO*t*-Bu (75 mg, 0.78 mmol) were dissolved in DMF at ice bath under N₂. Then, CH₃I (49 μL, 0.78 mmol) was slowly added to the mixture, and stirred for 2 h. The solution was poured into water and a precipitate was formed. The product was filtered, washed with water, and air-dried. Without any purification, **31** (89 mg, 80%) was obtained as a yellow solid. ¹H NMR (DMSO-*d*₆, δ = 2.5 ppm, 400 MHz): 8.59 (d, 2H), 8.33 (m, 4H), 1.60 (s, 6H). ¹³C NMR (DMSO-*d*₆, δ = 39.52 ppm, 100 MHz): 156.2, 148.1, 142.7, 123.6, 122.9, 118.7, 47.9, 25.6.

9,9-Difluoro-9H-fluorene-2,7-diamine (32). A magnetic stirrer bar, Fe₃O₄ (purchased from Aldrich, 4 mg, 0.015 mmol), and DMF (0.5 mL) were added to an oven-dried Schlenk tube, and the mixture was sonicated in an ultrasound bath for 1 min under argon. Compound **31** (22 mg, 0.075 mmol) and hydrazine monohydrate (29 μL, 0.60 mmol) were then added to the mixture. The reaction mixture was stirred at 80°C under an argon atmosphere until the reaction was completed. After magnetic separation of the catalyst, the organic layer was concentrated in vacuo. The residue was partitioned between CH₂Cl₂ and H₂O. The organic layer was washed with brine, dried over MgSO₄, filtered, and concentrated in vacuo. Without any purification, **32** (17 mg, 98%) was obtained as a yellow solid. ¹H NMR (DMSO-*d*₆, δ = 2.5 ppm, 400 MHz): 7.19 (s, 1H), 7.17 (s, 1H), 6.8 (d, 2H), 6.61 (d, 1H), 6.59(d, 1H), 5.3 (s, 4H). ¹³C NMR

(DMSO-*d*₆, δ = 39.52 ppm, 100 MHz): 148.0, 137.3, 137.1, 127.7, 123.7, 119.8, 116.45, 109.1. ¹⁹F NMR (DMSO-*d*₆, 377 MHz): δ -106.7. HRMS: Anal. calcd. for [M+H]⁺ C₁₃H₁₀F₂N₂: 233.0885; found 233.0885.

9,9-Dimethyl-9H-fluorene-2,7-diamine (33). Yield of 69 mg (98%) was obtained as a yellow solid. ¹H NMR (DMSO-*d*₆, δ = 2.5 ppm, 400 MHz): 7.21 (s, 1H), 7.19 (s, 1H), 6.6 (d, 2H), 6.47 (d, 1H), 6.45 (d, 1H), 4.9 (s, 4H), 1.3 (s, 6H). ¹³C NMR (DMSO-*d*₆, δ = 39.52 ppm, 100 MHz): 153.5, 146.7, 128.4, 118.6, 112.6, 108.5, 45.6, 27.7. HRMS: Anal. calcd. for [M+H]⁺ C₁₅H₁₆N₂: 225.1386; found 225.1383.

2,7-Diamino-9H-fluoren-9-one (35). A mixture of 9H-fluorene-2,7-diamine (294 mg, 1.5 mmol) and Cs₂CO₃ (1.5 g, 4.5 mmol) in DMSO (7 mL) was stirred under an atmosphere of air. When TLC showed that no starting material remained, the solution was poured into water and a precipitate was formed. The product was filtered, washed with water, and air-dried. Without any purification, **35** (239 mg, 76%) was obtained as a solid. ¹H NMR (DMSO-*d*₆, δ = 2.5 ppm, 400 MHz): 7.10 (s, 1H), 7.08 (s, 1H), 6.70 (d, 2H), 6.57 (d, 1H), 6.57 (d, 1H), 5.30 (s, 4H). ¹³C NMR (DMSO-*d*₆, δ = 39.52 ppm, 100 MHz): 194.9, 148.2, 134.6, 133.3, 119.9, 118.6, 109.7. HRMS: Anal. calcd. for [M+H]⁺ C₁₃H₁₀N₂O: 211.0866; found 211.0867.

(2*S*,2'*S*)-Di-tert-butyl 2,2'-(((9H-fluorene-2,7-diyl)bis(azanediyl))bis(carbonyl))bis(pyrrolidine-1-carboxylate) (36). A mixture of *N*-Boc-L-proline (323 mg, 1.5 mmol), EDCI (312 mg, 1.63 mmol), and 2,7-diaminofluorene (123 mg, 0.63 mmol) in CH₂Cl₂ (2 mL) was stirred at ambient temperature for 2 h. The resulting residue was partitioned between CH₂Cl₂ and H₂O. The organic layer was washed with 1.0 N aq HCl solution and brine, dried over MgSO₄, filtered, and concentrated in vacuo. Without any purification, **36** was obtained as a solid (359 mg, 97%). ¹H NMR (DMSO-*d*₆, δ = 2.5 ppm, 400 MHz): 10.0 (d, 2H), 7.69 (d, 2H), 7.72 (d, 2H), 7.57-7.51 (m,

2H), 4.31-4.21 (m, 2H), 3.88 (s, 2H), 3.45-3.37 (m, 4H), 2.23 (m, 2H), 1.94-1.80 (m, 6H), 1.41 (app br s, 9H), 1.29 (app br s, 9H). ^{13}C NMR (DMSO- d_6 , δ = 39.52 ppm, 100 MHz): 171.4, 153.2, 143.5, 137.6, 136.3, 119.5, 118.0, 116.1, 78.6, 78.5, 60.4, 46.6, 31.1, 28.2, 28.0, 24.0, 23.4. HRMS: Anal. calcd. for $[\text{M}+\text{H}]^+ \text{C}_{33}\text{H}_{42}\text{N}_4\text{O}_6$: 591.3177; found 591.3168.

(2*S*,2'*S*)-di-*tert*-butyl 2,2'-(((9-oxo-9*H*-fluorene-2,7-diyl)bis(azanediyl))bis(carbonyl))bis(pyrrolidine-1-carboxylate) (37). Yield 131 mg (91%). ^1H NMR (DMSO- d_6 , δ = 2.5 ppm, 400 MHz): 10.24 (s, 2H), 7.91 (m, 2H), 7.91 (m, 2H), 7.62 (m, 2H), 4.26-4.16 (m, 2H), 3.46-3.40 (m, 2H), 3.37-3.31 (m, 2H), 2.24-2.16 (m, 2H), 1.94-1.76 (m, 6H), 1.40 (app br s, 9H), 1.27 (app br s, 9H). ^{13}C NMR (DMSO- d_6 , δ = 39.52 ppm, 100 MHz): 192.9, 171.9, 171.4, 153.6, 153.1, 139.6, 138.8, 134.2, 125.0, 121.1, 115.0, 78.8, 78.6, 60.5, 60.1, 46.6, 46.1, 31.0, 30.2, 28.2, 28.0, 24.0, 23.4. HRMS: Anal. calcd. for $[\text{M}+\text{H}]^+ \text{C}_{33}\text{H}_{40}\text{N}_4\text{O}_7$: 605.2970; found 605.2980.

(2*S*,2'*S*)-di-*tert*-butyl 2,2'-(((9,9-dimethyl-9*H*-fluorene-2,7-diyl)bis(azanediyl))bis(carbonyl))bis(pyrrolidine-1-carboxylate) (38). Yield 201 mg (97%). ^1H NMR (DMSO- d_6 , δ = 2.5 ppm, 400 MHz): 10.10 (app br s, 2H), 7.84 (s, 1H), 7.79 (s, 1H), 7.66 (d, 2H), 7.51 (t, 2H), 4.31-4.28 (m, 1H), 4.24-4.21 (m, 1H), 3.44-3.40 (m, 2H), 3.37-3.31 (m, 2H), 2.21-2.16 (m, 2H), 1.95-1.80 (m, 6H), 1.40 (app br s, 9H), 1.34 (s, 6H), 1.28 (app br s, 9H). ^{13}C NMR (DMSO- d_6 , δ = 39.52 ppm, 100 MHz): 174.3, 173.9, 171.4, 171.0, 153.6, 153.2, 138.1, 138.0, 133.7, 133.6, 119.7, 118.4, 118.2, 113.8, 113.6, 78.6, 78.5, 60.4, 60.0, 46.6, 46.1, 42.2, 42.1, 31.0, 30.3, 28.2, 28.1, 27.9, 27.1, 24.0, 23.4. HRMS: Anal. calcd. for $[\text{M}+\text{H}]^+ \text{C}_{35}\text{H}_{42}\text{N}_4\text{O}_6$: 619.3490; found 619.3496.

(2*S*,2'*S*)-Di-*tert*-butyl 2,2'-(((9,9-difluoro-9*H*-fluorene-2,7-diyl)bis(azanediyl))bis(carbonyl))bis(pyrrolidine-1-carboxylate) (39). Yield 28 mg (95%). ^1H NMR (DMSO- d_6 , δ = 2.5 ppm, 400 MHz): 10.29 (app br s, 2H), 8.06 (s, 1H), 8.02 (s, 1H), 7.69-7.66 (m, 4H), 4.30-4.25 (m, 1H), 4.21-4.18

(m, 1H), 3.45-3.41 (m, 2H), 3.37-3.34 (m, 2H), 2.23-2.16 (m, 2H), 1.92-1.80 (m, 6H), 1.40 (app br s, 9H), 1.27 (app br s, 9H). ^{13}C NMR (DMSO- d_6 , δ = 39.52 ppm, 100 MHz): 174.3, 173.9, 171.9, 171.5, 153.6, 153.1, 139.4, 133.56, 133.49, 122.8, 122.7, 121.2, 114.5, 114.4, 78.8, 78.6, 60.5, 59.3, 58.6, 46.6, 46.2, 46.1, 31.0, 30.3, 28.2, 28.0, 27.9, 27.7, 24.0, 23.4. ^{19}F NMR (DMSO- d_6 , 377 MHz,): δ -108.9, -109.0. HRMS: Anal. calcd. for $[\text{M}+\text{H}]^+$ $\text{C}_{33}\text{H}_{40}\text{F}_2\text{N}_4\text{O}_6$: 627.2989; found 627.2997.

Dimethyl ((1*R*,1'*R*)-((2*S*,2'*S*)-2,2'-(((9*H*-fluorene-2,7-diyl)bis(azanediyl))bis(carbonyl))bis(pyrrolidine-2,1-diyl))bis(2-oxo-1-phenylethane-2,1-diyl))dicarbamate (40). A mixture of biphenyl **36** (300 mg, 0.51 mmol) in $\text{CF}_3\text{CO}_2\text{H}$ (2 mL) and CH_2Cl_2 (2 mL) was stirred at room temperature for 5 h. The volatile component was removed in vacuo. EDCI (253 mg, 1.3 mmol) and **9** (255 mg, 1.3 mmol) were added in batches over 4 min to a solution of *i*-Pr₂NEt (441 μL , 2.5 mmol) in CH_2Cl_2 (2 mL), and the reaction mixture was stirred at room temperature for 75 min. The residue was partitioned between CH_2Cl_2 and H_2O . The organic layer was washed with H_2O and brine, dried over MgSO_4 , filtered, and concentrated in vacuo. A silica gel mesh was prepared from the residue and submitted to flash chromatography (silica gel: EtOAc/hexane as eluent) to provide **40** as a white solid (198 mg, 50%). ^1H NMR (DMSO- d_6 , δ = 2.5 ppm, 400 MHz): 9.92 (s, 2H), 7.91 (s, 2H), 7.75-7.69 (m, 4H), 7.56 (d, 2H), 7.44-7.13 (m, 10H), 5.52 (d, 2H), 4.43 (m, 2H), 3.88-3.83 (m, 2H), 3.55 (s, 6H), 3.21 (m, 2H), 2.04-1.78 (m, 8H). ^{13}C NMR (DMSO- d_6 , δ = 39.52 ppm, 100 MHz): 170.2, 168.5, 156.2, 143.6, 137.5, 137.2, 136.4, 128.7, 128.1, 127.9, 119.6, 118.1, 116.2, 60.8, 56.8, 51.7, 47.0, 36.7, 29.4, 24.3. HRMS: Anal. calcd. for $[\text{M}+\text{H}]^+$ $\text{C}_{43}\text{H}_{44}\text{N}_6\text{O}_8$: 773.3293; found 773.3296.

Dimethyl ((1*R*,1'*R*)-((2*S*,2'*S*)-2,2'-(((9-oxo-9*H*-fluorene-2,7-diyl)bis(azanediyl))bis(carbonyl))bis(pyrrolidine-2,1-diyl))bis(2-oxo-1-phenylethane-2,1-diyl))dicarbamate (41). Yield 12 mg (66%). ^1H NMR (DMSO- d_6 , δ = 2.5 ppm, 400 MHz): 10.10 (s, 2H), 7.91 (s, 2H), 7.76 (t, 4H),

7.64 (d, 2H), 7.43-7.10 (m, 10H), 5.51 (d, 2H), 4.39 (m, 2H), 3.85 (m, 2H), 3.55 (s, 6H), 3.20 (m, 2H), 2.05-1.79 (m, 8H). ^{13}C NMR (DMSO- d_6 , δ = 39.52 ppm, 100 MHz): 192.8, 170.6, 168.5, 156.2, 139.5, 138.8, 137.1, 134.2, 128.6, 128.1, 127.9, 125.0, 121.1, 115.0, 60.8, 56.7, 51.7, 47.0, 29.3, 24.3. HRMS: Anal. calcd. for $[\text{M}+\text{H}]^+ \text{C}_{43}\text{H}_{42}\text{N}_6\text{O}_9$: 787.3086; found 787.3089.

Dimethyl ((1*R*,1'*R*)-((2*S*,2'*S*)-2,2'-(((9,9-dimethyl-9*H*-fluorene-2,7-diyl))bis(azanediyl))bis(carbonyl))bis(pyrrolidine-2,1-diyl))bis(2-oxo-1-phenylethane-2,1-diyl))dicarbamate (42). Yield 135 mg (53%). ^1H NMR (DMSO- d_6 , δ = 2.5 ppm, 400 MHz): 9.96 (s, 2H), 7.86 (s, 2H), 7.74 (d, 2H), 7.69 (d, 2H), 7.51 (dd, 2H), 7.43-7.10 (m, 10H), 5.52 (d, 2H), 4.43 (m, 2H), 3.83 (m, 2H), 3.55 (s, 6H), 3.20 (m, 2H), 2.05-1.78 (m, 8H), 1.41 (s, 6H). ^{13}C NMR (DMSO- d_6 , δ = 39.52 ppm, 100 MHz): 170.1, 168.3, 156.1, 153.7, 138.0, 137.2, 133.7, 128.6, 128.1, 127.8, 119.8, 118.3, 113.7, 60.7, 56.7, 51.6, 47.0, 46.5, 29.3, 27.2, 24.3. HRMS: Anal. calcd. for $[\text{M}+\text{H}]^+ \text{C}_{45}\text{H}_{48}\text{N}_6\text{O}_8$: 801.3606; found 801.3611.

Dimethyl ((1*R*,1'*R*)-((2*S*,2'*S*)-2,2'-(((9,9-difluoro-9*H*-fluorene-2,7-diyl))bis(azanediyl))bis(carbonyl))bis(pyrrolidine-2,1-diyl))bis(2-oxo-1-phenylethane-2,1-diyl))dicarbamate (43). Yield 18 mg (52%). ^1H NMR (DMSO- d_6 , δ = 2.5 ppm, 400 MHz): 10.14 (s, 2H), 8.05 (s, 2H), 7.77 (d, 2H), 7.71 (s, 4H), 7.43-7.10 (m, 10H), 5.51 (d, 2H), 4.39 (m, 2H), 3.85 (m, 2H), 3.55 (s, 6H), 3.21 (m, 2H), 2.06-1.79 (m, 8H). ^{13}C NMR (DMSO- d_6 , δ = 39.52 ppm, 100 MHz): 170.6, 168.5, 156.2, 139.3, 137.3, 137.0, 128.6, 128.4, 128.1, 127.9, 127.6, 122.8, 121.2, 114.5, 60.8, 56.7, 51.6, 47.0, 29.3, 24.3. HRMS: Anal. calcd. for $[\text{M}+\text{H}]^+ \text{C}_{43}\text{H}_{42}\text{F}_2\text{N}_6\text{O}_8$: 809.3105; found 809.3109.

Biological Studies

1. Measurement of the anti-HCV activities of compounds using HCVcc

- Cell line and cell culture

Huh 7.5.1 cells were grown in Dulbecco's Modified Eagle's medium (DMEM; Gibco) supplemented with antibiotics (100 U/mL penicillin, 10 µg/mL streptomycin) and 10% heat-inactivated fetal bovine serum (ΔFBS; Thermo) at 37°C in a humidified 6.0% CO₂ incubator.

- Virus production

In vitro transcription and RNA electroporation were performed as described in the previous report.¹⁰¹ *In vitro* transcribed RNA of JFH5a-Rluc-ad34, which is a derivative of JFH1 with adaptive mutations in the E2 and p7 regions,²⁸ was transfected into Huh7.5.1 cells by electroporation. JFH5a-Rluc-ad34 virus contains a reporter *Renilla* luciferase (Rluc) for convenient assay of virus proliferation.²⁸ Cell culture media containing HCV were collected 3~5 days after electroporation and then filtered through a 0.45 µm pore size filter.

- Antiviral activity test with infectious HCV particles

Huh 7.5.1 cells were inoculated with a JFH5a-Rluc-ad34 virus stock and cultivated for 3 h. At 3 h after the virus inoculation, HCV-infected Huh7.5.1 cells were cultivated with media containing serially diluted compounds. At 3 days after chemical treatment (All of the compounds purity were 92% at least), the cells were harvested and luciferase activities in the cells were measured using a *Renilla* luciferase assay system (Promega) according to the manufacturer's direction. Finally the luciferase activities were normalized to those obtained from mock-treated cells.

2. Measurement of anti-HCV activities of compounds using HCV replicon

- Cell line and cell culture

Huh 7.5.1 cells containing a bicistronic HCV replicon NK/R2AZ (genotype 1b) were used to test the anti-HCV activities of the compounds (Figure I-6). The first and second open reading frames (ORFs) of the replicon contain the

Renilla luciferase gene fused with the neomycin phosphotransferase gene and the HCV nonstructural genes NS3-5, respectively. The replicon-containing cells were cultivated under the same conditions as described above with an additional antibiotic G418 (0.5 mg/ml, Calbiochem).

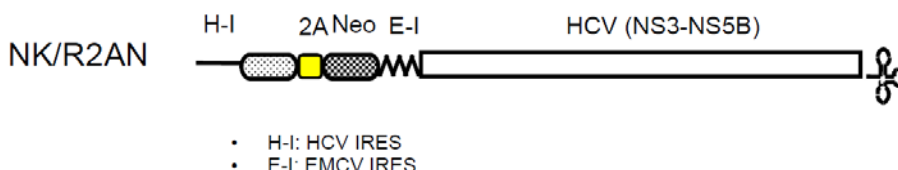


Figure I-6. The structure of replicon NK/R2AN

- Antiviral activity assay test with HCV replicon

Huh 7.5.1 cells containing HCV replicon (NK/R2AN) were plated on a 12-well plate (5×10^4 cells per well). At 16 h after cultivation, NK/R2AN-containing cells were incubated with media containing serially diluted compounds for 3 days. After the chemical treatment, the cells were harvested and luciferase activities were measured. Luciferase activities were measured using the *Renilla* luciferase assay system (Promega) according to the manufacturer's direction, and then normalized to those obtained from mock-treated cells.

3. Observation of the effects of co-treatment of two compounds

Huh 7.5.1 cells containing HCV replicon (NK/R2AN) were plated on a 12-well plate (5×10^4 cells per well). At 16 h after cultivation, NK/R2AN cells were treated with serially diluted compounds in the presence of 123 nM of sofosbuvir (EC_{30}). At 3 days after treatment, luciferase activities were measured using the *Renilla* luciferase assay system (Promega) according to the manufacturer's direction.

4. Observation of the effects of compounds on drug-resistant HCV mutants

We selected HCV mutants showing resistance against BMK-20113 by continuous cultivation of Huh 7.5.1 cells containing HCV replicon NK/R2AN in the presence of BMK-20113. We found that the majority of mutants had mutations at the N-terminal region of NS5A protein (L31V and/or Y93H in NS5A) similarly to the daclatasvir resistant mutants described previously.^{96,102} We used NK/R2AN derivatives containing single mutations (L31V or Y93H in NS5A) to investigate the drug resistance of lead compounds. Briefly, Huh 7.5.1 cells were electroporated with RNAs containing resistant mutations and cultivated on 12-well plates. At 4 h after transfection, media were replaced with DMEM containing serially diluted compounds and further cultivated. At 3 days after compound treatment, the cells were harvested and luciferase activities were measured. Luciferase activities were normalized to those obtained from mock-treated cells.

5. hERG ligand binding assay⁸²

The hERG ligand binding assay was performed by using the hERG Fluorescence Polarization Assay Kit (Cat No. PV5365), containing predictorTM hERG tracer red, predictorTM hERG membrane, and predictorTM hERG FP assay buffer. Test compounds (10 μ M) and positive control (Astemizole) were added to the 384-well plate (5 μ L each; low-volume polystyrene plate, corning #3677). Then, 10 μ L of membrane and 5 μ L of tracer were added to each plate by using a multi-pipette (Multi 16 channel pipette type 5–50 μ L, Thermo). The plate was then covered with aluminum foil and was kept for 2–3 h at room temperature. Lastly, the fluorescence polarization of the hERG red tracer was measured using a microplate reader (molecular devices, SpectraMax M5e, excitation (540 nm) emission (585 nm) filters).

6. Plasma stability measurement

Rat plasma (297 μ L) was pre-incubated for 5 min at 37°C in a water bath. The plasma and 100 μ M test compounds (3 μ L) were mixed using a vortex, and

incubated for 37°C in a water bath. Then the mixture was sampled multiple times (0, 15, 30, 60, and 120 min). A mixture of crude sample (50 µL) and acetonitrile (100 µL) was then treated by centrifugation at 10,000 rpm for 10 min at 25°C. Finally, supernatant was isolated and analyzed using a LC-MS/MS.

7. Method to determine stability in rat and human liver microsomes⁸⁴

The metabolic stability of the compounds was evaluated in pooled rat (BD Gentest® Cat No. 452501) or human livers (BD GentestCat. 452161) microsomal fractions with β-NADPH over 30 m using 1 µM of compounds. The compounds in the supernatants were analyzed by LC-MS/MS.

8. Method of CYP₄₅₀ Inhibition

The interaction of human cytochrome CYP450 with compounds was studied on a cytochrome panel consisting of CYP1A2, CYP2C9, CYP2C19, CYP2D6, and CYP3A4 (P450-glo, promega kit) according to the manufacturer's protocols. The inhibition effects were measured at 100, 50, 10, 5, 1, 0.1, and 0.01 µM of compounds using a luminometer (GENios, TECAN).

9. PK study

Pharmacokinetic studies were conducted in a parallel format with 2 male and 1 female Sprague-Dawley rats (supplied by Sippr-BK Lab Animal Ltd., Shanghai, China) for compounds per each dose routes. For Intravenous (IV) dose, administrated via tail vein as a bolus injection by nominal 5 mg/kg as a solution (5% DMSO, 10% solutol, 85% (2-hydroxypropyl)-β-cyclodextrin (HPBCD)). Blood samples were collected into polypropylene tubes containing K2-EDTA as anticoagulant at different time points and stored on wet ice. The samples were centrifuged at 8,000 rpm for 6 min and the plasma samples were determined with LC/MS/MS. Non-compartmental pharmacokinetic analysis was performed with drug and statistics (DAS) 2.1.1 pharmacokinetic program.

10. Ames test⁹⁹

The Ames test of compound was carried out with the Maron's method¹³³ using histidine-dependent strains of *Salmonella typhimurium* (TA98, and TA100). Histidine requiring bacteria of each strain was treated with inhibitor compound **43** at 200 µg/plate and with positive (2-nitrofluorene, sodium azide, and benzo[a]pyrene) and negative controls. The number of colonies was counted three times for each medium to provide acceptable data for statistical analysis.

Reference - Part I.

1. Kim, W. R. *Microbes Infect.* **2002**, *4*, 1219.
2. Negro, F.; Alberti, A. *Liver Int.* **2011**, *31 Suppl 2*, 1.
3. Di Bisceglie, A. M. *Hepatology* **2000**, *31*, 1014.
4. Brillanti, S.; Mazzella, G.; Roda, E. *Dig. Liver Dis.* **2011**, *43*, 425.
5. Sheridan, C. *Nat. Biotechnol.* **2011**, *29*, 553.
6. De Francesco, R.; Migliaccio, G. *Nature* **2005**, *436*, 953.
7. Ishii, S.; Koziel, M. J. *Clin. Immunol.* **2008**, *128*, 133.
8. Jones, D. M.; McLauchlan, J. *J. Biol. Chem.* **2010**, *285*, 22733.
9. Bartenschlager, R.; Penin, F.; Lohmann, V.; Andre, P. *Trends in microbiology* **2011**, *19*, 95.
10. Appel, N.; Pietschmann, T.; Bartenschlager, R. *J. Virol.* **2005**, *79*, 3187.
11. Kim, J.; Lee, D.; Choe, J. *Biochem. Biophys. Res. Commun.* **1999**, *257*, 777.
12. Lim, P. J.; Chatterji, U.; Cordek, D.; Sharma, S. D.; Garcia-Rivera, J. A.; Cameron, C. E.; Lin, K.; Targett-Adams, P.; Gallay, P. A. *J. Biol. Chem.* **2012**, *287*, 30861.
13. Tellinghuisen, T. L.; Marcotrigiano, J.; Rice, C. M. *Nature* **2005**, *435*, 374.
14. Tan, S. L.; Katze, M. G. *Virology* **2001**, *284*, 1.
15. Gao, M.; Nettles, R. E.; Belema, M.; Snyder, L. B.; Nguyen, V. N.; Fridell, R. A.; Serrano-Wu, M. H.; Langley, D. R.; Sun, J. H.; O'Boyle, D. R., 2nd; Lemm, J. A.; Wang, C.; Knipe, J. O.; Chien, C.; Colonno, R. J.; Grasela, D. M.; Meanwell, N. A.; Hamann, L. G. *Nature* **2010**, *465*, 96.
16. Asselah, T. *J. Hepatol.* **2011**, *54*, 1069.
17. Romine, J. L.; St. Laurent, D. R.; Leet, J. E.; Martin, S. W.; Serrano-Wu, M. H.; Yang, F.; Gao, M.; O'Boyle, D. R.; Lemm, J. A.; Sun, J.-H.; Nower, P. T.; Huang, X.; Deshpande, M. S.; Meanwell, N. A.; Snyder, L. B. *ACS Med. Chem. Lett.* **2011**, *2*, 224.
18. Chang, W.; Mosley, R. T.; Bansal, S.; Keilman, M.; Lam, A. M.; Furman, P. A.; Otto, M. J.; Sofia, M. J. *Bioorg. Med. Chem. Lett.* **2012**, *22*, 2938.

19. Lopez, O. D.; Nguyen, V. N.; St. Laurent, D. R.; Belema, M.; Serrano-Wu, M. H.; Goodrich, J. T.; Yang, F.; Qiu, Y.; Ripka, A. S.; Nower, P. T.; Valera, L.; Liu, M.; O'Boyle, D. R.; Sun, J.-H.; Fridell, R. A.; Lemm, J. A.; Gao, M.; Good, A. C.; Meanwell, N. A.; Snyder, L. B. *Bioorg. Med. Chem. Lett.* **2013**, *23*, 779.
20. St. Laurent, D. R.; Belema, M.; Gao, M.; Goodrich, J.; Kakarla, R.; Knipe, J. O.; Lemm, J. A.; Liu, M.; Lopez, O. D.; Nguyen, V. N.; Nower, P. T.; O'Boyle, D.; Qiu, Y.; Romine, J. L.; Serrano-Wu, M. H.; Sun, J.-H.; Valera, L.; Yang, F.; Yang, X.; Meanwell, N. A.; Snyder, L. B. *Bioorg. Med. Chem. Lett.* **2012**, *22*, 6063.
21. St. Laurent, D. R.; Serrano-Wu, M. H.; Belema, M.; Ding, M.; Fang, H.; Gao, M.; Goodrich, J. T.; Krause, R. G.; Lemm, J. A.; Liu, M.; Lopez, O. D.; Nguyen, V. N.; Nower, P. T.; O'Boyle, D. R., II; Pearce, B. C.; Romine, J. L.; Valera, L.; Sun, J.-H.; Wang, Y.-K.; Yang, F.; Yang, X.; Meanwell, N. A.; Snyder, L. B. *J. Med. Chem.* **2014**, *57*, 1976.
22. Schlutter, J. *Nature* **2011**, *474*, S5.
23. Amblard, F.; Zhang, H.; Zhou, L.; Shi, J.; Bobeck, D. R.; Nettles, J. H.; Chavre, S.; McBrayer, T. R.; Tharnish, P.; Whitaker, T.; Coats, S. J.; Schinazi, R. F. *Bioorg. Med. Chem. Lett.* **2013**, *23*, 2031.
24. Zhang, H.; Zhou, L.; Amblard, F.; Shi, J.; Bobeck, D. R.; Tao, S.; McBrayer, T. R.; Tharnish, P. M.; Whitaker, T.; Coats, S. J.; Schinazi, R. F. *Bioorg. Med. Chem. Lett.* **2012**, *22*, 4864.
25. Shi, J.; Zhou, L.; Amblard, F.; Bobeck, D. R.; Zhang, H.; Liu, P.; Bondada, L.; McBrayer, T. R.; Tharnish, P. M.; Whitaker, T.; Coats, S. J.; Schinazi, R. F. *Bioorg. Med. Chem. Lett.* **2012**, *22*, 3488.
26. El-Faham, A.; Albericio, F. *Chem. Rev.* **2011**, *111*, 6557.
27. Gibson, F. S.; Bergmeier, S. C.; Rapoport, H. *J. Org. Chem.* **1994**, *59*, 3216.
28. Kim, C. S.; Keum, S. J.; Jang, S. K. *PloS one* **2011**, *6*, e22808.
29. Belema, M.; Nguyen, V. N.; Serrano-Wu, M.; St. Laurent, D. R.; Qiu, Y.; Ding, M.; Meanwell, N. A.; Snyder, L. B. Preparation of Biarylacetylenes and Biheteroarylacetylenes End-Capped with Amino Acid or Peptide Derivatives as Hepatitis C Virus Inhibitors. World Patent WO-2010039793 A1, April 8,

2010.

30. Bachand, C.; Belema, M.; Deon, D. H.; Good, A. C.; Goodrich, J.; James, C. A.; Lavoie, R.; Lopez, O. D.; Martel, A.; Meanwell, N. A.; Nguyen, V. N.; Romine, J. L.; Ruediger, E. H.; Snyder, L. B.; St. Laurent, D. R.; Yang, F.; Langley, D. R.; Wang, G.; Hamann, L. G. Preparation of Biphenyls and Biheteroaryls End-Capped with Amino Acid or Peptide Derivatives as Hepatitis C Virus Inhibitors. World Patent WO-2008021927 A2/A3, February 21, 2008
31. Stuyver, L. J.; Whitaker, T.; McBrayer, T. R.; Hernandez-Santiago, B. I.; Lostia, S.; Tharnish, P. M.; Ramesh, M.; Chu, C. K.; Jordan, R.; Shi, J.; Rachakonda, S.; Watanabe, K. A.; Otto, M. J.; Schinazi, R. F. *Antimicrob. Agents Chemother.* **2003**, *47*, 244.
32. Horscroft, N.; Lai, V. C. H.; Cheney, W.; Yao, N.; Wu, J. Z.; Hong, Z.; Zhong, W. *Antiviral Chem. Chemother.* **2005**, *16*, 1.
33. Gleeson, M. P. *J. Med. Chem.* **2008**, *51*, 817.
34. Piper, D. R.; Duff, S. R.; Eliason, H. C.; Frazee, W. J.; Frey, E. A.; Fuerstenau-Sharp, M.; Jachec, C.; Marks, B. D.; Pollok, B. A.; Shekhani, M. S.; Thompson, D. V.; Whitney, P.; Vogel, K. W.; Hess, S. D. *Assay Drug Dev. Technol.* **2008**, *6*, 213.
35. Aptula, A. O.; Cronin, M. T. *SAR QSAR Environ. Res.* **2004**, *15*, 399.
36. Funato, K.; Yoda, R.; Kiwada, H. *Biochim. Biophys. Acta Biomem.* **1992**, *1103*, 198.
37. Di, L.; Kerns, E. H.; Hong, Y.; Chen, H. *Int. J. Pharm.* **2005**, *297*, 110.
38. Lewis, D. *Curr. Med. Chem.* **2003**, *10*, 1955.
39. Lok, A. S.; Gardiner, D. F.; Lawitz, E.; Martorell, C.; Everson, G. T.; Ghalib, R.; Reindollar, R.; Rustgi, V.; McPhee, F.; Wind-Rotolo, M.; Persson, A.; Zhu, K.; Dimitrova, D. I.; Eley, T.; Guo, T.; Grasela, D. M.; Pasquinelli, C. *N. Engl. J. Med.* **2012**, *366*, 216.
40. Asselah, T.; Marcellin, P. *Liver Int.* **2011**, *31 Suppl 1*, 68.
41. Belema, M.; Lopez, O. D.; Bender, J. A.; Romine, J. L.; St. Laurent, D. R.; Langley, D. R.; Lemm, J. A.; O'Boyle, D. R., II; Sun, J.-H.; Wang, C.; Fridell,

- R. A.; Meanwell, N. A. *J. Med. Chem.* **2014**, *57*, 1643.
42. Nettles, R. E.; Gao, M.; Bifano, M.; Chung, E.; Persson, A.; Marbury, T. C.; Goldwater, R.; DeMicco, M. P.; Rodriguez-Torres, M.; Vutikullird, A.; Fuentes, E.; Lawitz, E.; Lopez-Talavera, J. C.; Grasele, D. M. *Hepatology* **2011**, *54*, 1956.
43. Pol, S.; Ghalib, R. H.; Rustgi, V. K.; Martorell, C.; Everson, G. T.; Tatum, H. A.; Hezode, C.; Lim, J. K.; Bronowicki, J.-P.; Abrams, G. A.; Braeu, N.; Morris, D. W.; Thuluvath, P. J.; Reindollar, R. W.; Yin, P. D.; Diva, U.; Hindes, R.; McPhee, F.; Hernandez, D.; Wind-Rotolo, M.; Hughes, E. A.; Schnittman, S. *Lancet Infect. Dis.* **2012**, *12*, 671.
44. Belema, M.; Meanwell, N. A. *J. Med. Chem.* **2014**, *57*, 5057.
45. Herbst, D. A.; Reddy, K. R. *Expert Opin. Invest. Drugs* **2013**, *22*, 1337.
46. Belema, M.; Nguyen, V. N.; St. Laurent, D. R.; Lopez, O. D.; Qiu, Y.; Good, A. C.; Nower, P. T.; Valera, L.; O'Boyle, D. R.; Sun, J.-H.; Liu, M.; Fridell, R. A.; Lemm, J. A.; Gao, M.; Knipe, J. O.; Meanwell, N. A.; Snyder, L. B. *Bioorg. Med. Chem. Lett.* **2013**, *23*, 4428.
47. Giroux, S.; Xu, J.; Reddy, T. J.; Morris, M.; Cottrell, K. M.; Cadilhac, C.; Henderson, J. A.; Nicolas, O.; Bilimoria, D.; Denis, F.; Mani, N.; Ewing, N.; Shawgo, R.; L'Heureux, L.; Selliah, S.; Chan, L.; Chauret, N.; Berlioz-Seux, F.; Namchuk, M. N.; Grillot, A. L.; Bennani, Y. L.; Das, S. K.; Maxwell, J. P. *ACS Med. Chem. Lett.* **2014**, *5*, 240.
48. Kwong, A. D. *ACS Med. Chem. Lett.* **2014**, *5*, 214.
49. Tan, S. L.; Pause, A.; Shi, Y.; Sonenberg, N. *Nat. Rev. Drug Discovery* **2002**, *1*, 867.
50. Belema, M.; Nguyen, V. N.; Romine, J. L.; St. Laurent, D. R.; Lopez, O. D.; Goodrich, J. T.; Nower, P. T.; O'Boyle, D. R., II; Lemm, J. A.; Fridell, R. A.; Gao, M.; Fang, H.; Krause, R. G.; Wang, Y.-K.; Oliver, A. J.; Good, A. C.; Knipe, J. O.; Meanwell, N. A.; Snyder, L. B. *J. Med. Chem.* **2014**, *57*, 1995.
51. Coburn, C. A.; Meinke, P. T.; Chang, W.; Fandozzi, C. M.; Graham, D. J.; Hu, B.; Huang, Q.; Kargman, S.; Kozlowski, J.; Liu, R.; McCauley, J. A.; Nomeir, A. A.; Soll, R. M.; Vacca, J. P.; Wang, D.; Wu, H.; Zhong, B.; Olsen, D. B.; Ludmerer, S. W. *ChemMedChem* **2013**, *8*, 1930.

52. Tran, T. D.; Wakenhut, F.; Pickford, C.; Shaw, S.; Westby, M.; Smith-Burchnell, C.; Watson, L.; Paradowski, M.; Milbank, J.; Brimage, R. A.; Halstead, R.; Glen, R.; Wilson, C. P.; Adam, F.; Hay, D.; Chiva, J. Y.; Nichols, C.; Blakemore, D. C.; Gardner, I.; Dayal, S.; Pike, A.; Webster, R.; Pryde, D. C. *ChemMedChem* **2014**, *9*, 1378.
53. Belema, M.; Nguyen, V. N.; Bachand, C.; Deon, D. H.; Goodrich, J. T.; James, C. A.; Lavoie, R.; Lopez, O. D.; Martel, A.; Romine, J. L.; Ruediger, E. H.; Snyder, L. B.; St Laurent, D. R.; Yang, F.; Zhu, J.; Wong, H. S.; Langley, D. R.; Adams, S. P.; Cantor, G. H.; Chimalakonda, A.; Fura, A.; Johnson, B. M.; Knipe, J. O.; Parker, D. D.; Santone, K. S.; Fridell, R. A.; Lemm, J. A.; O'Boyle, D. R., 2nd; Colonna, R. J.; Gao, M.; Meanwell, N. A.; Hamann, L. G. *J. Med. Chem.* **2014**, *57*, 2013.
54. DeGoey, D. A.; Randolph, J. T.; Liu, D.; Pratt, J.; Hutchins, C.; Donner, P.; Krueger, A. C.; Matulenko, M.; Patel, S.; Motter, C. E.; Nelson, L.; Keddy, R.; Tufano, M.; Caspi, D. D.; Krishnan, P.; Mistry, N.; Koev, G.; Reisch, T. J.; Mondal, R.; Pilot-Matias, T.; Gao, Y.; Beno, D. W. A.; Maring, C. J.; Molla, A.; Dumas, E.; Campbell, A.; Williams, L.; Collins, C.; Wagner, R.; Kati, W. M. *J. Med. Chem.* **2014**, *57*, 2047.
55. Ivachtchenko, A. V.; Mitkin, O. D.; Yamanushkin, P. M.; Kuznetsova, I. V.; Bulanova, E. A.; Shevkun, N. A.; Koryakova, A. G.; Karapetian, R. N.; Bichko, V. V.; Trifelenkov, A. S.; Kravchenko, D. V.; Vostokova, N. V.; Veselov, M. S.; Chufarova, N. V.; Ivanenkov, Y. A. *J. Med. Chem.* **2014**, *57*, 7716.
56. Kazmierski, W. M.; Maynard, A.; Duan, M.; Baskaran, S.; Botyanszki, J.; Crosby, R.; Dickerson, S.; Tallant, M.; Grimes, R.; Hamatake, R.; Leivers, M.; Roberts, C. D.; Walker, J. *J. Med. Chem.* **2014**, *57*, 2058.
57. Link, J. O.; Taylor, J. G.; Xu, L.; Mitchell, M.; Guo, H.; Liu, H.; Kato, D.; Kirschberg, T.; Sun, J.; Squires, N.; Parrish, J.; Keller, T.; Yang, Z. Y.; Yang, C.; Matles, M.; Wang, Y.; Wang, K.; Cheng, G.; Tian, Y.; Mogalian, E.; Mondou, E.; Cornpropst, M.; Perry, J.; Desai, M. C. *J. Med. Chem.* **2014**, *57*, 2033.
58. Wakenhut, F.; Tran, T. D.; Pickford, C.; Shaw, S.; Westby, M.; Smith-Burchnell, C.; Watson, L.; Paradowski, M.; Milbank, J.; Stonehouse, D.;

- Cheung, K.; Wybrow, R.; Daverio, F.; Crook, S.; Statham, K.; Leese, D.; Stead, D.; Adam, F.; Hay, D.; Roberts, L. R.; Chiva, J. Y.; Nichols, C.; Blakemore, D. C.; Goetz, G. H.; Che, Y.; Gardner, I.; Dayal, S.; Pike, A.; Webster, R.; Pryde, D. C. *ChemMedChem* **2014**, 9, 1387.
59. http://www.hepmag.com/pdfs/hepatitis_c_drug_list.pdf
60. Bae, I. H.; Choi, J. K.; Chough, C.; Keum, S. J.; Kim, H.; Jang, S. K.; Kim, B. M. *ACS Med. Chem. Lett.* **2014**, 5, 255.
61. Srinivasan, N.; Yurek-George, A.; Ganesan, A. *Mol. Diversity* **2005**, 9, 291.
62. Saroja, G.; Pingzhu, Z.; Ernsting, N. P.; Liebscher, J. *J. Org. Chem.* **2004**, 69, 987.
63. Kim, S.; Kim, E.; Kim, B. M. *Chem. Asian J.* **2011**, 6, 1921.
64. Hamilton, A.; Park, K.; Tsou, L. *Synthesis* **2006**, 2006, 3617.
65. Lindenbach, B. D.; Evans, M. J.; Syder, A. J.; Woelk, B.; Tellinghuisen, T. L.; Liu, C. C.; Maruyama, T.; Hynes, R. O.; Burton, D. R.; McKeating, J. A.; Rice, C. M. *Science* **2005**, 309, 623.
66. Blight, K. J.; Kolykhalov, A. A.; Rice, C. M. *Science* **2000**, 290, 1972.
101. Lu, Y.; Shi, T.; Wang, Y.; Yang, H.; Yan, X.; Luo, X.; Jiang, H.; Zhu, W. *J. Med. Chem.* **2009**, 52, 2854.
67. Lu, Y.; Liu, Y.; Xu, Z.; Li, H.; Liu, H.; Zhu, W. *Expert Opin. Drug Discovery* **2012**, 7, 375.
68. Parisini, E.; Metrangolo, P.; Pilati, T.; Resnati, G.; Terraneo, G. *Chem. Soc. Rev.* **2011**, 40, 2267.
69. Wilcken, R.; Zimmermann, M. O.; Lange, A.; Joerger, A. C.; Boeckler, F. *M. J. Med. Chem.* **2013**, 56, 1363.
70. *C&EN Suppl.* **2014**, <http://cen.acs.org/content/dam/cen/supplements/CEN>.
71. Kosaka, K.; Imamura, M.; Hayes, C. N.; Abe, H.; Hiraga, N.; Yoshimi, S.; Murakami, E.; Kawaoka, T.; Tsuge, M.; Aikata, H.; Miki, D.; Ochi, H.; Matsui, H.; Kanai, A.; Inaba, T.; Chayama, K. *J. Viral. Hepat.* **2014**.
72. Fontana, R. J.; Hughes, E. A.; Bifano, M.; Appelman, H.; Dimitrova, D.; Hindes, R.; Symonds, W. T. *Am. J. Transplant.* **2013**, 13, 1601.
73. Rustgi, V. K. *Expert Opin. Drug Saf.* **2010**, 9, 883.

74. Autran, B. *Science* **1997**, 277, 112.
75. Kumada, H.; Suzuki, Y.; Ikeda, K.; Toyota, J.; Karino, Y.; Chayama, K.; Kawakami, Y.; Ido, A.; Yamamoto, K.; Takaguchi, K.; Izumi, N.; Koike, K.; Takehara, T.; Kawada, N.; Sata, M.; Miyagoshi, H.; Eley, T.; McPhee, F.; Damokosh, A.; Ishikawa, H.; Hughes, E. *Hepatology* **2014**, 59, 2083.
76. Sulkowski, M. S.; Gardiner, D. F.; Rodriguez-Torres, M.; Reddy, K. R.; Hassanein, T.; Jacobson, I.; Lawitz, E.; Lok, A. S.; Hinestrosa, F.; Thuluvath, P. J.; Schwartz, H.; Nelson, D. R.; Everson, G. T.; Eley, T.; Wind-Rotolo, M.; Huang, S.-P.; Gao, M.; Hernandez, D.; McPhee, F.; Sherman, D.; Hindes, R.; Symonds, W.; Pasquinelli, C.; Grasela, D. M. *N. Engl. J. Med.* **2014**, 370, 211.
78. Pockros, P. J. *Expert Opin. Biol. Ther.* **2011**, 11, 1611.
79. *J. Org. Chem.* **1962**, 27, 700.
80. Howard, J. A. K.; Hoy, V. J.; O'Hagan, D.; Smith, G. T. *Tetrahedron* **1996**, 52, 12613.
81. Perola, E. *J. Med. Chem.* **2010**, 53, 2986.
82. Burke, T. J.; Loniello, K. R.; Beebe, J. A.; Ervin, K. M. *Comb. Chem. High Throughput Screening* **2003**, 6, 183.
83. Vaz, R. J.; Li, Y.; Rampe, D. **2005**, 43, 1.
84. Fonsi, M.; Orsale, M. V.; Monteagudo, E. *J. Biomol. Screening* **2008**, 13, 862.
85. Rettie, A. E.; Korzekwa, K. R.; Kunze, K. L.; Lawrence, R. F.; Eddy, A. C.; Aoyama, T.; Gelboin, H. V.; Gonzalez, F. J.; Trager, W. F. *Chem. Res. Toxicol.* **1992**, 5, 54.
86. Akhila, J. S.; Shyamjith, D.; Alwar, M. C. *Curr. Sci.* **2007**, 93, 917.
87. Kiser, J. J.; Burton, J. R., Jr.; Everson, G. T. *Nat. Rev. Gastroenterol. Hepatol.* **2013**, 10, 596.
88. Lipinski, C. A. *Drug Discovery Today: Technol.* **2004**, 1, 337.
89. Veber, D. F.; Johnson, S. R.; Cheng, H. Y.; Smith, B. R.; Ward, K. W.; Kopple, K. D. *J. Med. Chem.* **2002**, 45, 2615.
90. Lipinski, C. A. *J. Pharmacol. Toxicol. Methods* **2000**, 44, 235.
91. Wenlock, M. C.; Austin, R. P.; Barton, P.; Davis, A. M.; Leeson, P. D. *J.*

Med. Chem. **2003**, *46*, 1250.

92. Lovering, F.; Bikker, J.; Humblet, C. *J. Med. Chem.* **2009**, *52*, 6752.

93. Lipinski, C. A.; Lombardo, F.; Dominy, B. W.; Feeney, P. J. *Adv. Drug Deliv. Rev.* **2001**, *46*, 3.

94. Ritchie, T. J.; MacDonald, S. J. F. *Drug Discovery Today* **2009**, *14*, 1011.

95. Meanwell, N. A. *Chem. Res. Toxicol.* **2011**, *24*, 1420.

96. Wang, C.; Jia, L.; Huang, H.; Qiu, D.; Valera, L.; Huang, X.; Sun, J. H.; Nower, P. T.; O'Boyle, D. R., 2nd; Gao, M.; Fridell, R. A. *Antimicrob. Agents Chemother.* **2012**, *56*, 1588.

97. Wong, K. A.; Worth, A.; Martin, R.; Svarovskaia, E.; Brainard, D. M.; Lawitz, E.; Miller, M. D.; Mo, H. *Antimicrob. Agents Chemother.* **2013**, *57*, 6333.

98. Hickman, D.; Vasavanonda, S.; Nequist, G.; Colletti, L.; Kati, W. M.; Bertz, R.; Hsu, A.; Kempf, D. J. *Antimicrob. Agents Chemother.* **2004**, *48*, 2911.

99. Maron, D. M.; Ames, B. N. *Mutat. Res.* **1983**, *113*, 173.

100. Kugler-Steigmeier, M. E.; Friederich, U.; Graf, U.; Lutz, W. K.; Maier, P.; Schlatter, C. *Mutat. Res.* **1989**, *211*, 279.

101. Wakita, T.; Pietschmann, T.; Kato, T.; Date, T.; Miyamoto, M.; Zhao, Z.; Murthy, K.; Habermann, A.; Krausslich, H. G.; Mizokami, M.; Bartenschlager, R.; Liang, T. J. *Nat. Med.* **2005**, *11*, 791.

102. Wang, C.; Huang, H.; Valera, L.; Sun, J.-H.; O'Boyle, D. R., II; Nower, P. T.; Jia, L.; Qiu, D.; Huang, X.; Altaf, A.; Gao, M.; Fridell, R. A. *Antimicrob. Agents Chemother.* **2012**, *56*, 1350.

Part II.

Synthesis of conjugated polymers using palladium iron oxide nanocrystals

1. Introduction

Conjugated polymers (CPs) have received much attention as the key materials for organic electronic devices, such as organic photovoltaics (OPVs),^{1,2} organic light emitting diodes (OLEDs),³ and organic thin film transistors (OTFTs)⁴ owing to their intriguing optoelectronic property, solution processability, flexibility, and low-cost manufacturing potential. Therefore, much interest has been concentrated on developing efficient synthetic methods for well-defined CPs. The syntheses of CPs have been mostly accomplished using two types of transition metal-catalyzed polymerization reactions. The first method involves a chain-growth polymerization approach, such as nickel (Ni)-catalyzed Kumada catalyst-transfer polycondensation (KCTP),^{5,6} palladium (Pd)-catalyzed catalyst-transfer Suzuki-Miyaura coupling polymerization,⁷ as well as ruthenium (Ru)-catalyzed cyclopolymerization⁸⁻¹⁰ and ring opening metathesis polymerization (ROMP).^{11,12} The second method, a more commonly used one, involves a step-growth polymerization approach based on Pd-catalyzed Heck, Suzuki, and Stille reactions as well as Ni-catalyzed Yamamoto coupling reaction.^{2,13,14} Although homogeneous catalysis using transition metals has achieved great success in the synthesis of CPs, it suffers from residual contamination from the use of metal catalysts and ligands. This is because it is difficult to remove those contaminants by simple physical methods such as filtration and centrifugation. The residual contaminants reduce the electrical properties of CPs; this affects the evaluation of intrinsic properties of the CPs and makes the comparison of the properties of various CPs difficult.¹⁵⁻¹⁸ Therefore, easy and convenient separation methods to reduce the residual contaminant level are highly desirable. Moreover, from the economic and environmental perspectives, the recycling of the catalysts for polymerization by employing heterogeneous catalysts is most desired. In 2012, the Chen group successfully achieved the synthesis of the CPs using heterogeneous Pd on carbon by (Pd/C)-catalyzed Heck, Suzuki, and Stille coupling reactions.¹⁹ However, the catalytic activity of the recovered heterogeneous catalyst

diminished after a single reaction, and attempts to recycle the catalyst were not successful.¹⁹

Recently, because of greater surface-to-volume ratio and well-defined three-dimensional structures, nanocrystals have attracted much attention as heterogeneous catalysts; they exhibit significantly increased activity and sometimes even selectivity over the conventional heterogeneous catalysts.²⁰⁻²² Because the metal nanoparticle catalysts are well dispersed in solution, they almost act as semi-homogeneous catalysts.²⁰ In particular, Pd-Fe₃O₄ HNCs have exhibited consistent high catalytic activities in many organic reactions owing to their relatively uniform size (approximately 8 and 65 nm for Pd and Fe₃O₄, respectively). Furthermore, because of their soft ferrimagnetic property, the magnetic HNCs can be easily recovered using an external magnet and recycled without resorting to cumbersome filtration or centrifugation.²³ Recently, we synthesized gram quantities of Pd-Fe₃O₄ HNCs and successfully applied the magnetic nanocrystals, in the absence of extra ligands, to various organic reactions such as Suzuki,²³ Heck,²⁴ and Sonogashira coupling reactions,²⁴ as well as direct C-H arylation²⁵ and Wacker oxidation reaction.²⁶ Herein, we report the first application of nanocrystal catalysis toward the synthesis of CPs via Suzuki polymerization using Pd-Fe₃O₄ HNCs. In the synthesis of CPs, we particularly focused on the recycling of the catalyst; this is one of the most important goals toward sustainable or green chemistry.^{27,28}

2. Result and Discussion

To test the feasibility of the polycondensation via nanocatalysis, 1,4-diiodobenzene, 9,9-di(2'-ethylhexyl)fluorene-2,7-diboronic acid, and 2 mol% Pd-Fe₃O₄ catalyst were subjected to various polymerization conditions. We observed that several factors affected the efficiency of the polymerization. Because Pd-catalyzed Suzuki coupling reactions are known to be dependent upon a base,^{29,30} several bases such as potassium acetate (KOAc), dipotassium hydrogen phosphate (K₂HPO₄), potassium phosphate (K₃PO₄), and sodium carbonate (Na₂CO₃) were investigated first (Table II-1, entries 1–4). The best result was obtained when 5 equiv of K₃PO₄ was used to afford the conjugated polymer in a good yield after the precipitation (Table II-1, entry 4). When less than 5 equiv of K₃PO₄ was used, both the yields and number average molecular weights (Mn) of the CPs decreased dramatically (Table II-1, entry 5). We then examined the solvents for the polymerization, considering that the Pd-Fe₃O₄ catalyst is well dispersed in polar solvents. While choosing solvents, the solubility of the CPs was also taken into consideration. First, *N,N'*-dimethylformamide (DMF) was investigated because it is well known to stabilize Pd catalysts;^{14,31} however, a low molecular weight polymer was obtained in low yield (Table II-1, entry 11). When ethereal solvents such as 1,4-dioxane and tetrahydrofuran (THF) were used, good conversions were obtained (Table II-1, entries 10 and 4, respectively). Because the solubility of the polymer was better in THF than in 1,4-dioxane, slightly higher yields and Mn of the polymer in THF were observed than that in 1,4-dioxane. When a 3:1 v/v mixture of THF and water was used, the dispersion of the catalyst was poor, resulting in an aggregation of the catalyst in the reaction vessel, i.e., the Schlenk tube; this led to a low Mn of the resulting polymer (Table II-1, entry 16). Therefore, THF was selected as the reaction solvent. With the optimum base (5 equiv of K₃PO₄) and solvent (THF) in hand, we examined the reaction temperature by comparing the reactions at 70 and 110 °C. At both the temperatures, the reactions proceeded well (Table II-1, entries 4 and 6). Next,

the catalyst loading was varied from 0.5 to 5 mol%; 2 mol% catalyst was found optimal. This is because a higher catalyst loading did not increase the molecular weight and only a small amount of the polymer was produced when the catalyst loading was reduced to 0.5 mol% (Table II-1, entries 7 and 8). Thus, the optimized reaction conditions are as follows: 0.15 M substrate in the presence of 2 mol% Pd-Fe₃O₄ and 5 equiv K₃PO₄ in THF.

Table II-1. Condition optimization for Suzuki polymerization

Entry	Solvent	Base	Time (hr)	temp (°C)	M_n^a	M_w^a	PDI ^a	Yield
1	THF	Na ₂ CO ₃ (5 eq)	72	110			trace amount	
2	THF	K ₂ HPO ₄ (5 eq)	72	110			trace amount	
3	THF	KOAc (5 eq)	72	110			trace amount	
4	THF (0.15M)	K ₃ PO ₄ (5 eq)	72	110	15.2k	41.4k	2.72	96%
5	THF	K ₃ PO ₄ (3 eq)	72	110			trace amount	
6	THF (0.15M)	K ₃ PO ₄ (5 eq)	72	70	15.6k	56.7k	3.63	95%
7 ^{b,c}	THF (0.15M)	K ₃ PO ₄ (5 eq)	72	110	12.7k	53.3k	4.20	94%
8 ^d	THF (0.15M)	K ₃ PO ₄ (5 eq)	72	110	n.d.			13%
9 ^e	THF (0.15M)	K ₃ PO ₄ (5 eq)	72	70			no precipitates	
10	1,4-dioxane	K ₃ PO ₄ (5 eq)	72	105	13.0k	32.8k	2.52	84%
11	DMF	K ₃ PO ₄ (5 eq)	72	160	4.3k	8.9k	2.07	31%
12	Toluene	K ₃ PO ₄ (5 eq)	72	100			no precipitates	
13 ^f	toluene/H ₂ O (v/v=3/1)	K ₃ PO ₄ (5 eq)	72	100	4.8k	11.2k	2.33	49%
14 ^f	toluene/H ₂ O (v/v=1/1)	K ₂ CO ₃ (10 eq)	72	100	n.d.			24%
15 ^f	toluene/H ₂ O (v/v=1/1)	Na ₂ CO ₃ (10 eq)	72	100	n.d.			29%
16	THF/H ₂ O (v/v=3/1)	K ₃ PO ₄ (5 eq)	72	100	7.0k	13.3k	1.90	87%
17 ^b	THF/H ₂ O (v/v=3/1)	K ₂ CO ₃ (5 eq)	48	100	8.1k	27.2k	3.36	76%
18 ^b	THF/H ₂ O (v/v=3/1)	Cs ₂ CO ₃ (5 eq)	48	100	2.7k	7.1k	2.63	73%

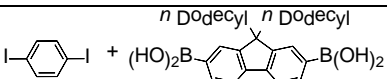
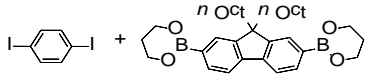
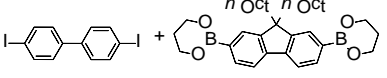
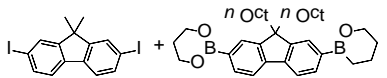
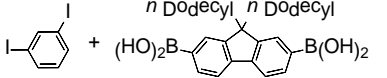
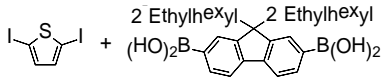
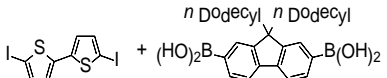
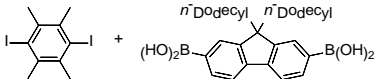
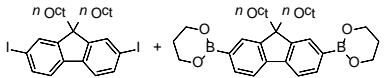
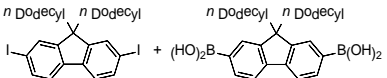
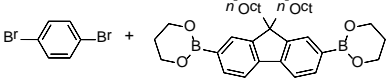
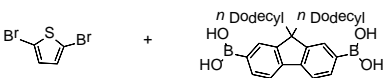
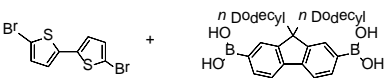
19	THF/MeOH (v/v=4/1)	Cs ₂ CO ₃ (5 eq)	72	100	n.d.	36%		
20 ^b	THF/DMA (v/v=4/1)	K ₃ PO ₄ (5 eq)	72	110	3.4k	15.4k	4.53	86%
21	THF/H ₂ O (v/v=14/1)	K ₃ PO ₄ (5 eq)	72	110	no precipitates			
22	1,4-dioxane/H ₂ O (v/v=3/1)	K ₂ CO ₃ (5 eq)	48	90	n.d.	29%		
23 ^b	1,4-dioxane/H ₂ O (v/v=3/1)	Cs ₂ CO ₃ (5 eq)	48	90	2.2k	6.1k	2.77	78%
24 ^b	DMA/H ₂ O (v/v=4/1)	K ₂ CO ₃ (5 eq)	72	100	1.9k	7.5k	3.95	83%
25 ^b	DMA/H ₂ O (v/v=4/1)	K ₃ PO ₄ (5 eq)	72	100	0.8k	2.1k	2.63	46%

^a Determined by THF size exclusion chromatography (SEC) calibrated using polystyrene (PS) standards. *M_n* is given in g/mol. ^b Determined by CHCl₃ SEC calibrated using PS standards. *M_n* is given in g/mol. ^c 5 mol% of Pd-Fe₃O₄ was used. ^d 0.5 mol% of Pd-Fe₃O₄ was used. ^e Fe₃O₄ was used rather than Pd-Fe₃O₄. ^f A drop of Aliquat 336 was added.

With the optimized reaction conditions in hand, the substrate scope of the Suzuki polymerization using the Pd-Fe₃O₄ HNC catalyst was investigated. Depending on the length and branching of the side chains, the properties of CPs such as the electronic performance could vary.^{32,33} With this consideration, we carried out the polymerization of 1,4-diiodobenzene with the fluorenes containing linear alkyl chains, such as 9,9-didodecylfluorene-2,7-diboronic acid (Table II-2, entry 1) and 9,9-dioctylfluorene-2,7-diboronic acid bis(1,3-propanediol) ester (Table II-2, entry 2). Regardless of the side-chain structures, moderate to high molecular weight polymers were obtained in high yields (Table II-1, entry 6; Table II-2, entries 1 and 2). The choice between a boronic acid and boronic ester may affect the efficiency of Suzuki polycondensation.^{34,35} In this study, the polymerizations between the diboronic ester and several diiodoarenes were also successful (Table II-2, entries 2-4). However, the reaction of 1,4-diiodo-2,3,5,6-tetramethylbenzene, 2,7-diiodo-9,9-dioctyl-9*H*-fluorene, or 2,7-diiodo-9,9-didodecyl-9*H*-fluorene with the boronic ester did not proceed smoothly to afford the desired polymers (Table

II-2, entries 8–10). It appears that the oxidative addition of the diiodo monomers containing bulky side chains is challenging, resulting in lower conversions. Next we attempted couplings of 1,4-dibromobenzene or dibromothiophene derivatives as monomers with a boronic acid or ester, but only a trace to small amount of desired polymer was obtained (Table II-2, entries 11–13). The low conversion of dibromoarenes is similar to the results observed with monomer reactions using bromoarenes with the same Pd-Fe₃O₄ nanoparticles.²³ Therefore, the diiodo compounds, substituted with either short or no side chains such as meta-diiodobenzene and monomers of thiophene derivatives, were used to ensure successful Suzuki polymerization (Table II-2, entries 4–7). The most notable example in this regard is reported in entry 7 of Table II-2, where the bithiophene unit was successfully incorporated into the polymer to give F12T2, the didodecyl analog of the well-known polymer, poly(9,9-dioctylfluorene-alt-bithiophene) (F8T2), for OTFT applications.³⁶ All the polymers dissolved well in common organic solvents such as chloroform and THF.

Table II-2. Synthesis of conjugated polymers using Pd-Fe₃O₄ catalyst

Entry	Monomers	M_n^a	PDI ^a	Yield
1		16.2 k	2.90	>99%
2		19.5 k	3.32	78%
3		27.1 k	2.72	74%
4		10.7 k	2.21	99%
5		14.9 k	2.47	>99%
6 ^b		13.0 k	3.62	85%
7		20.2 k	3.33	95%
8		2.5k	1.20	80%
9		4.3k	1.58	90%
10			trace amount	
11			trace amount	
12			trace amount	
13		n.d.		13%

^a Determined by THF SEC calibrated using PS standards. M_n is given in g/mol. ^b Reaction was run at 110 °C.

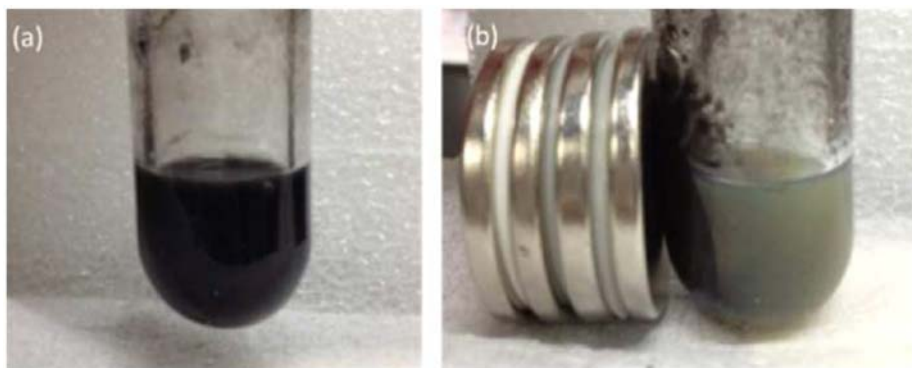


Figure II-1. Recovery of Pd-Fe₃O₄ HNC using external magnet after polymerization (a) without magnet (b) with magnet.

The ferrimagnetic characteristics of Pd-Fe₃O₄ HNCs allowed for easy recycling of the catalyst using an external magnet (Figure II-1). Because of the relationship between the *Mn* and conversion in step-growth polymerization, the resulting polymers would be obtained with significantly lower *Mn* and lower yield if the catalyst activity decreases during the recycling. Therefore, it is of utmost interest to maintain the performance of the heterogeneous catalyst system in repetitive polymerization. When the recycling experiments of the Pd-Fe₃O₄ HNC catalyst for the polymerization of 1,4-diiodobenzene and 9,9-didodecylfluorene-2,7-diboronic acid were carried out, the corresponding CPs were obtained in high yield and with a similar level of *Mn* (≥ 11.3 kg/mol) up to at least sixth recycling (Table II-3). In the case of the polymerization of 1,4-diiodobenzene and 9,9-di(2'-ethylhexyl)fluorene-2,7-diboronic acid, the recycling experiments were carried out at both 70 and 110 °C. At 70 °C, the catalyst in the polymerization was reused for at least 11 times, (or 10 times at 110 °C, Table II-4 (a) and (b), respectively). It was crucial to sonicate the reaction flask containing the recycled catalyst and fresh batch of monomers before the reaction, because the Pd-Fe₃O₄ HNC catalyst should be well-

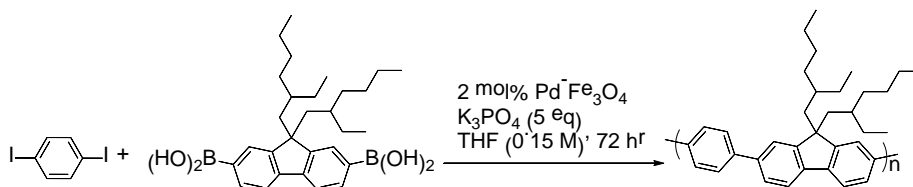
dispersed in THF for successful polymerization. Without the sonication treatment, the catalytic activity dropped precipitously, presumably because of the aggregation of the Pd-Fe₃O₄ HNC catalyst during the recycling process (Table II-4 (c)).³⁶ The transmission electron microscopy (TEM) images of the fresh Pd-Fe₃O₄ HNC catalyst and that after the fifth recycling at 70 °C showed the same morphology (Figure II-2, inset (b) shows the image after 11 times recycling). Moreover, even after 11 times recycling, the recovered weight of the Pd-Fe₃O₄ HNC catalyst was 89% of the original amount. The Pd content of the catalyst, determined by ICP-MS, changed from 2.45 wt% to 2.07 wt% after the fifth recycling. It appears that the degree of Pd leaching caused by the catalyst recycling during the Suzuki polymerization was not significant.²³

Table II-3. Recycling of Pd-Fe₃O₄ HNC catalyst for Suzuki polymerization

run	M_n^a	PDI ^a	yield	Pd _{re} ^b
1	16.2 k	2.90	>99%	52 ppm
2	19.9 k	2.49	>99%	28 ppm
3	17.5 k	2.82	98%	21 ppm
4	15.3 k	2.41	>99%	5 ppm
5	18.9 k	2.49	94%	34 ppm
6	11.3 k	2.35	>99%	17 ppm
average	16.5 k	-	>98%	26 ppm

^a Determined by THF SEC calibrated using PS standards. M_n is given in g/mol. ^b Concentration of residual Pd in polymers detected by inductively coupled plasma-mass spectrometry (ICP-MS)

Table II-4. Recycle test of the Pd-Fe₃O₄ HNC catalyst for compare to sonication process



(a) recycling at 70 °C (with sonication)

run	M_n^a	PDI ^a	yield	Pd _{re} ^b
1	17.6k	4.03	>99%	38 ppm
2	14.2k	3.12	95%	17 ppm
3	8.6k	2.34	95%	38 ppm
4	12.6k	4.93	77%	28 ppm
5	11.3k	2.42	>99%	31 ppm
6	6.2k	3.82	34%	n.d.
7	7.0k	4.53	52%	n.d.
8	21.5k	3.05	81%	n.d.
9	14.1k	3.43	65%	n.d.
10	21.8k	7.99	82%	n.d.
11	15.1k	2.14	>99%	n.d.

(b) recycling at 110 °C (with sonication)

run	M_n^a	PDI ^a	yield	Pd _{re} ^b
1	8.2k	2.37	80%	56 ppm
2	15.9k	2.83	94%	3 ppm
3	11.9k	2.94	87%	24 ppm
4	8.1k	2.19	90%	4 ppm
5	4.3k	1.58	47%	n.d.
6	13.0k	3.12	86%	21 ppm
7	9.2k	2.78	80%	n.d.
8	5.8k	2.00	56%	n.d.
9	9.1k	2.24	68%	n.d.
10	14.6k	3.14	85%	n.d.

(c) recycling at 70 °C (without sonication)

run	M_n^a	PDI ^a	yield	Pd _{re} ^b
1	15.6k	3.63	95%	53
2	n.d.		26%	n.d.
3	n.d.		17%	n.d.

^a Determined by THF SEC calibrated using PS standards. M_n is given in g/mol. ^b Concentration of residual Pd in polymers detected by inductively coupled plasma-mass spectrometry (ICP-MS)

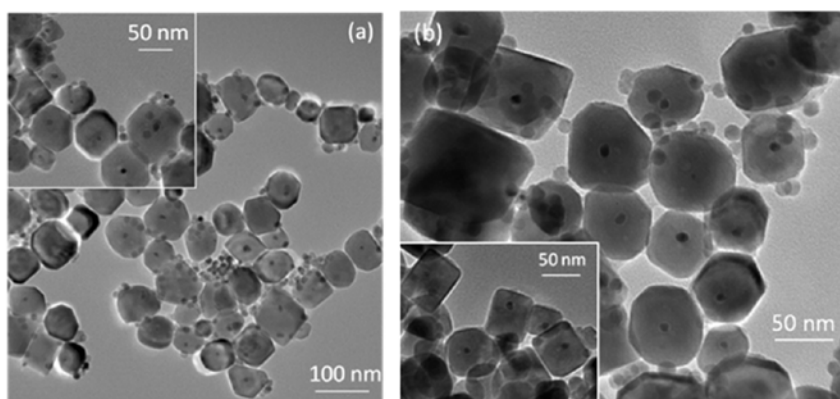


Figure II-2. TEM images of Pd-Fe₃O₄ HNC after recycling reactions in Table II-4 (a). (a) before reaction (b) after 5 runs of recycling reactions (inset : after 11 runs of recycling reactions).

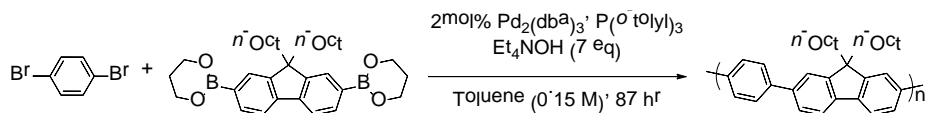
Next, we investigated the amount of Pd remaining in the CPs after the polymerization. The ICP-MS analysis of the polymers prepared from 1,4-diiodobenzene and 9,9-didodecylfluorene-2,7-diboronic acid showed that the residual Pd content after the first six reactions was 26 ppm on average with the lowest value of 5 ppm (Table II-3). In the case of the polymer from 9,9-di(2'-ethylhexyl)fluorene-2,7-diboronic acid, 30 and 22 ppm Pd were detected from the reaction at 70 and 110 °C, respectively (Table II-4 (a) and (b), respectively, the average value over five recycles). To make a comparison, we conducted the

analogous polymerization using homogenous $\text{Pd}(\text{PPh}_3)_4$ and $\text{Pd}_2(\text{dba})_3$ and obtained high level of Pd residue of 1996 and 151 ppm respectively (Table II-5). Although Pd residues could be reduced by additional rigorous purification, this showed that under the same conditions, the polymers prepared by the HNC contained much lower Pd residue. The Pd residue found in the polymer obtained from the $\text{Pd-Fe}_3\text{O}_4$ HNC-catalyzed polymerization is comparable to the value reported for the polymerization employing Pd/C catalyst (34–56 ppm for the Suzuki polymerization).¹⁹ Further reduction in the Pd content to a level of 32 ppm from 53 ppm and an increase in the M_n could be achieved through the purification by Soxhlet extraction using methanol and acetone (Table II-5, entry 2).

Table II-5. Homogeneous Pd-catalyzed Suzuki polymerization

Entry	Temp (°C)	M_n^a	PDI ^a	Yield	ICP-MS (ppm)
1	70	4.3k	1.88	73%	1996

^a Determined by THF SEC calibrated using PS standards. M_n is given in g/mol



Entry	Temp (°C)	M_n^a	PDI ^a	Yield	ICP-MS (ppm)
2	110	8.5k	2.76	69%	151
		(9.9k) ^b	(2.66) ^b	(62%) ^b	(101) ^b

^a Determined by THF SEC calibrated using PS standards. M_n is given in g/mol ^b Determined after Soxhlet extraction with methanol and acetone.

3. Conclusion

In conclusion, we demonstrated successful Suzuki polymerization using magnetically separable Pd-Fe₃O₄ heterobimetallic nanocrystals as the novel heterogeneous catalyst. The polymerizations using the Pd-Fe₃O₄ HNC catalyst showed good reactivity to afford various moderate to high molecular weight polymers. After the polymerization, the catalyst was easily separated and recovered using an external magnet. The nanocatalyst was reused in the polymerization for up to the 11th run, and the catalytic activity was maintained throughout the recycling process. Furthermore, less Pd remained in the CPs compared to that obtained from the analogous homogeneous reaction. The Pd leaching from each run was minimal, and the recovered catalyst maintained the original heterodimeric shape. The CPs, thus prepared are expected to exhibit better electrical performance than those obtained from the reactions using homogeneous catalysts. Therefore, the heterogeneous Pd-Fe₃O₄ HNCs have a great potential for application in large-scale and more environment-friendly polymerization.

4. Experimental

NMR spectra were recorded by Varian/Oxford As-500 (500 MHz for ^1H , 125 MHz for ^{13}C). THF Gel permeation chromatography (GPC) for polymer molecular weight analysis was carried out with Waters system (1515 pump, 2414 refractive index detector and 2489 UV detector) and Shodex GPC LF-804 column eluted with THF (GPC grade, Honeywell Burdick & Jackson). Flow rate was 1.0 mL/min and temperature of column was maintained at 35 °C. Samples were diluted in 0.001-0.005 wt% by THF and filtered with a 0.20 μm PTFE filter before injection into the GPC. Sonication was carried out with Powersonic 410 model devices from Hwashin Tech. Inductively coupled plasma mass spectrometry (ICP-MS) was performed by using ICPS-7500 spectrometer (Shimadzu).

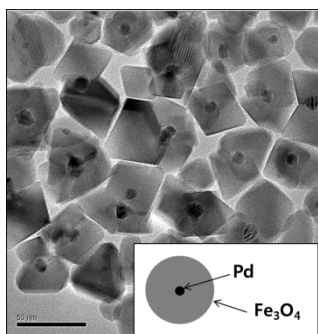
Materials

Without additional notes, all reagents were commercially available and used without further purification. THF was distilled over sodium and benzophenone, and degassed by argon bubbling for 10 minutes before using on polymerization. Toluene, 1,4-dioxane, methanol, DMF were purified by solvent purification system using alumina column, and degassed by argon bubbling. *N,N'*-dimethylacetamide (DMA) was purchased from Junsei and degassed by argon for 10 minutes before using on polymerization without further purification.

Preparation of Pd-Fe₃O₄ HNCs

The Pd-Fe₃O₄ HNCs were prepared according to the previously reported procedure. The synthesis was performed by one-pot thermal degradation of a mixture solution composed of iron acetylacetonate (14.0g, 40.0 mmol), palladium acetylacetonate (200 mg, 0.066 mmol), oleylamine (120 mL, 350

mmol), and oleic acid (80 mL, 250 mmol). The mixture was heated to 120 °C under reduced pressure while being vigorously stirred for 2 h. The resulting mixture was heated to 220 °C under Argon at a heating rate of 2 °C/min and kept at same temperature for 30 min. Then it was further heated to 300 °C at the 2 °C/min heating rate and aged for 30 min. Next the mixture was cooled to room temperature and washed with ethanol and a black supernatant was sore. The residue was dispersed in EtOH through sonication and products were collected by centrifugation (1750 rpm, 15 min). The Pd-Fe₃O₄ product was again dispersed in hexane and collected through the use of centrifugation (1750 rpm, 15 min). This washing process was rerun until the sore hexane did not show any color. Then, the Pd-Fe₃O₄ HNCs was collected and dried under vacuum to provided 2.45 g of dark solid.



General preparation of polymers

The mixture of 1 equiv of diiodo compounds (0.3 mmol), 1 equiv of diboronic acid (or diboronic ester) compounds (0.3 mmol), 5 equiv of base (1.5 mmol), 2 mol% of Pd-Fe₃O₄ (2 mol% loading of Pd-atom equivalents, 26 mg of 2.45 wt% Pd-Fe₃O₄) in Schlenk tube was evacuated and backfilled with argon four times, then degassed solvent (2-3 mL, 0.10-0.15 M) was added to the reaction mixture. The Schlenk tube was tightly sealed, and it was sonicated for 30 min at room temperature. The reaction mixture was immersed in 70 °C (or 110 °C) oil bath and stirred for 72 hr with stirring. The reaction mixture was cooled down to

room temperature, and the Pd-Fe₃O₄ catalyst was separated using a magnet. The resulting reaction mixture was diluted with chloroform, and washed with brine. The combined organic layers were dried with magnesium sulfate, and concentrated. The concentrated solution was precipitated into methanol, filtered, and dried under vacuum. The recovered Pd-Fe₃O₄ catalyst was washed many times by using chloroform, hexane, water, acetone, and tetrahydrofuran then it was dried and reused for the next run of the reaction.

Reference - Part II.

1. Gunes, S.; Neugebauer, H.; Sariciftci, N. S. *Chem. Rev.* **2007**, *107*, 1324.
2. Cheng, Y. J.; Yang, S. H.; Hsu, C. S. *Chem. Rev.* **2009**, *109*, 5868.
3. Grimsdale, A. C.; Chan, K. L.; Martin, R. E.; Jokisz, P. G.; Holmes, A. B. *Chem. Rev.* **2009**, *109*, 897.
4. Murphy, A. R.; Frechet, J. M. *Chem. Rev.* **2007**, *107*, 1066.
5. Loewe, R. S.; Ewbank, P. C.; Liu, J. S.; Zhai, L.; McCullough, R. D. *Macromolecules* **2001**, *34*, 4324.
6. Yokozawa, T.; Yokoyama, A. *Chem. Rev.* **2009**, *109*, 5595.
7. Yokoyama, A.; Suzuki, H.; Kubota, Y.; Ohuchi, K.; Higashimura, H.; Yokozawa, T. *J. Am. Chem. Soc.* **2007**, *129*, 7236.
8. Kang, E. H.; Lee, I. S.; Choi, T. L. *J. Am. Chem. Soc.* **2011**, *133*, 11904.
9. Lee, I. S.; Kang, E.-H.; Park, H.; Choi, T.-L. *Chem. Sci.* **2012**, *3*, 761.
10. Park, H.; Lee, H.-K.; Choi, T.-L. *Poly. Chem.* **2013**, *4*, 4676.
11. Klavetter, F. L.; Grubbs, R. H. *J. Am. Chem. Soc.* **1988**, *110*, 7807.
12. Yoon, K. Y.; Lee, I. H.; Kim, K. O.; Jang, J.; Lee, E.; Choi, T. L. *J. Am. Chem. Soc.* **2012**, *134*, 14291.
13. Sakamoto, J.; Rehahn, M.; Wegner, G.; Schluter, A. D. *Macromol. Rapid. Commun.* **2009**, *30*, 653.
14. Carsten, B.; He, F.; Son, H. J.; Xu, T.; Yu, L. *Chem. Rev.* **2011**, *111*, 1493.
15. Krebs, F. C.; Nyberg, R. B.; Jørgensen, M. *Chem. Mater.* **2004**, *16*, 1313.
16. Sonar, P.; Grimsdale, A. C.; Heeney, M.; Shkunov, M.; McCulloch, I.; Müllen, K. *Synth. Met.* **2007**, *157*, 872.
17. Björklund, N.; Lill, J.-O.; Rajander, J.; Österbacka, R.; Tierney, S.; Heeney, M.; McCulloch, I.; Cölle, M. *Org. Electron.* **2009**, *10*, 215.
18. Kaake, L.; Dang, X. D.; Leong, W. L.; Zhang, Y.; Heeger, A.; Nguyen, T. Q. *Adv. Mater.* **2013**, *25*, 1706.
19. Liu, S.-Y.; Li, H.-Y.; Shi, M.-M.; Jiang, H.; Hu, X.-L.; Li, W.-Q.; Fu, L.; Chen, H.-Z. *Macromolecules* **2012**, *45*, 9004.
20. Astruc, D.; Lu, F.; Aranzas, J. R. *Angew. Chem. Int. Ed.* **2005**, *44*, 7852.

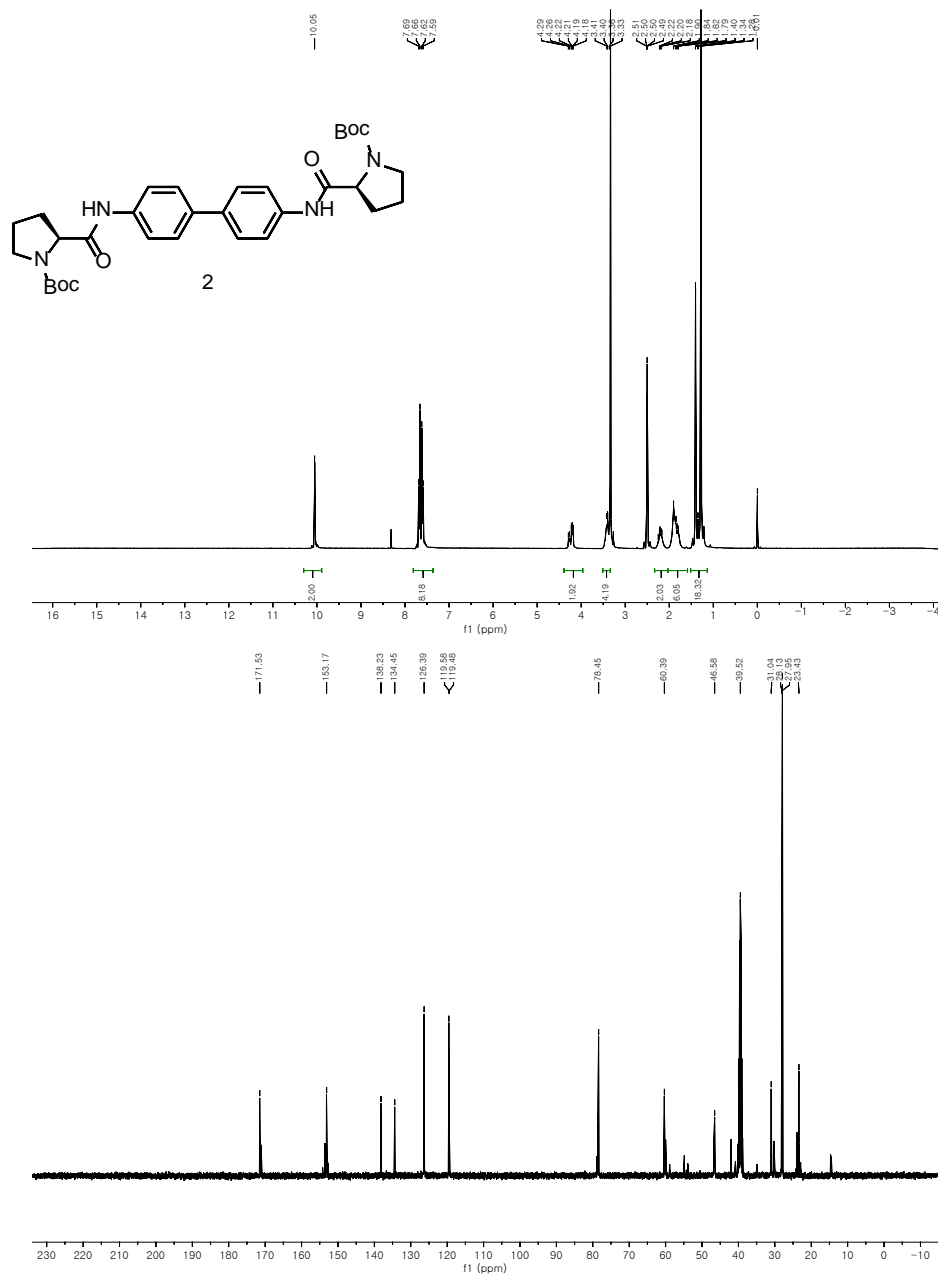
21. Huber, D. L. *Small* **2005**, *1*, 482.
22. Chung, J.; Kim, C.; Jeong, H.; Yu, T.; Binh do, H.; Jang, J.; Lee, J.; Kim, B. M.; Lim, B. *Chem. Asian. J.* **2013**, *8*, 919.
23. Jang, Y.; Chung, J.; Kim, S.; Jun, S. W.; Kim, B. H.; Lee, D. W.; Kim, B. M.; Hyeon, T. *Phys. Chem. Chem. Phys.* **2011**, *13*, 2512.
24. Chung, J.; Kim, J.; Jang, Y.; Byun, S.; Hyeon, T.; Kim, B. M. *Tetrahedron Lett.* **2013**, *54*, 5192.
25. Lee, J.; Chung, J.; Byun, S. M.; Kim, B. M.; Lee, C. *Tetrahedron* **2013**, *69*, 5660.
26. Byun, S.; Chung, J.; Jang, Y.; Kwon, J.; Hyeon, T.; Kim, B. M. *RSC Adv.* **2013**, *3*, 16296.
27. Gladysz, J. A. *Pure Appl. Chem.* **2001**, *73*.
28. Gladysz, J. A. *Chem. Rev.* **2002**, *102*, 3215.
29. Magano, J.; Dunetz, J. R. *Chem. Rev.* **2011**, *111*, 2177.
30. Molnar, A. *Chem. Rev.* **2011**, *111*, 2251.
31. Bao, Z.; Chan, W. K.; Yu, L. *J. Am. Chem. Soc.* **1995**, *117*, 12426.
32. Piliego, C.; Holcombe, T. W.; Douglas, J. D.; Woo, C. H.; Beaujuge, P. M.; Frechet, J. M. *J. Am. Chem. Soc.* **2010**, *132*, 7595.
33. Yiu, A. T.; Beaujuge, P. M.; Lee, O. P.; Woo, C. H.; Toney, M. F.; Frechet, J. M. *J. Am. Chem. Soc.* **2012**, *134*, 2180.
34. Ohe, T.; Miyaura, N.; Suzuki, A. *J. Org. Chem.* **1993**, *58*, 2201.
35. Miyaura, N.; Suzuki, A. *Chem. Rev.* **1995**, *95*, 2457.
36. Sirringhaus, H.; Kawase, T.; Friend, R. H.; Shimoda, T.; Inbasekaran, M.; Wu, W.; Woo, E. P. *Science* **2000**, *290*, 2123.

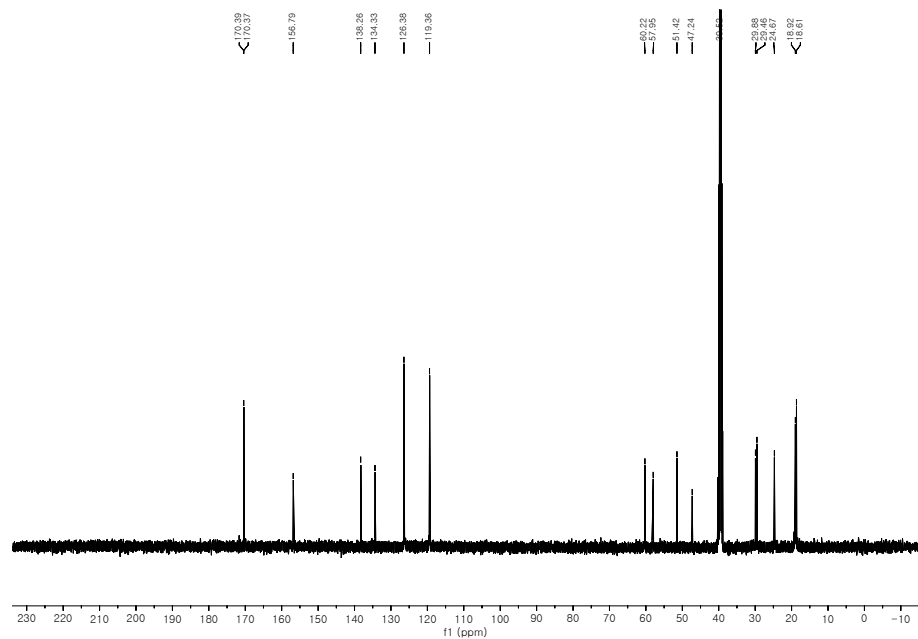
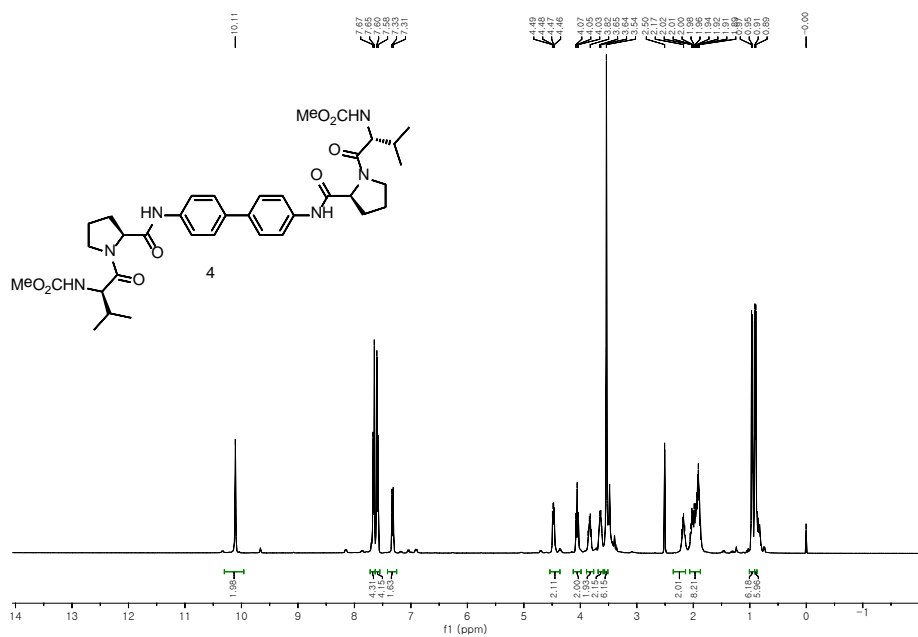
Appendix A

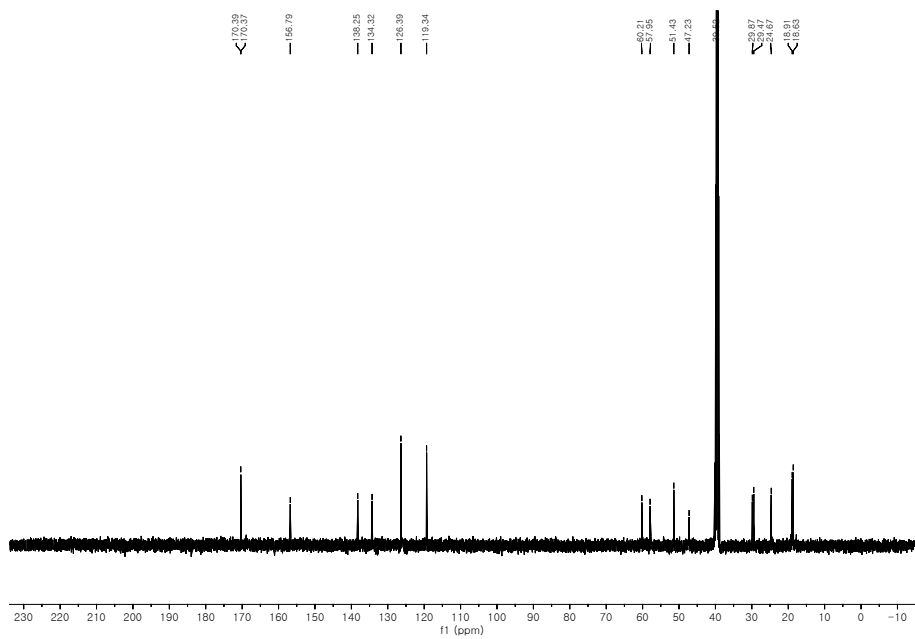
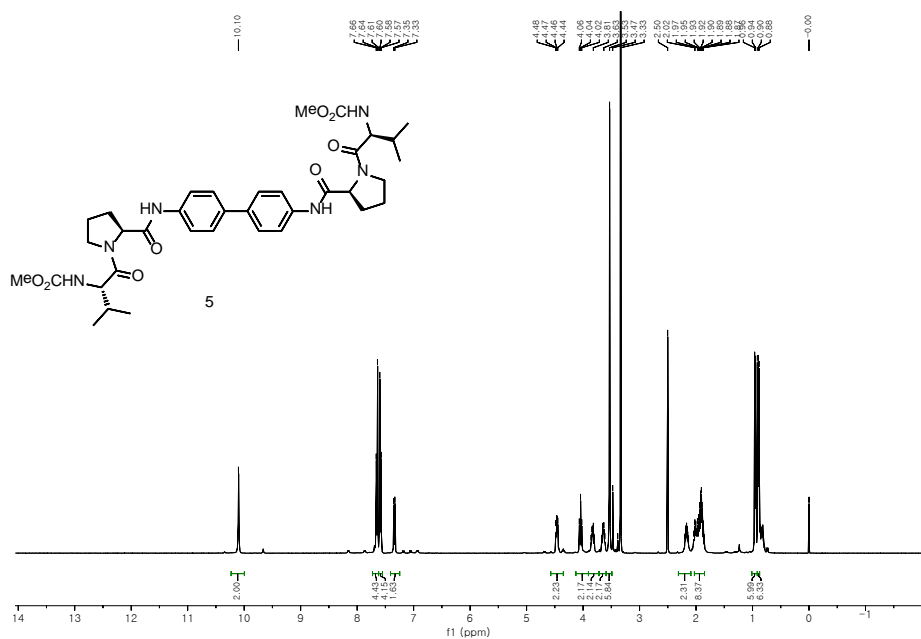
NMR spectra

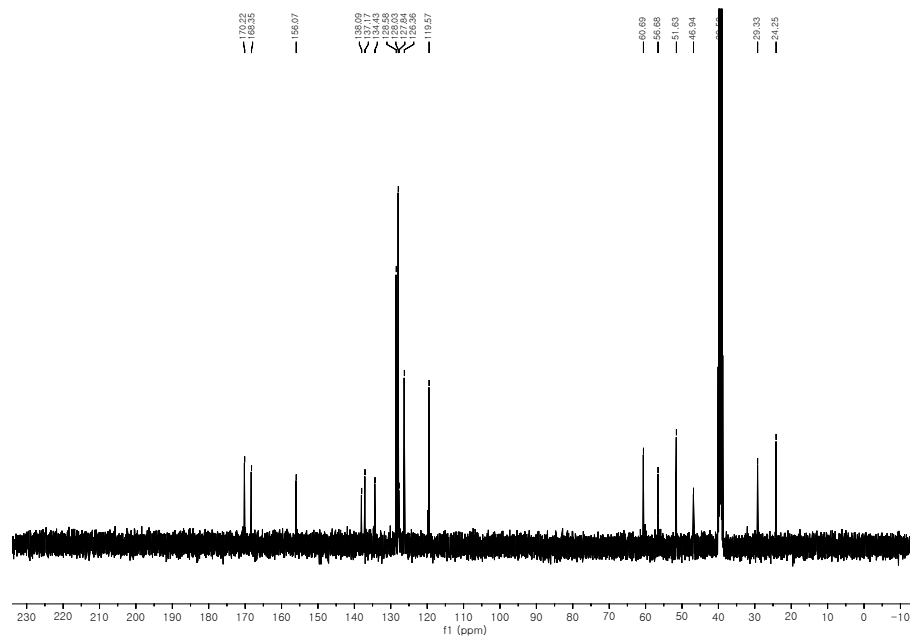
Part I.

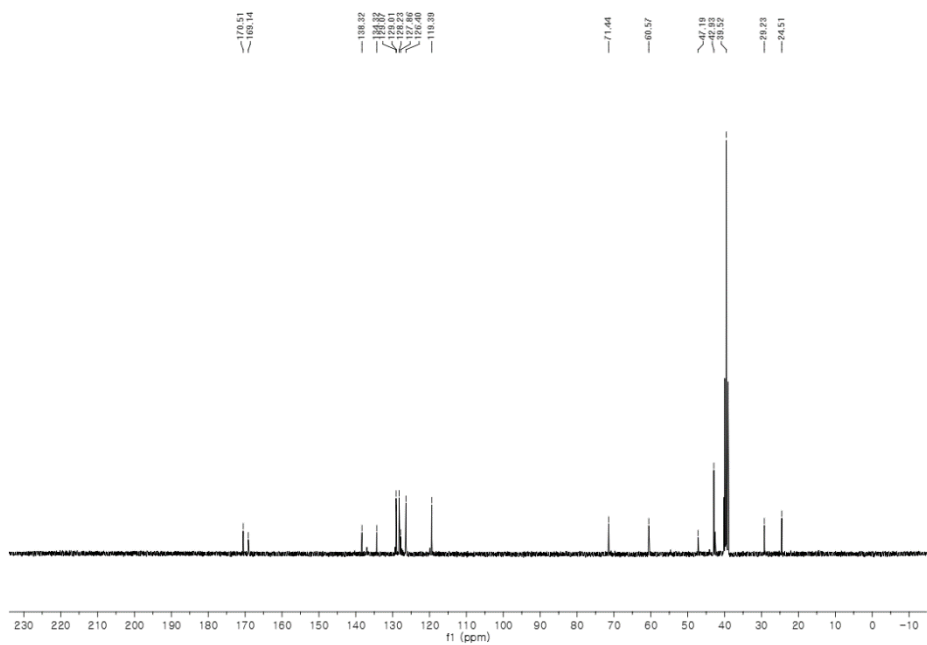
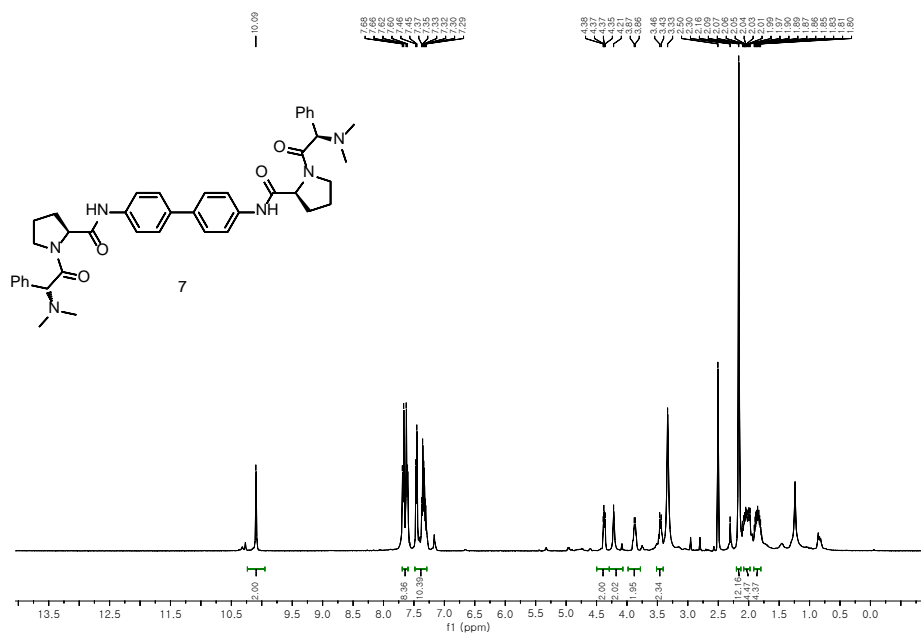
Chapter 1.

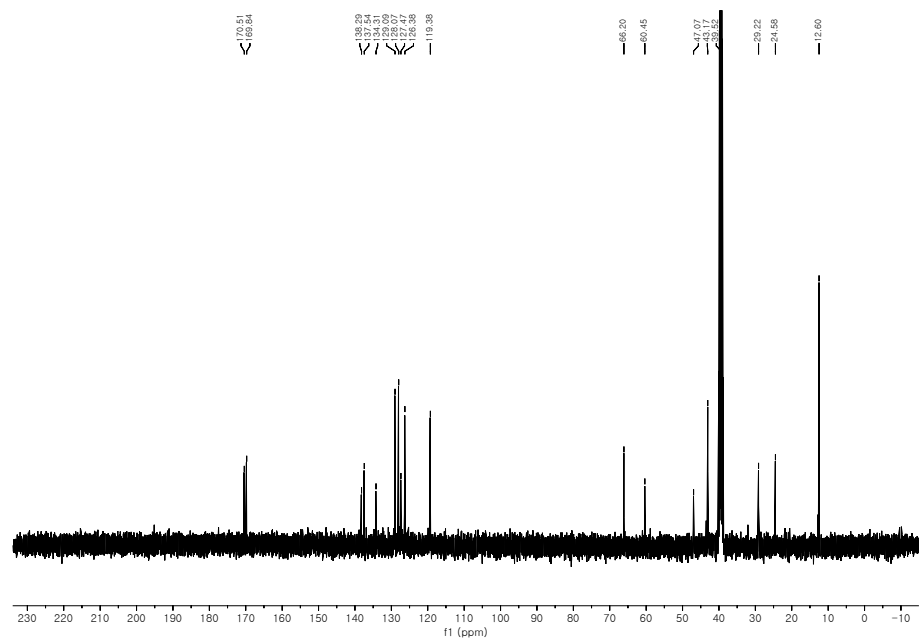
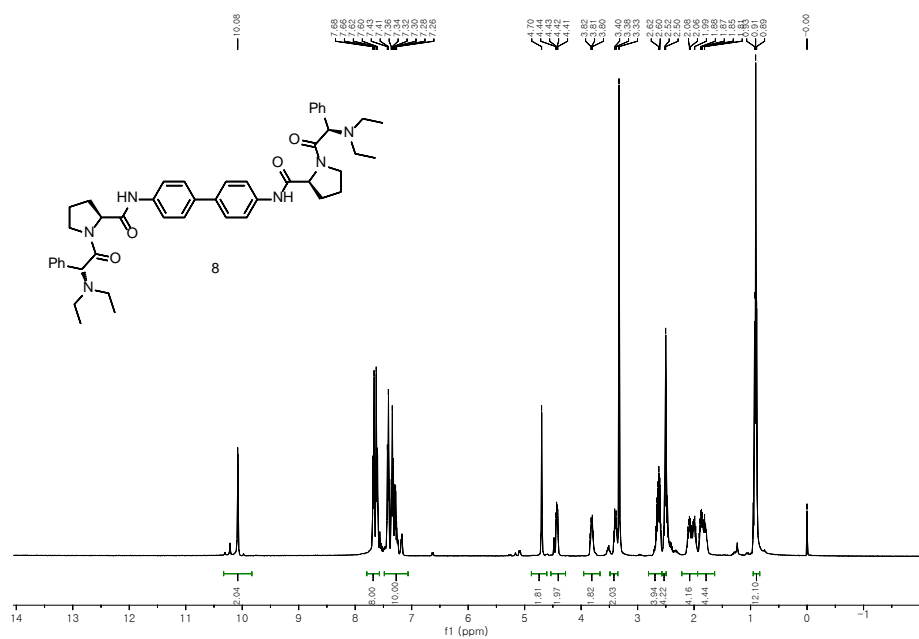


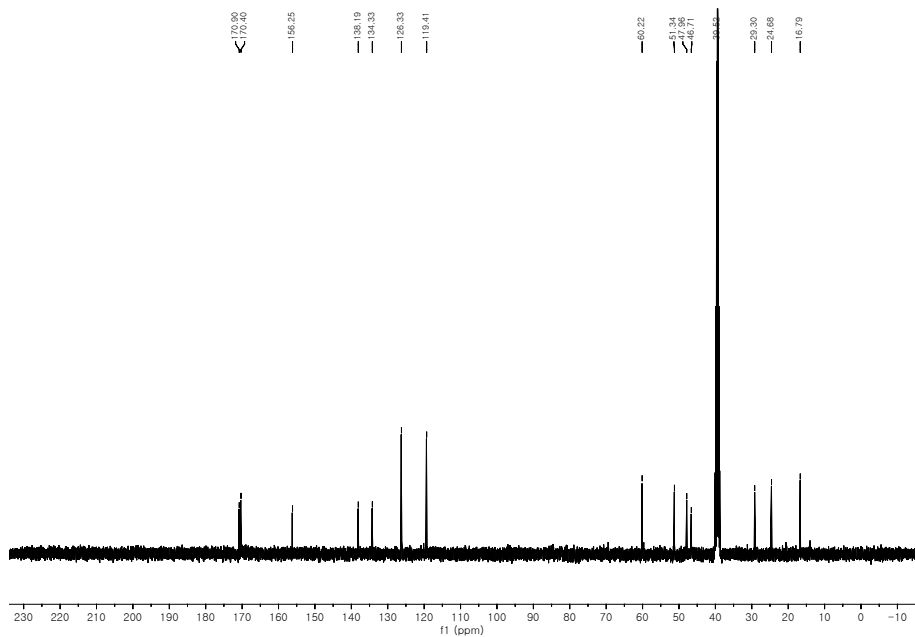
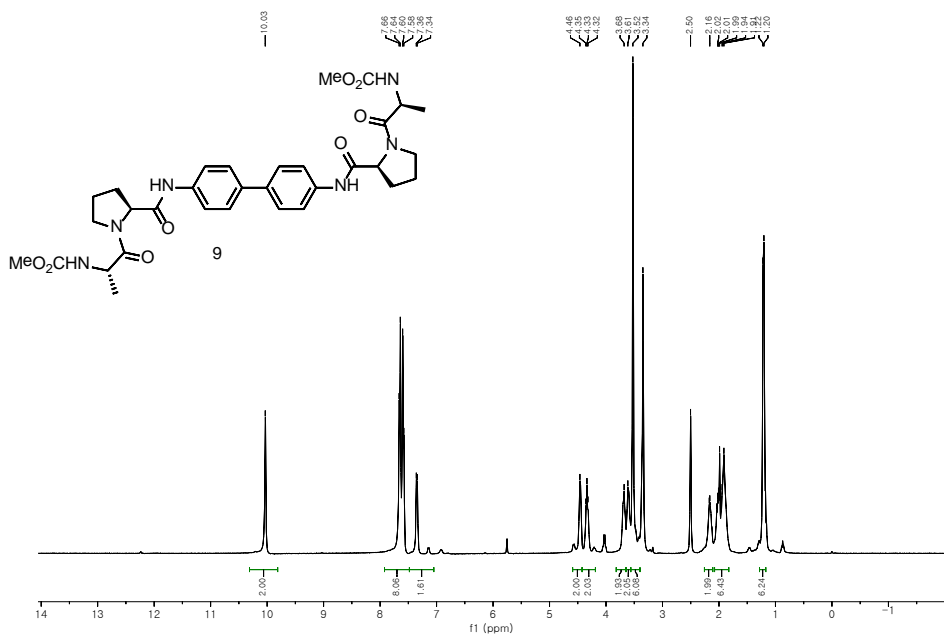


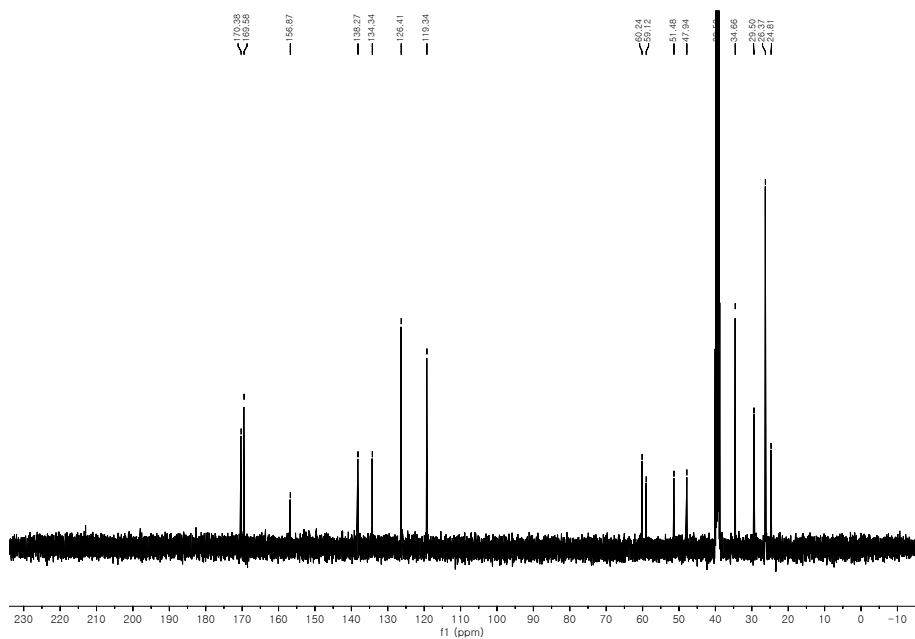
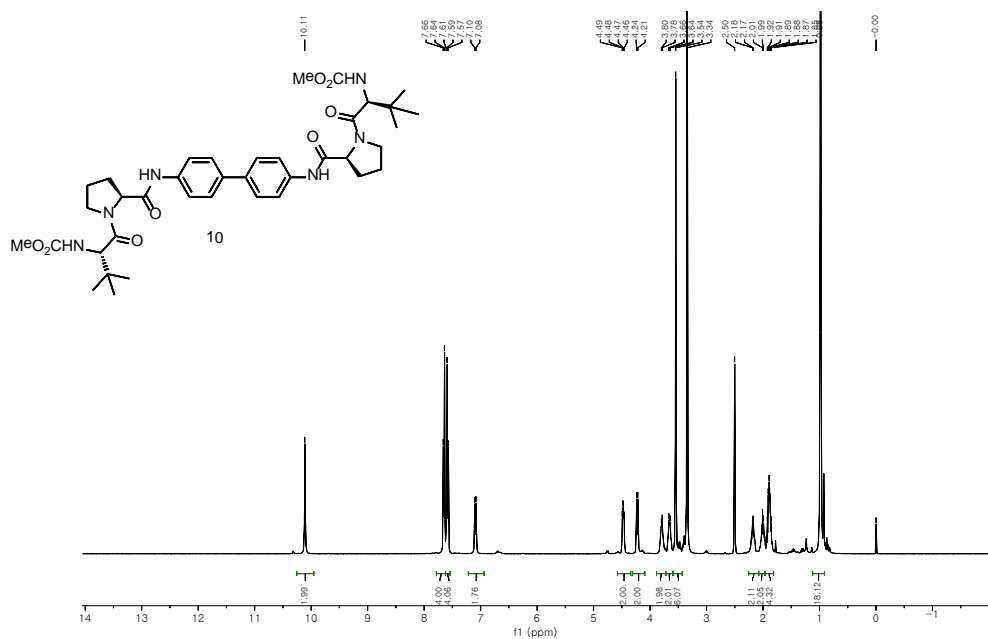


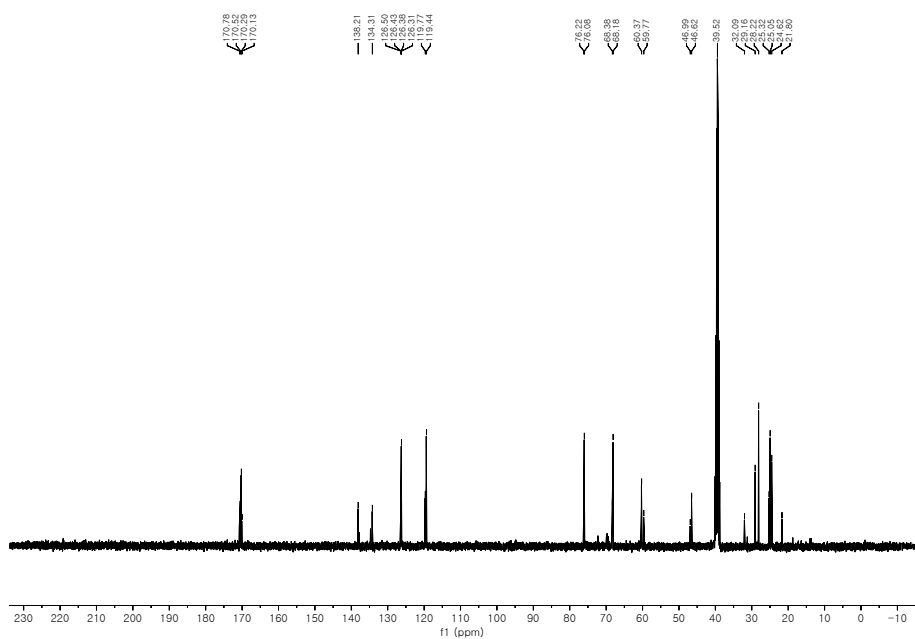
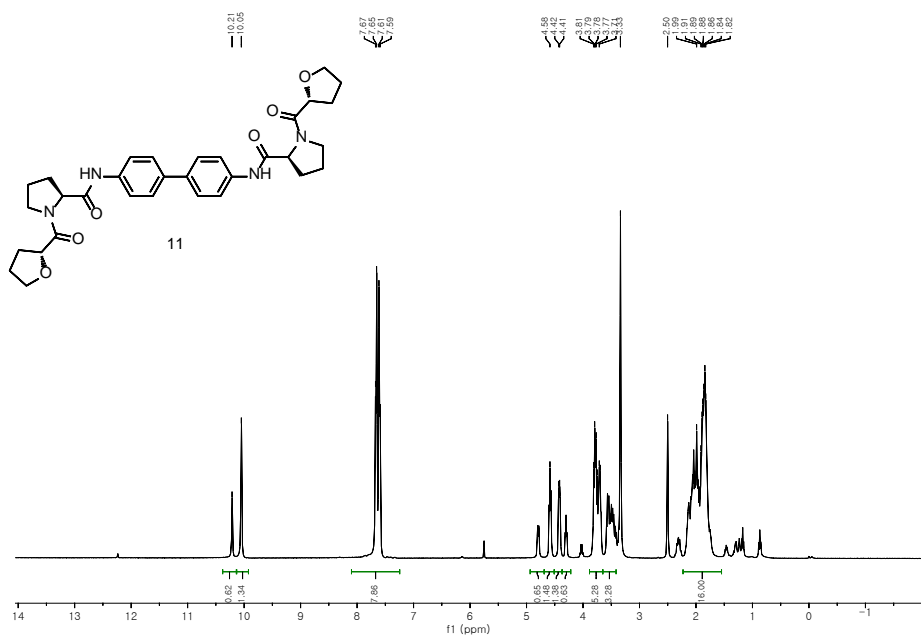








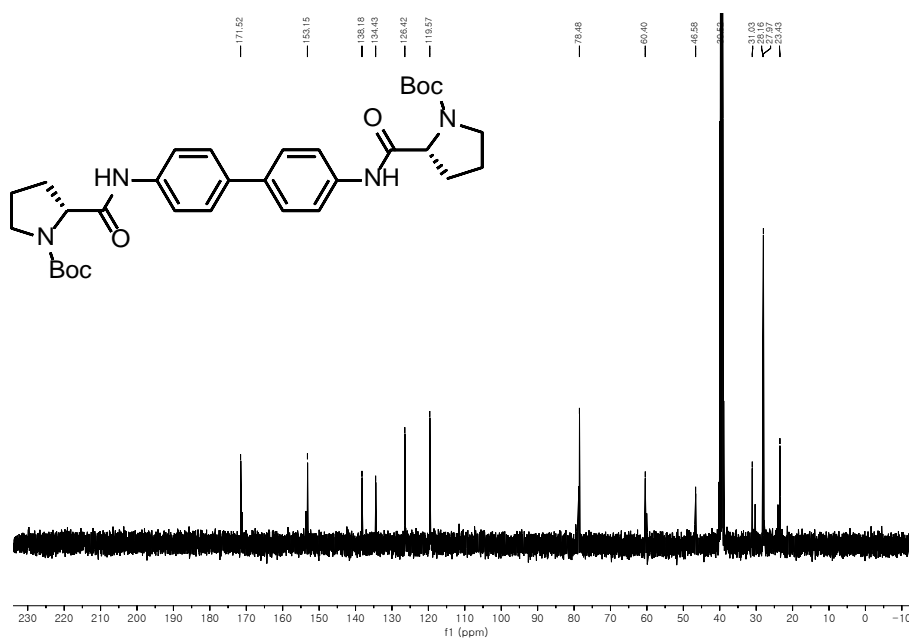
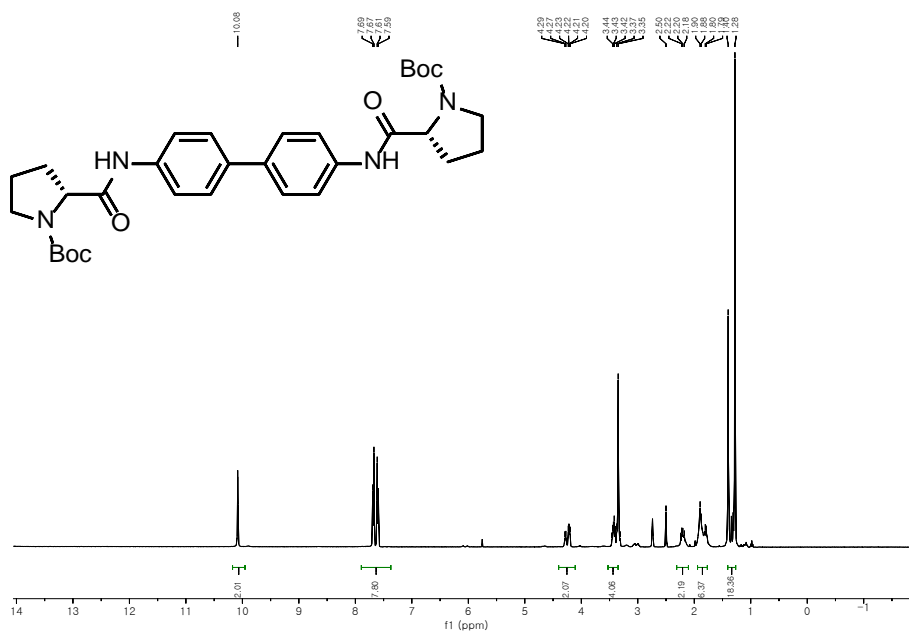




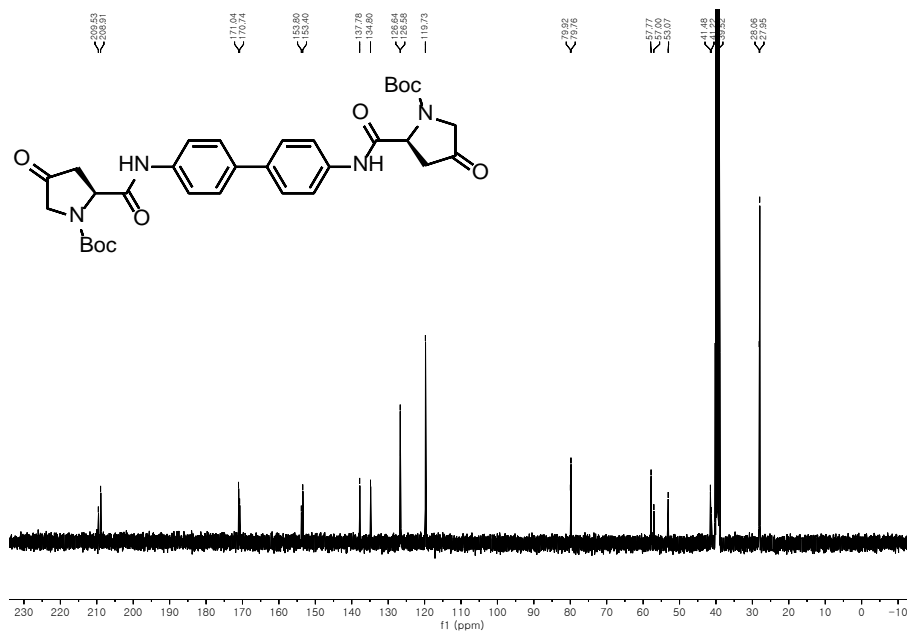
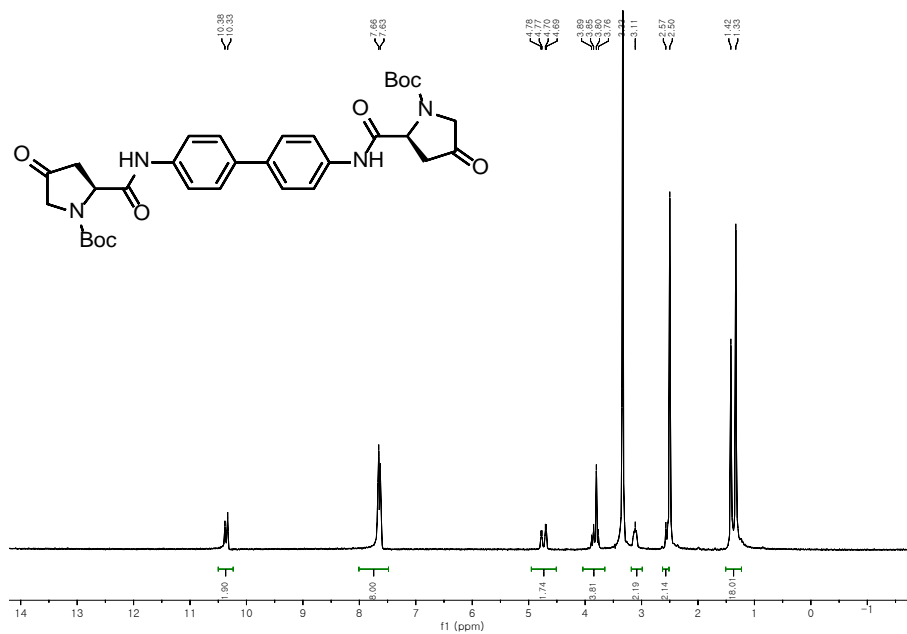
Part I.

Chapter 2.

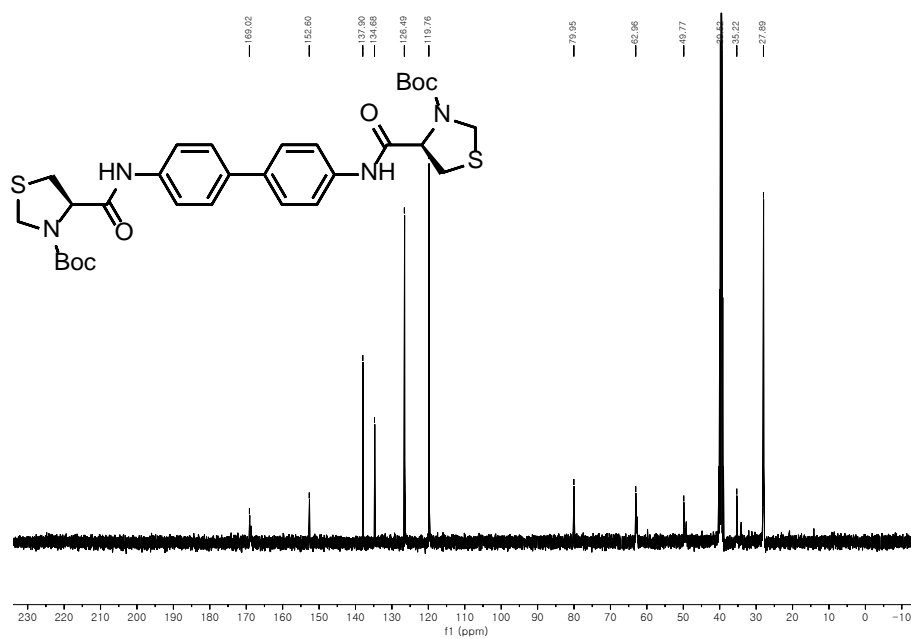
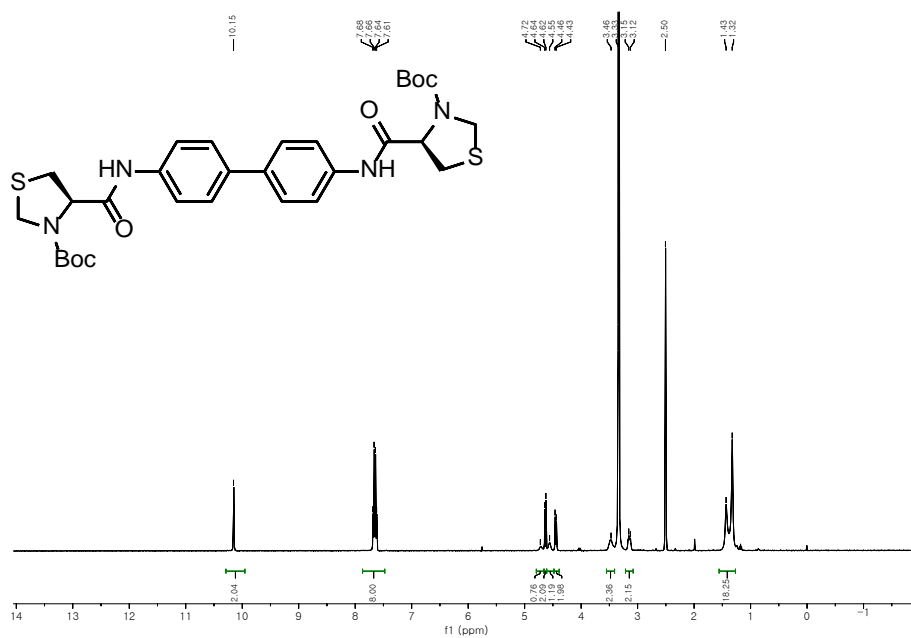
3



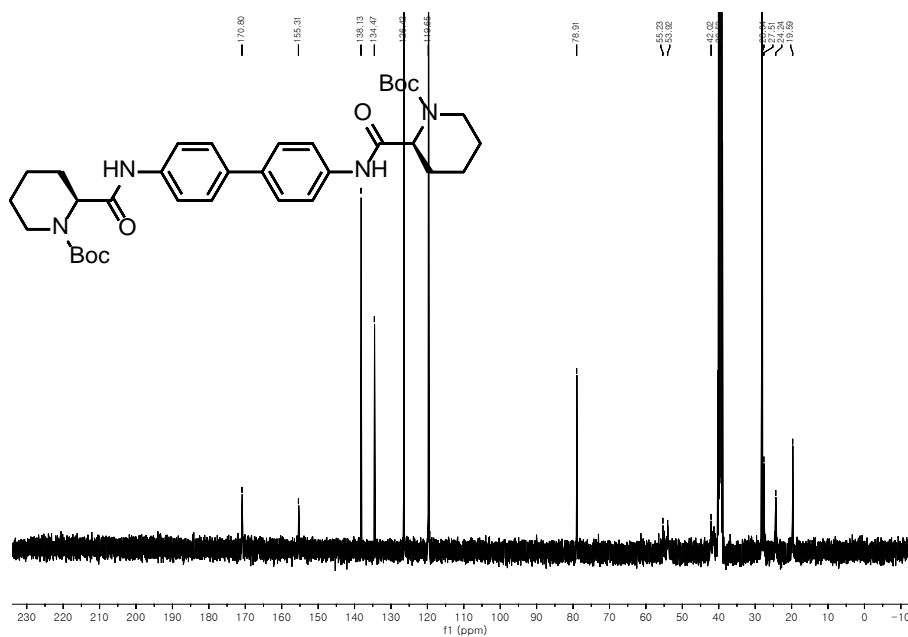
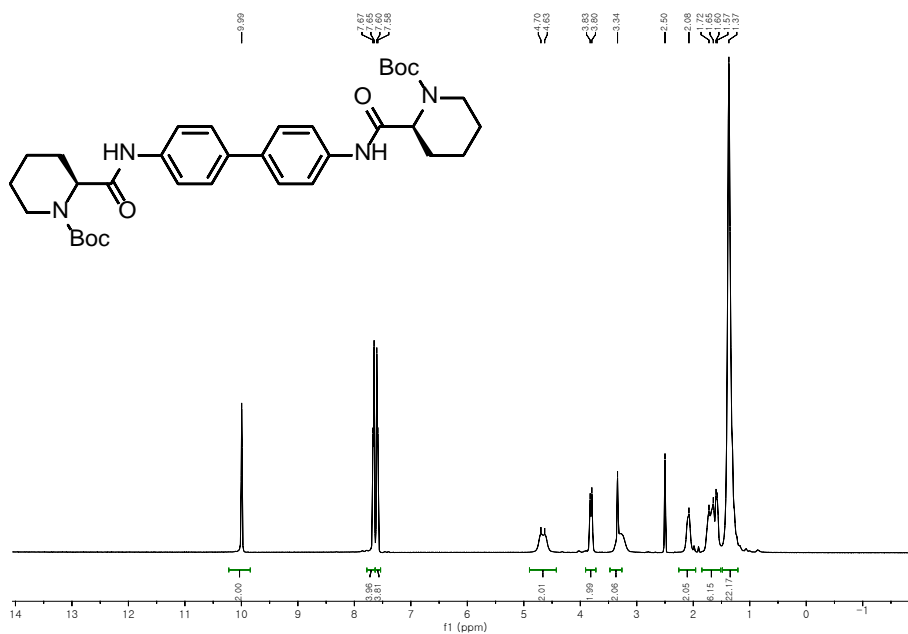
4



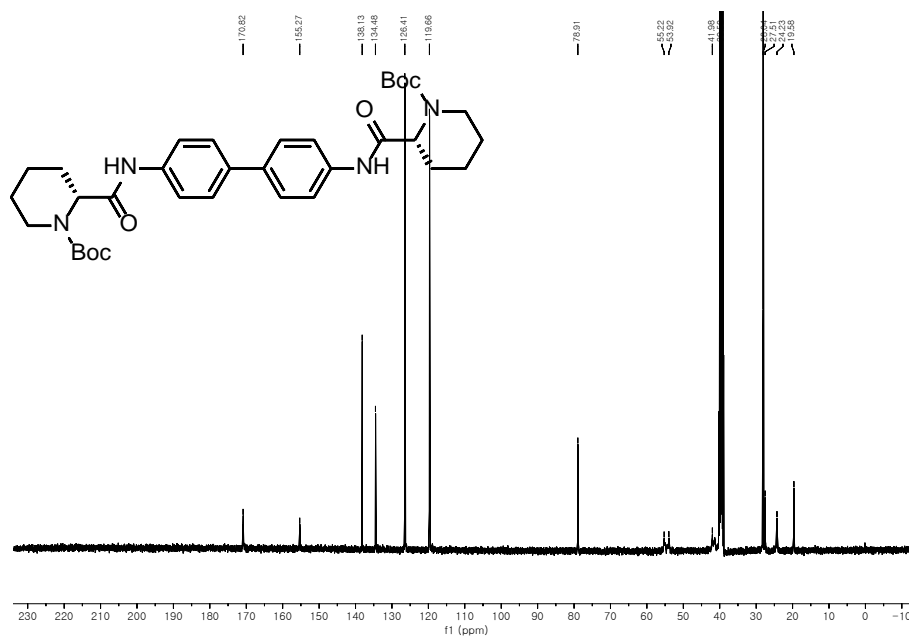
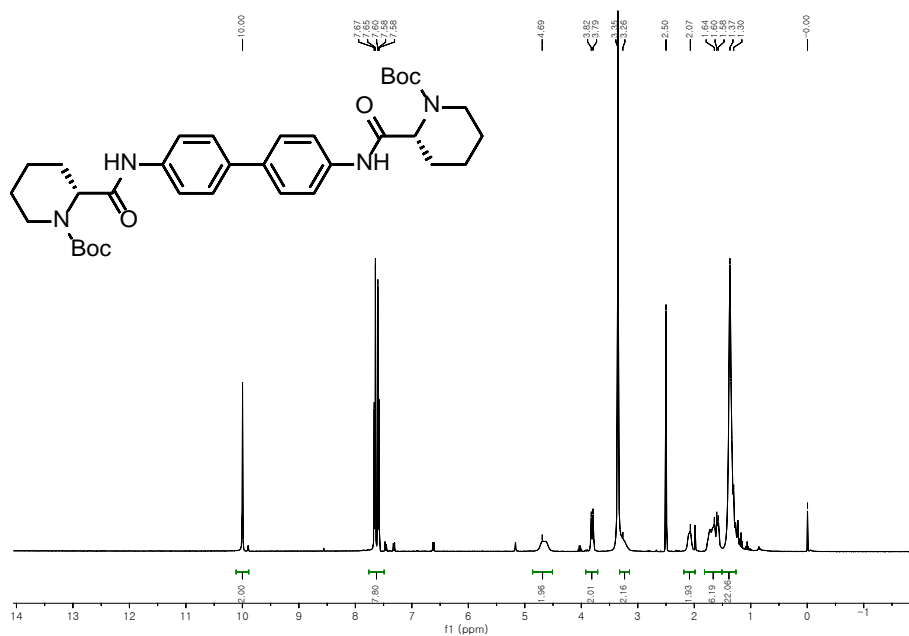
5



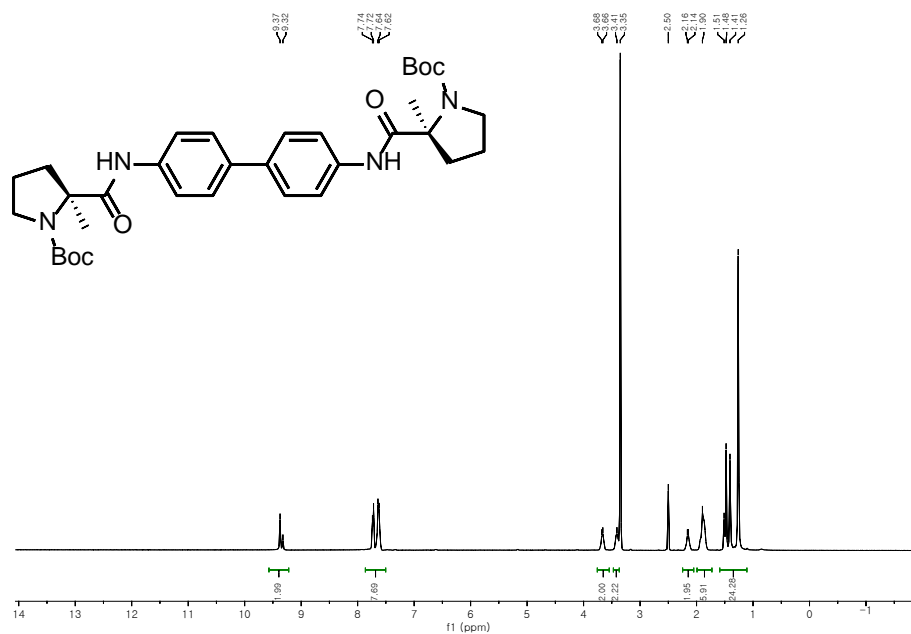
6

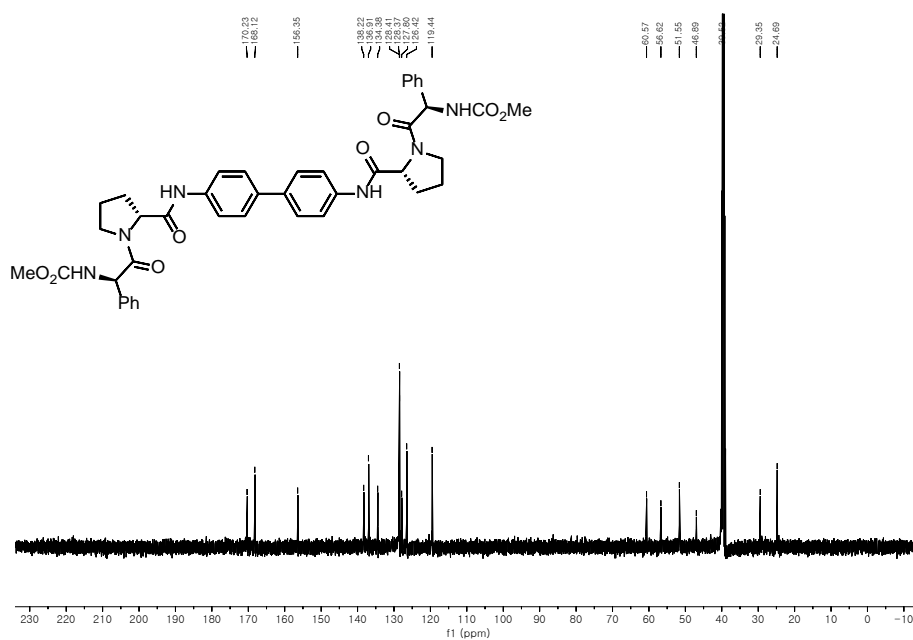


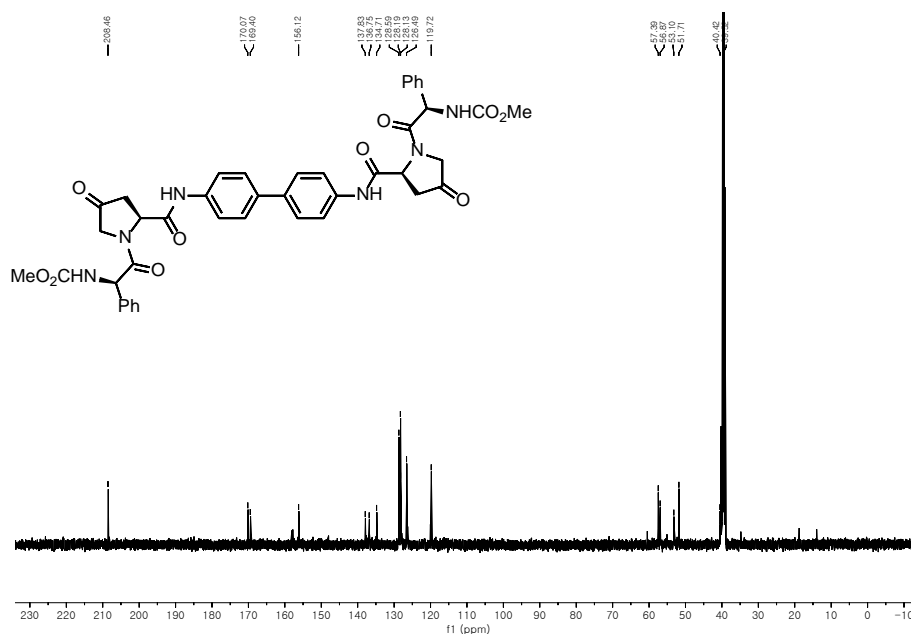
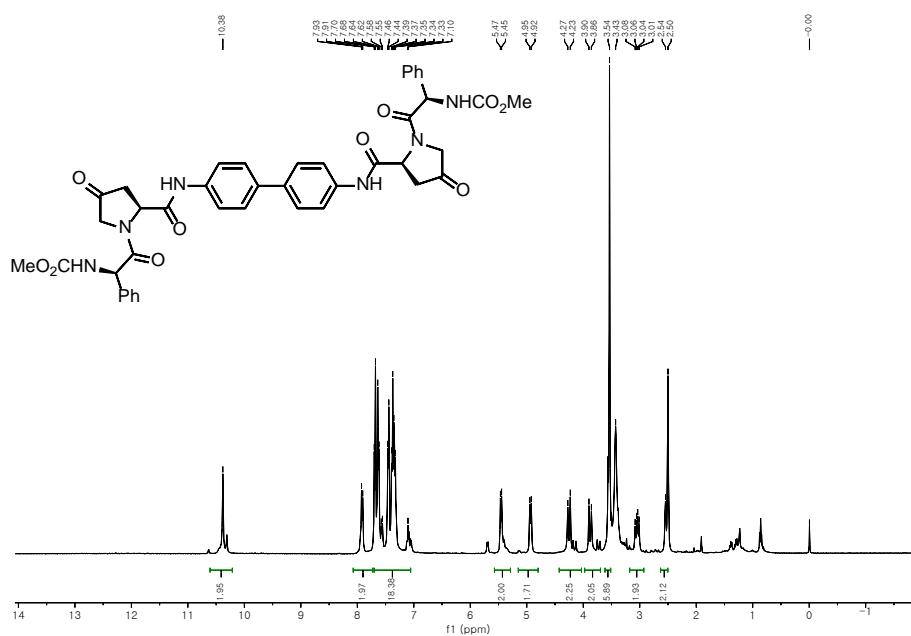
7

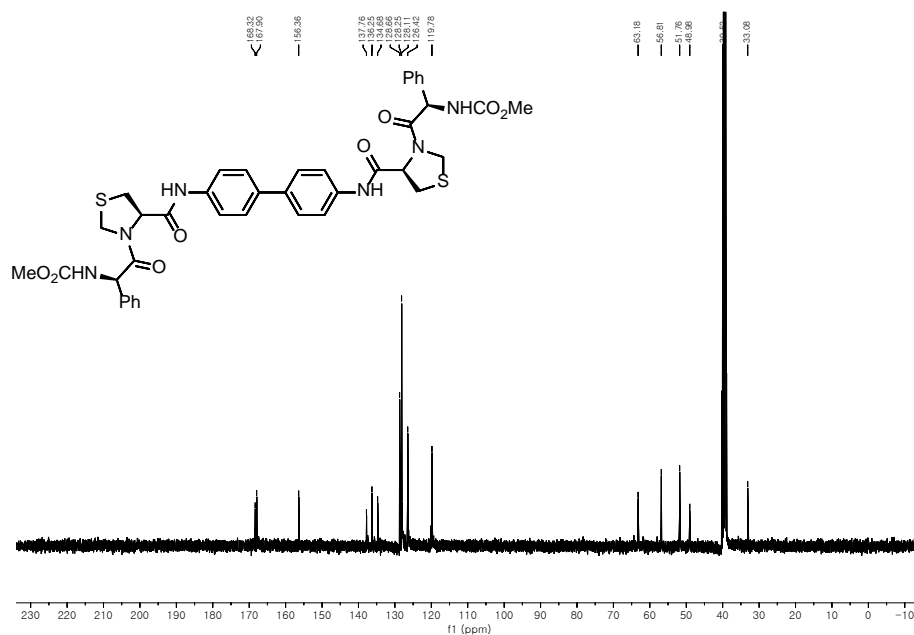
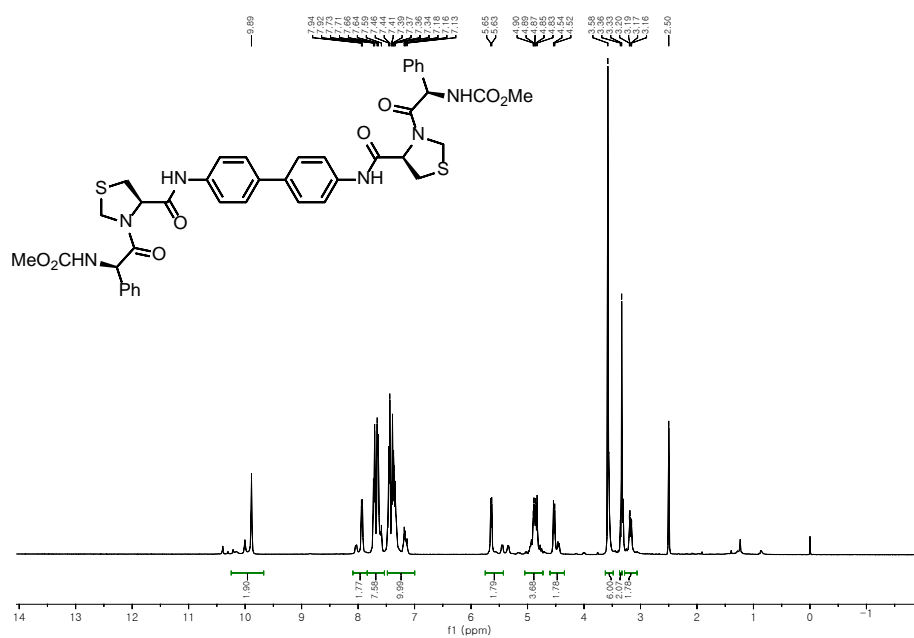


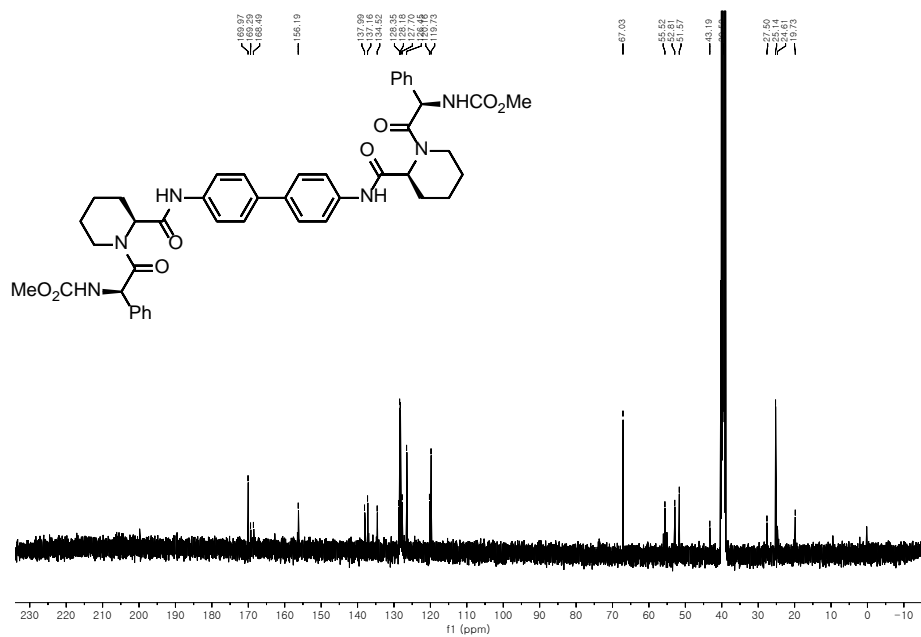
8

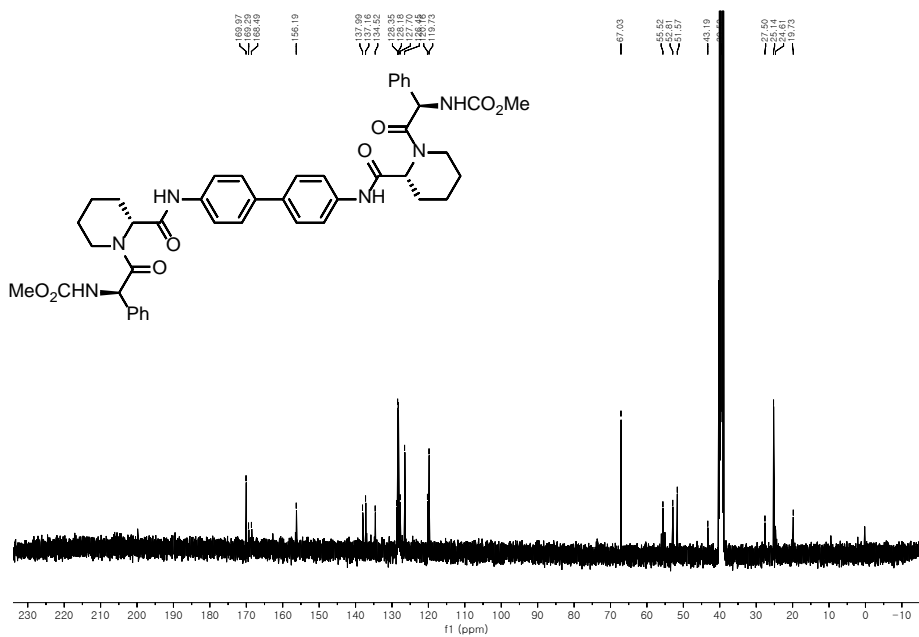


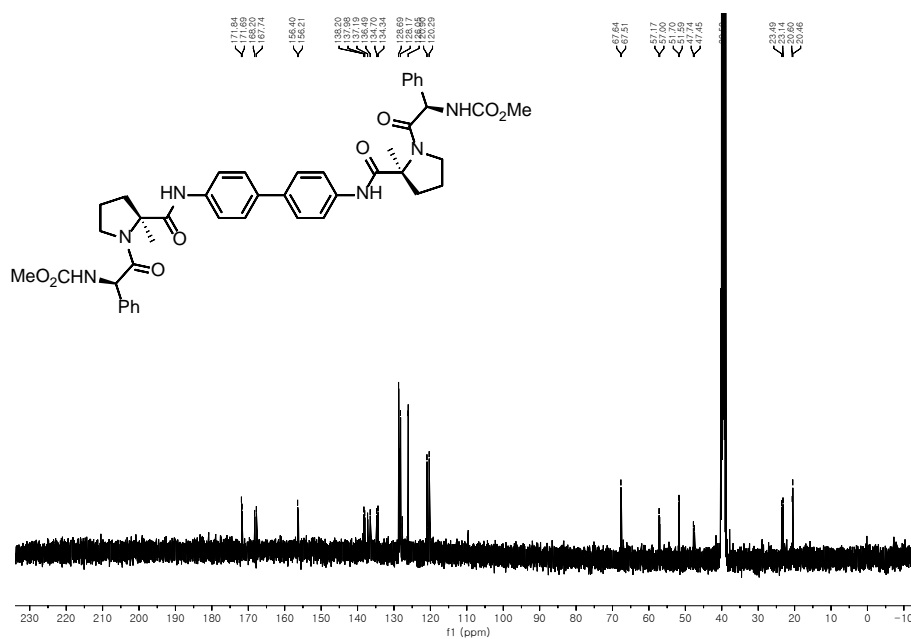








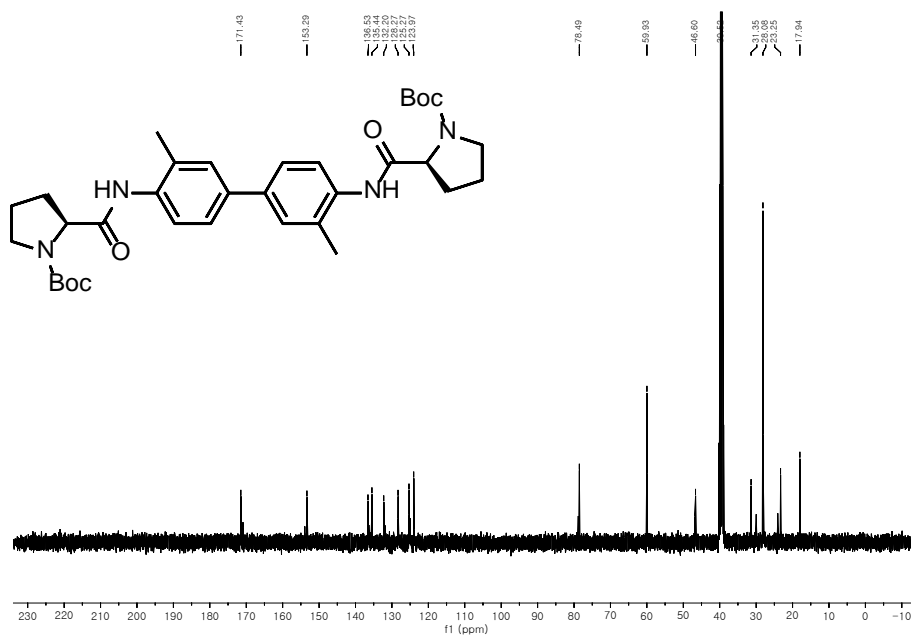


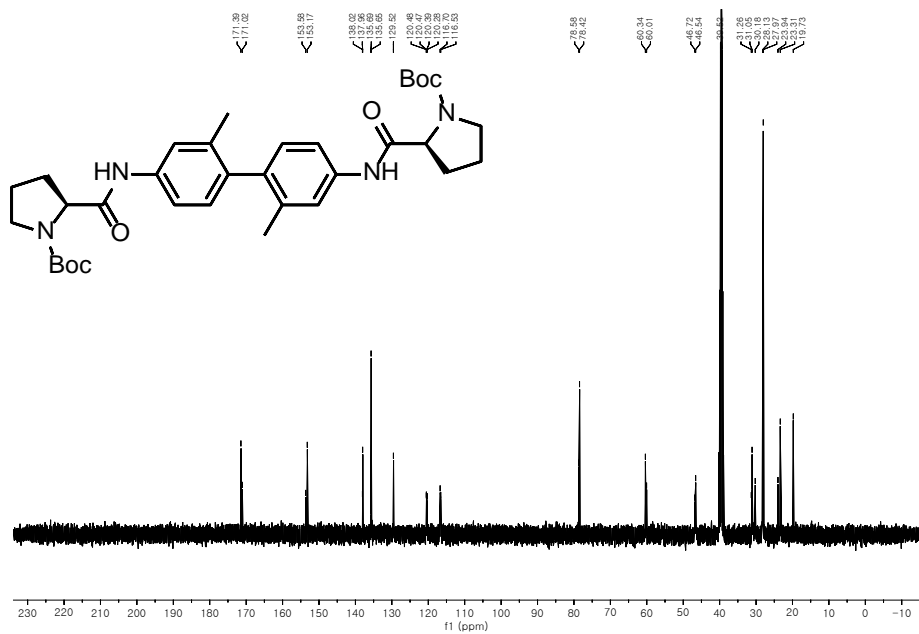


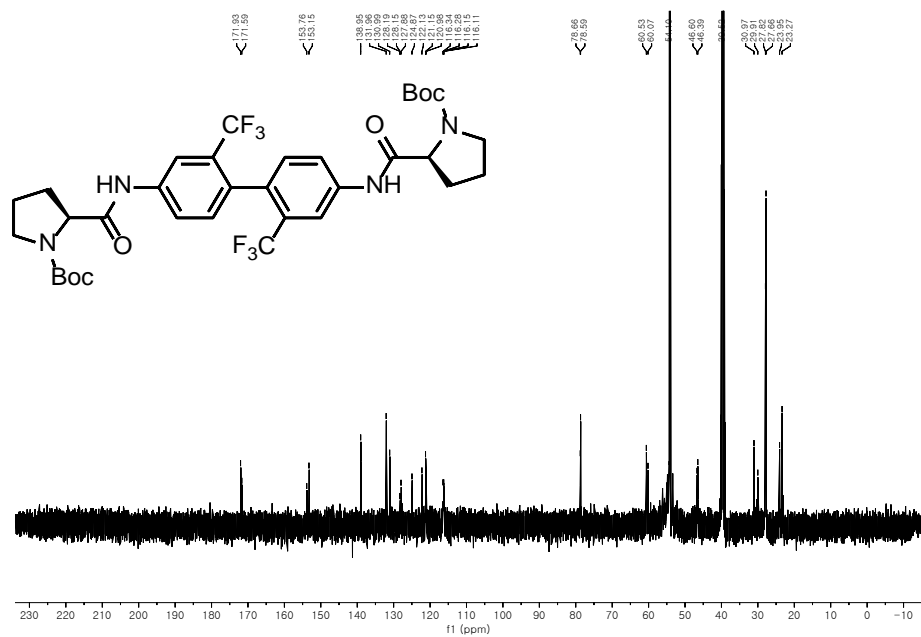
Chemical structure of compound 10 is shown above the ^1H NMR spectrum. The structure is a symmetrical molecule consisting of two 2-(Boc-2-oxo-2,3-dihydro-1H-pyrrol-1-yl)-4-methylphenyl groups linked by a biphenyl core.

The ^1H NMR spectrum (CDCl₃) shows the following peaks and integrations:

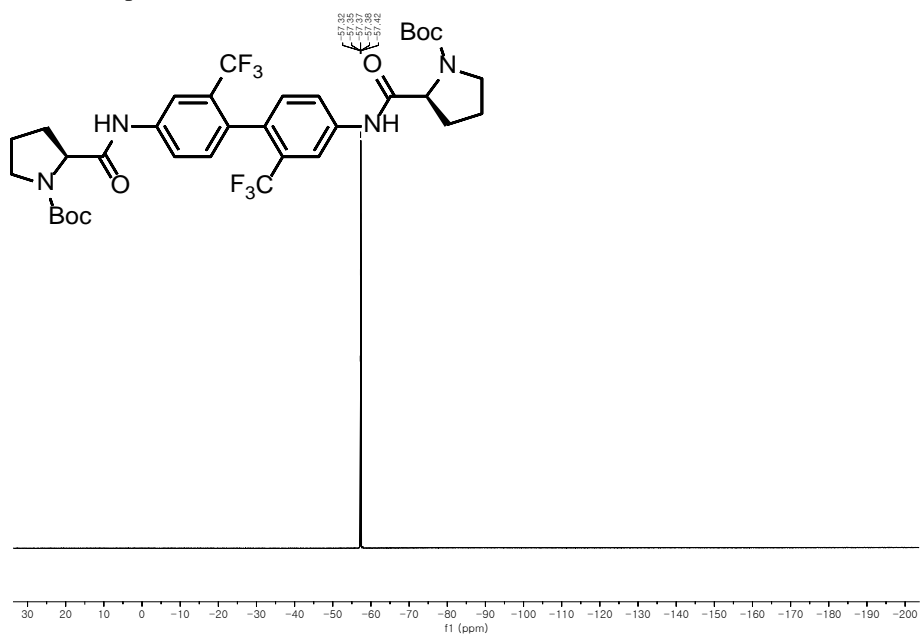
- 9.68 (d, 2H, integration 1.00)
- 7.41-7.44 (m, 8H, integration 0.97)
- 4.35-4.38 (m, 4H, integration 1.00)
- 2.41-2.44 (m, 8H, integration 0.99)
- 1.32-1.35 (s, 18H, integration 2.4, 1.00, 18.0)



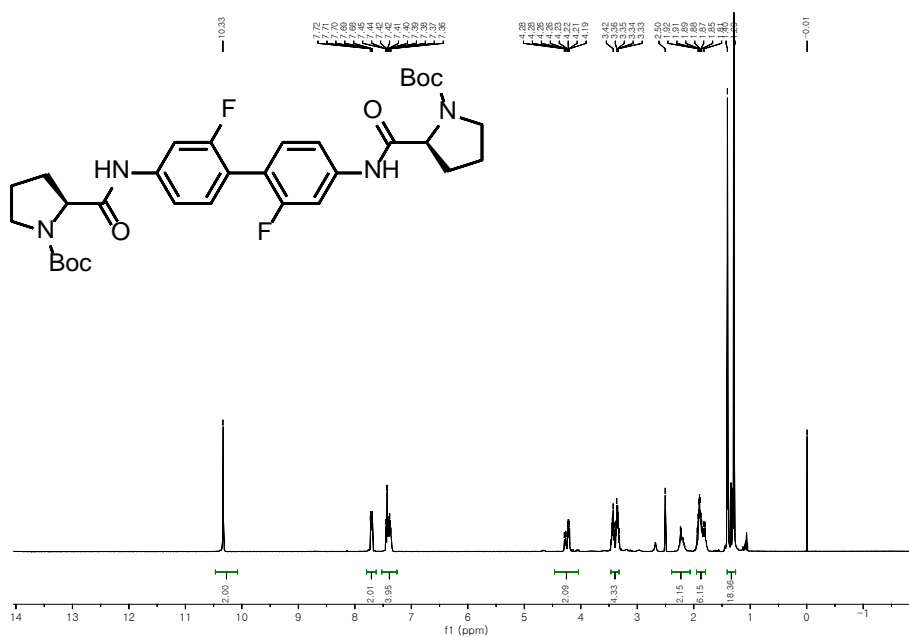


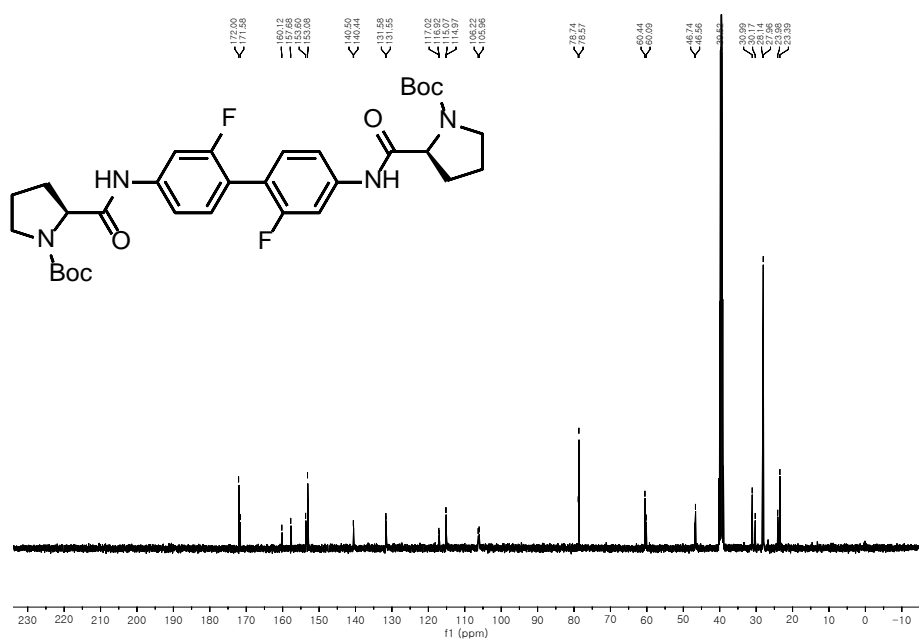


^{19}F NMR Spectrum of **19**

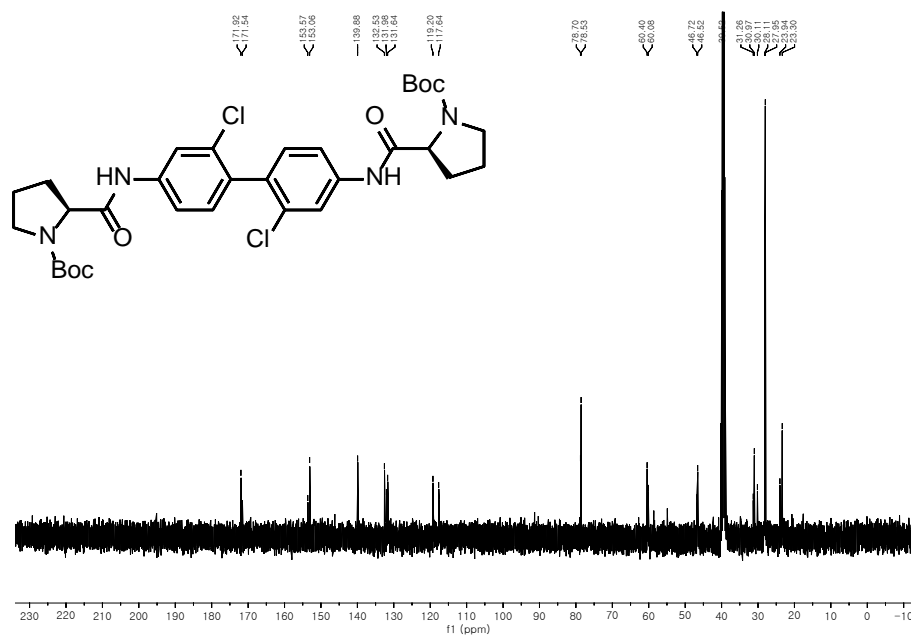
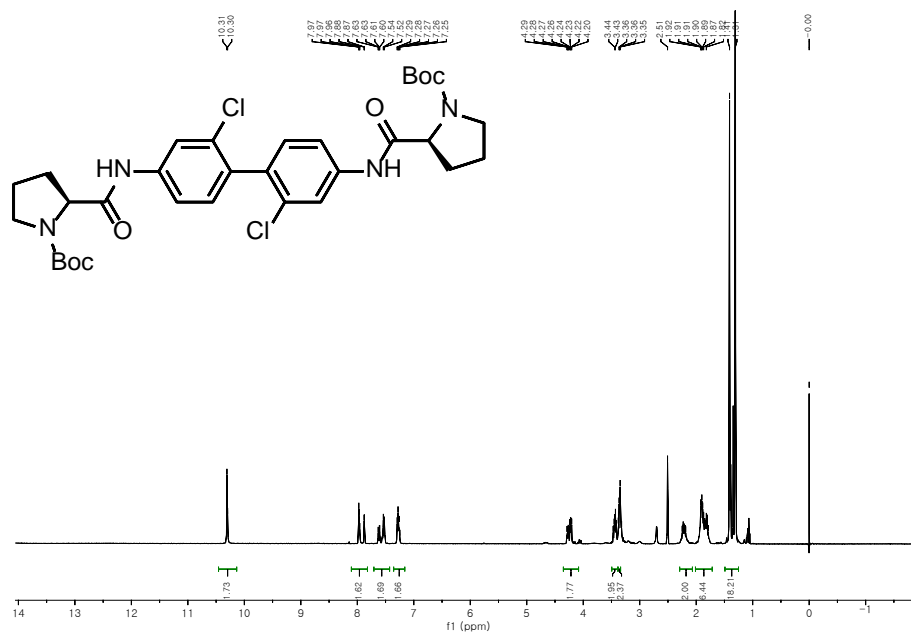


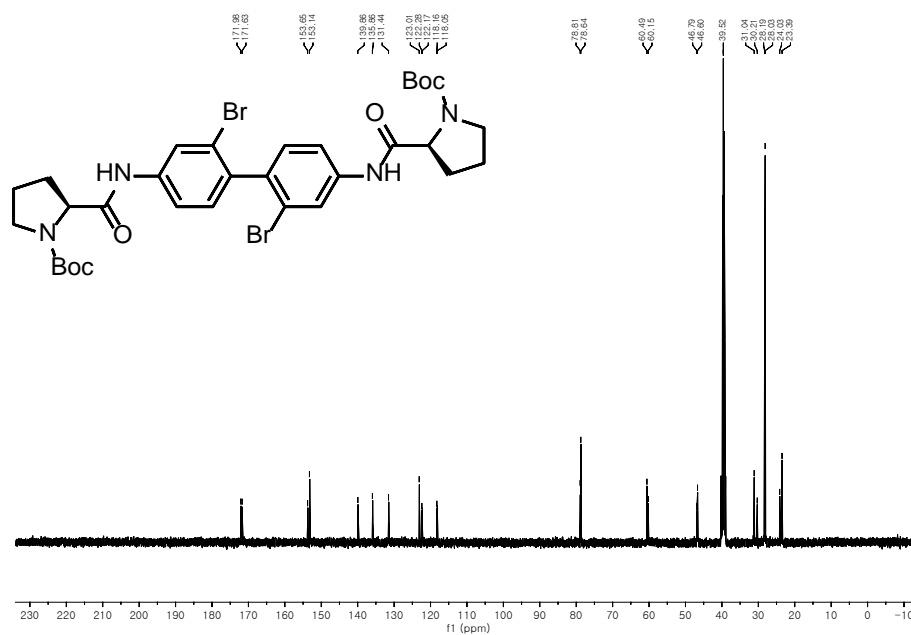
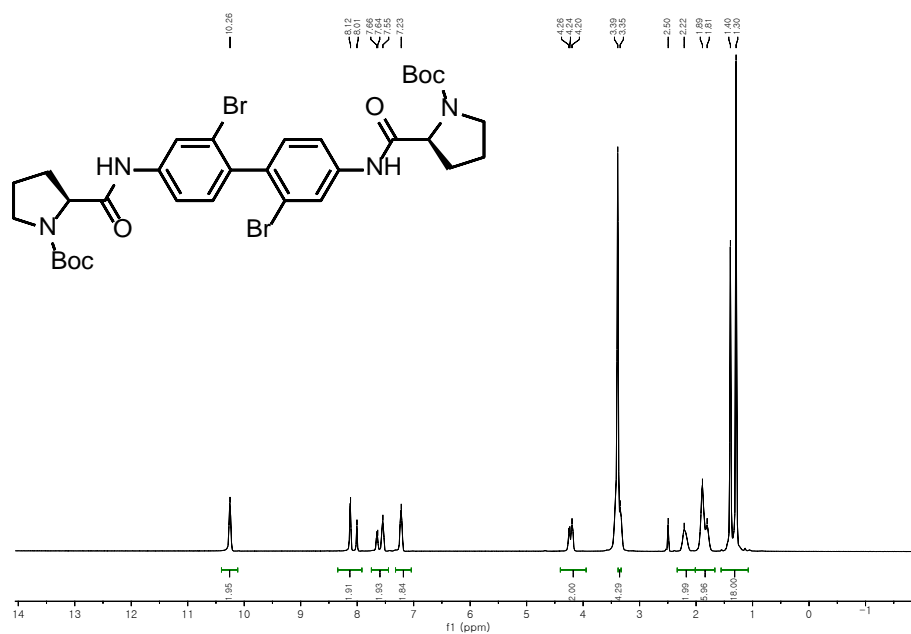
20

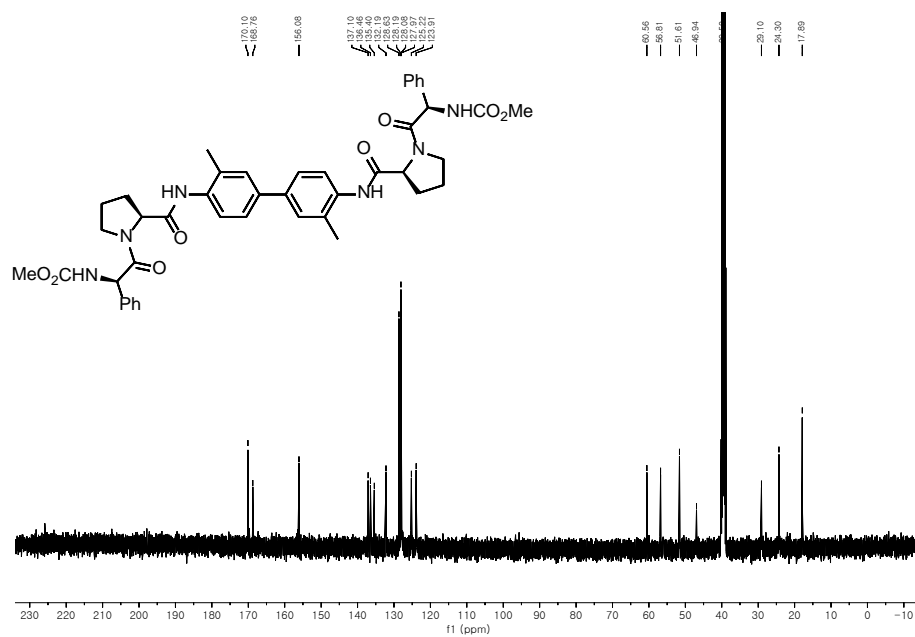
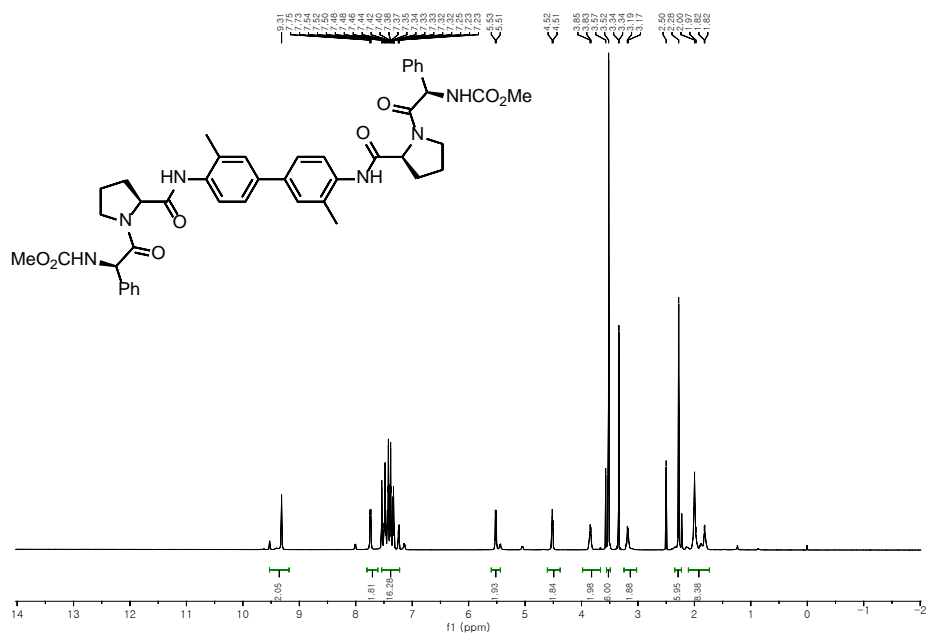


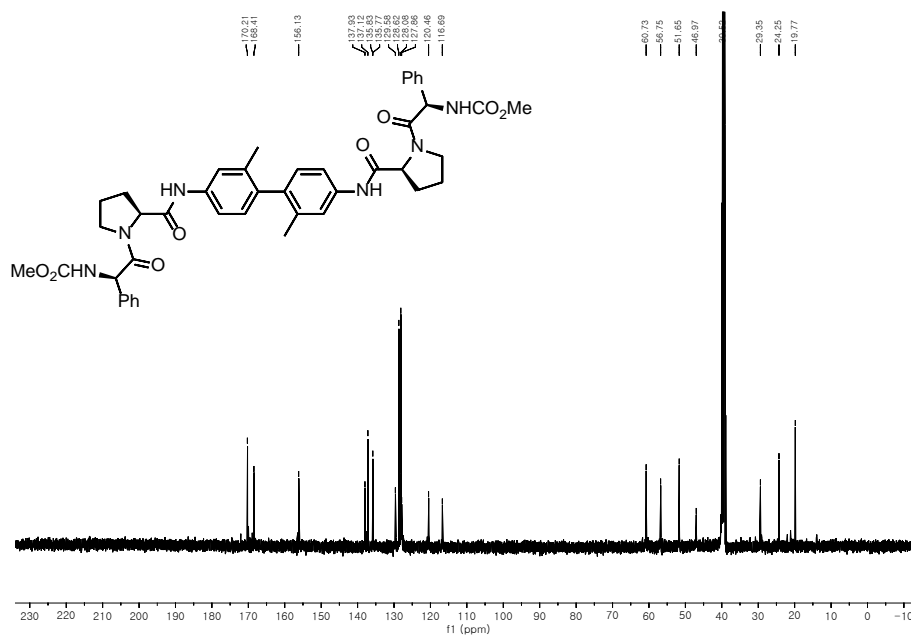
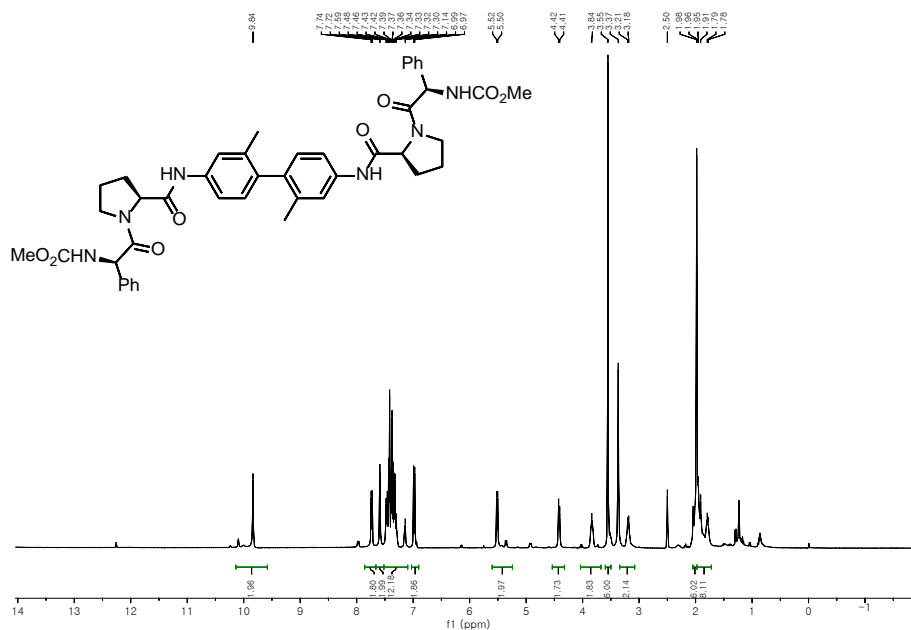


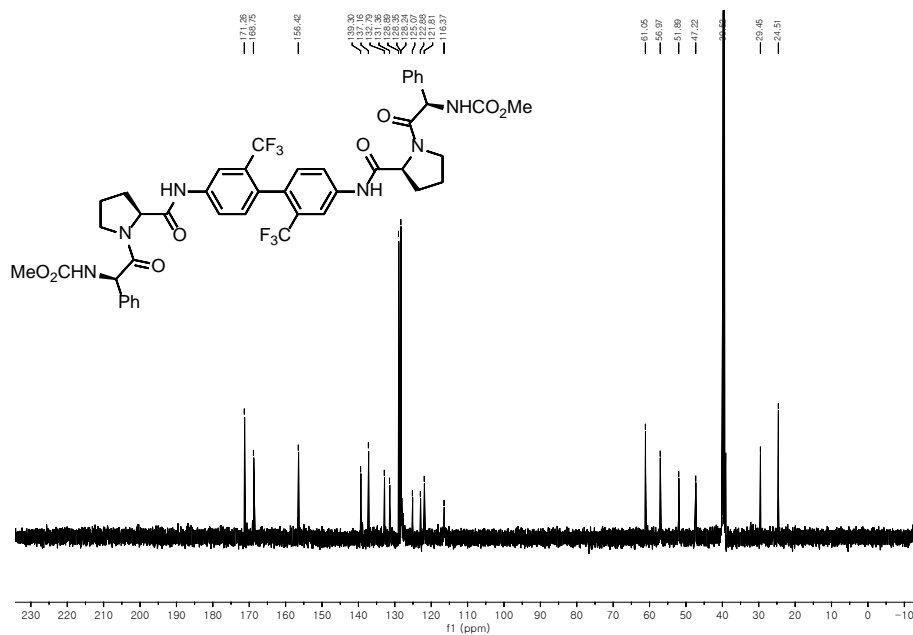
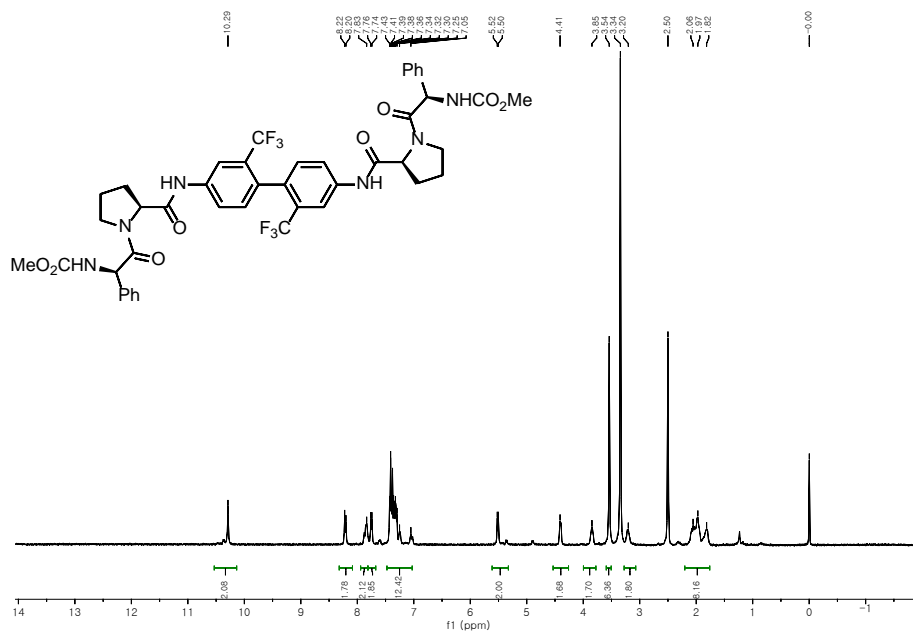
21



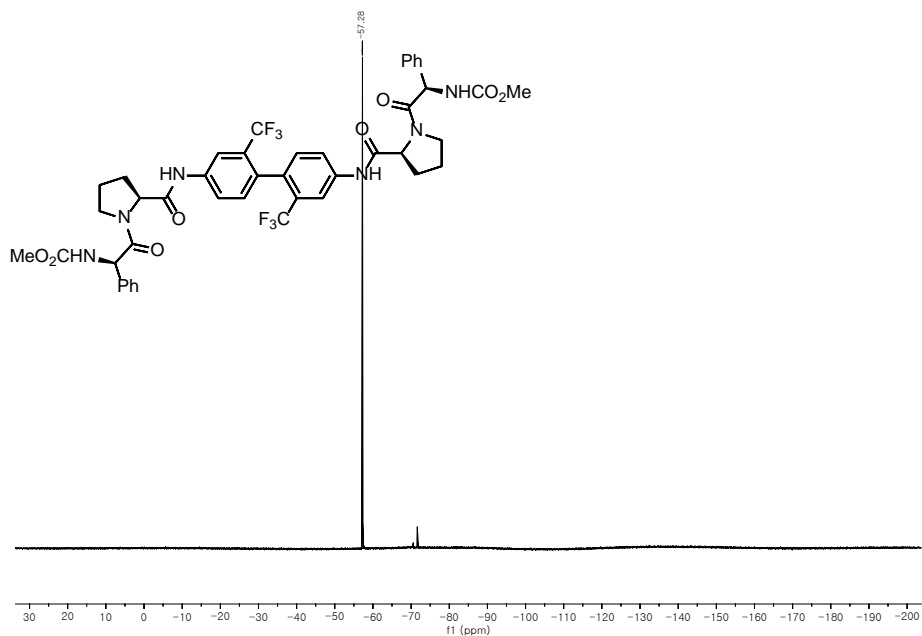




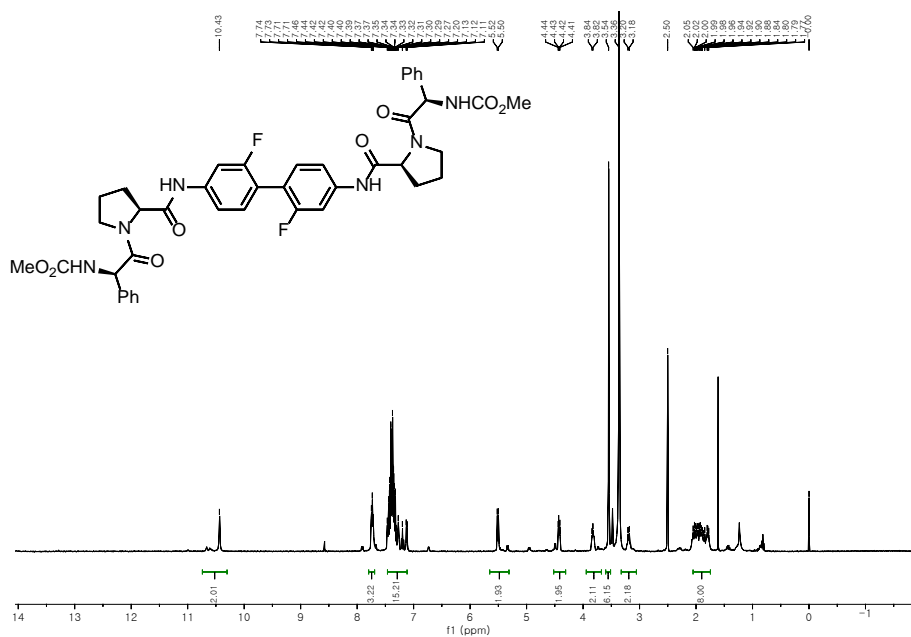


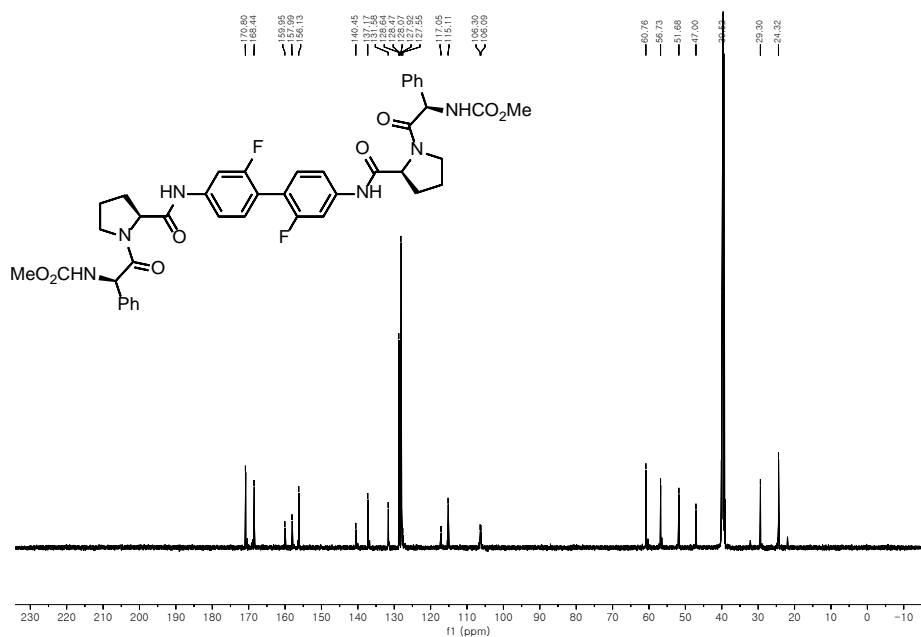


¹⁹F NMR Spectrum of **25**

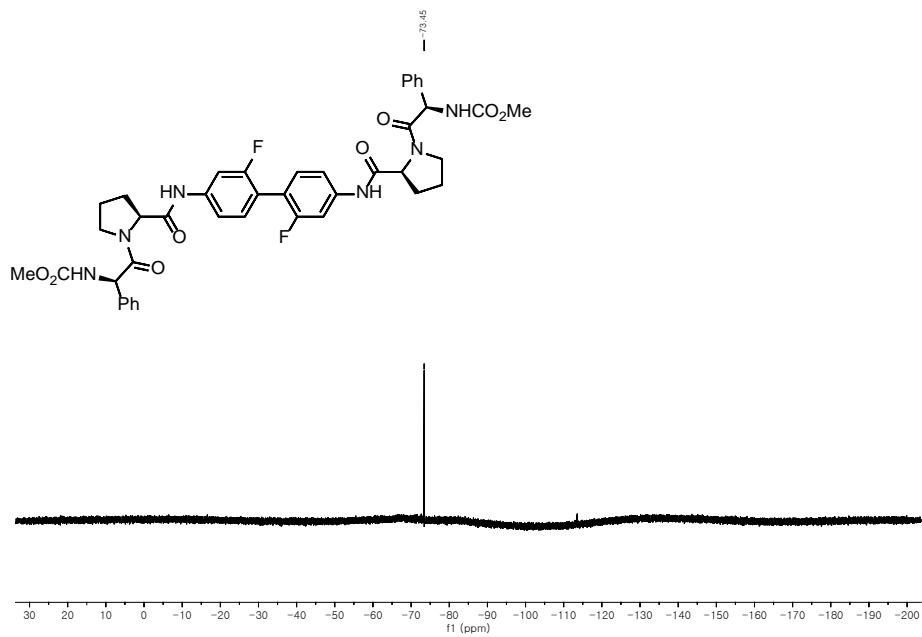


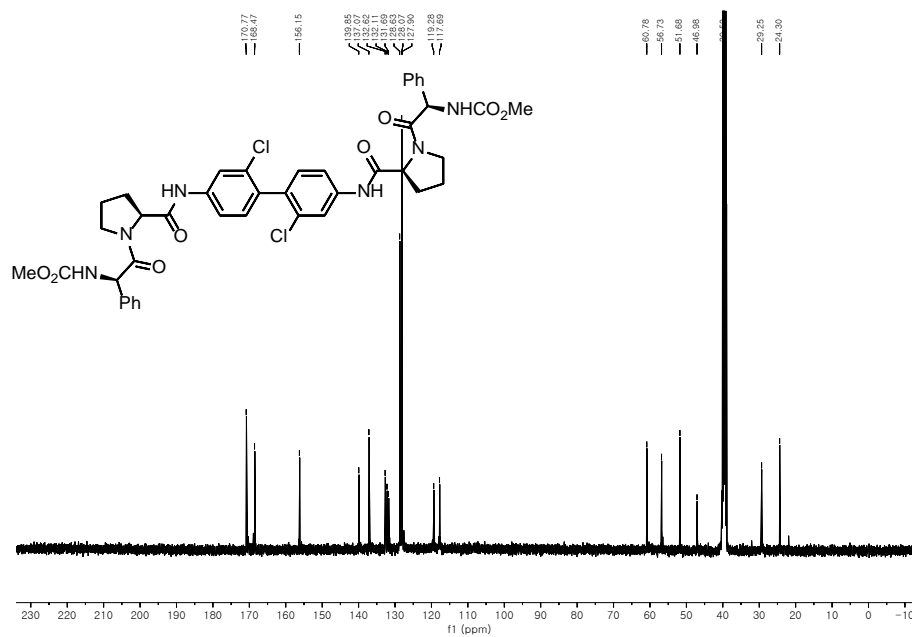
26

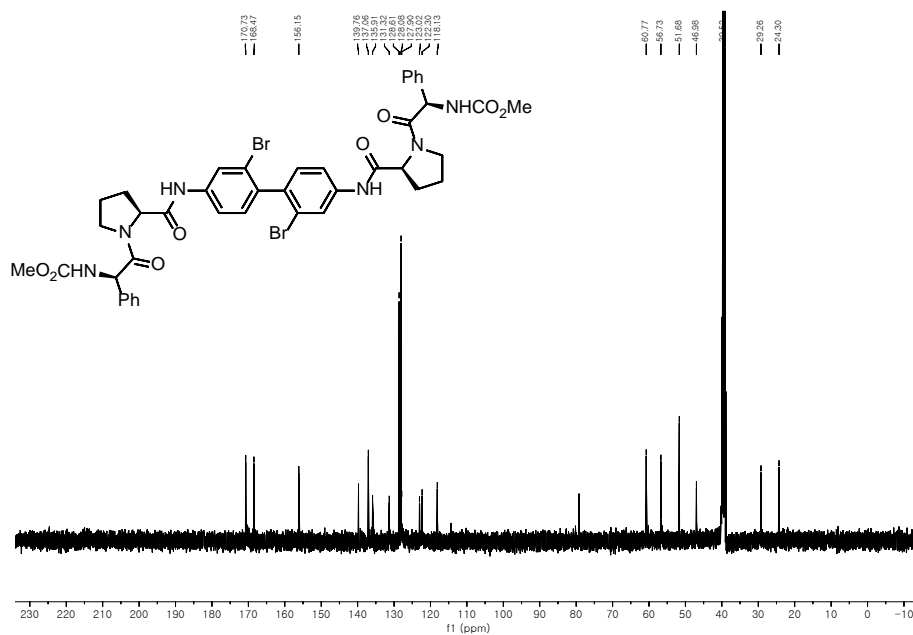


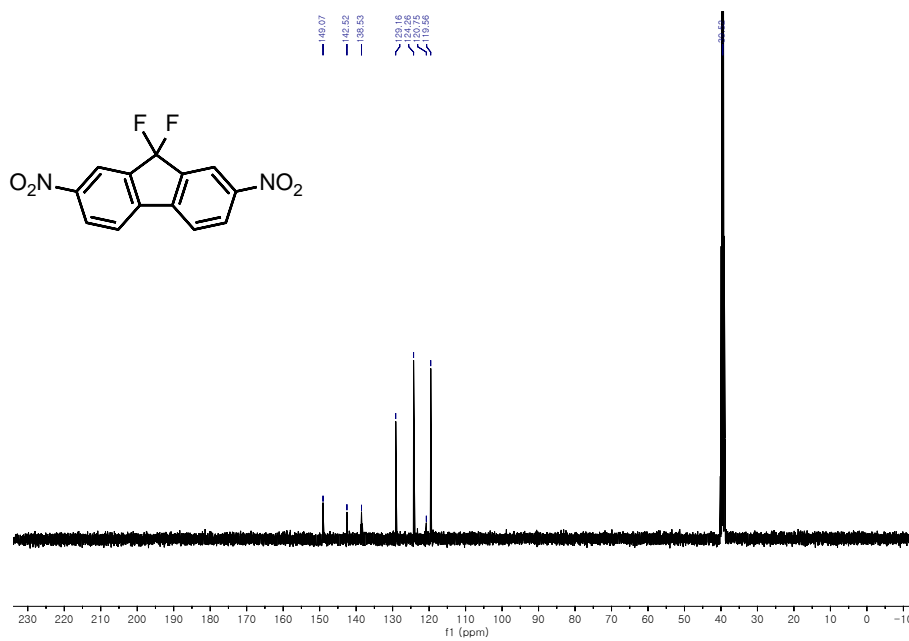


¹⁹F NMR Spectrum of 26

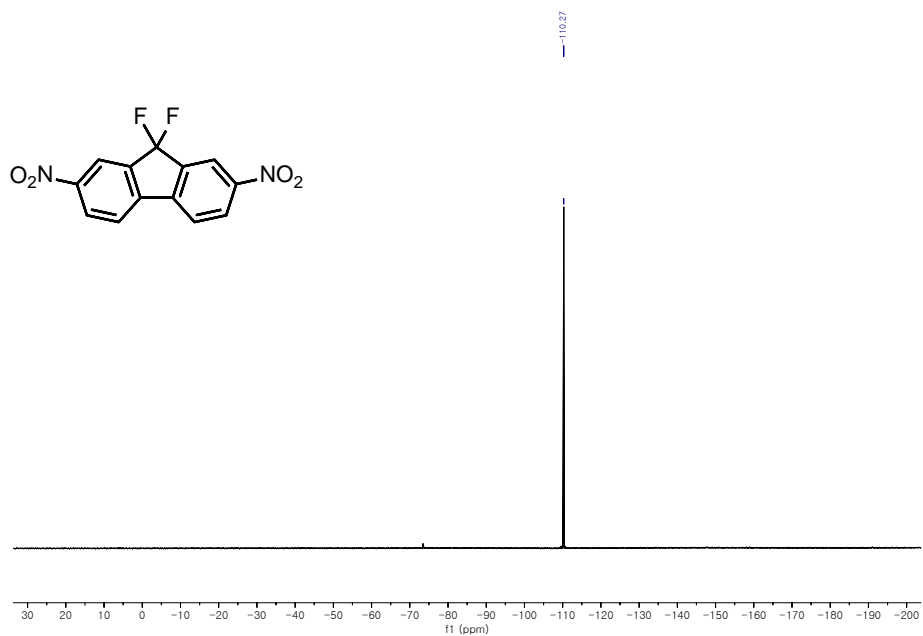




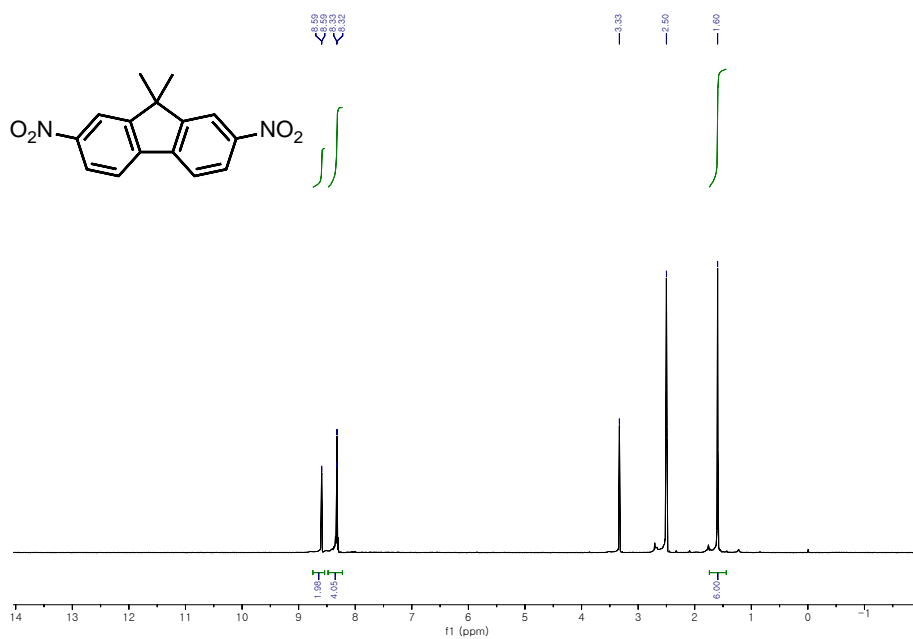


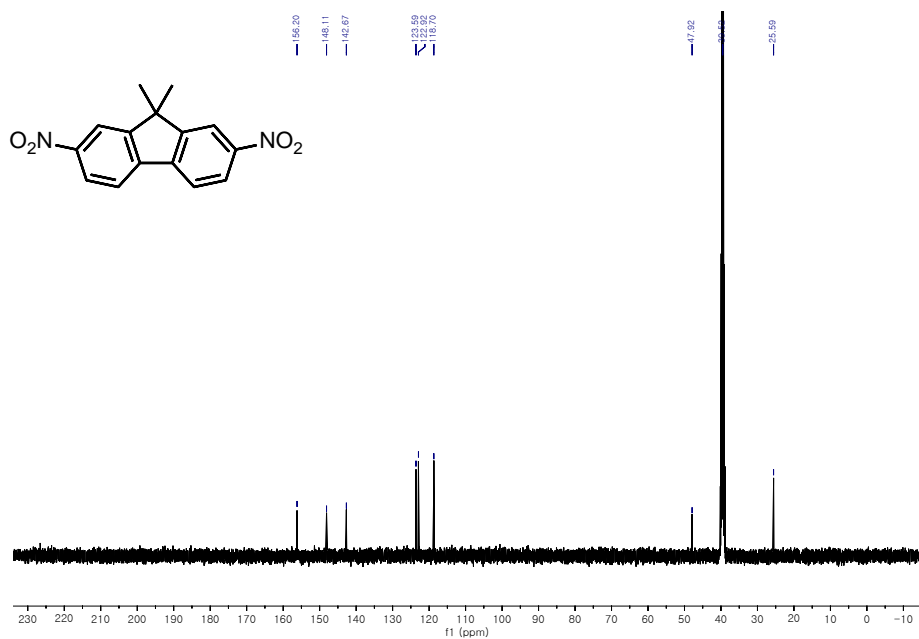


¹⁹F NMR Spectrum of **30**

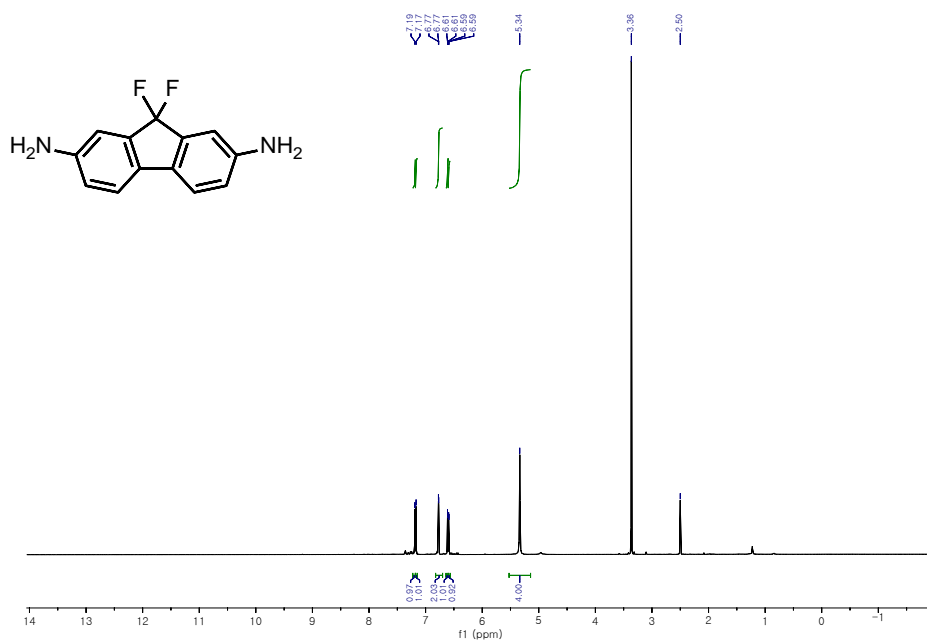


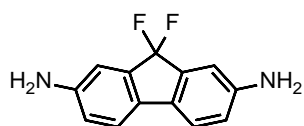
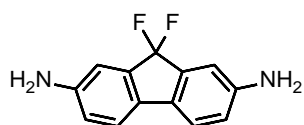
31



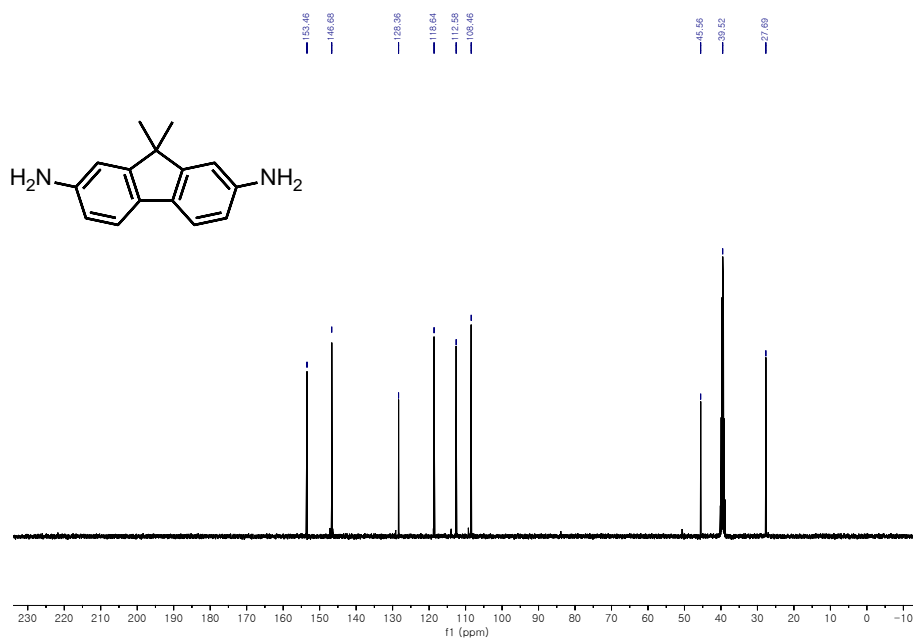
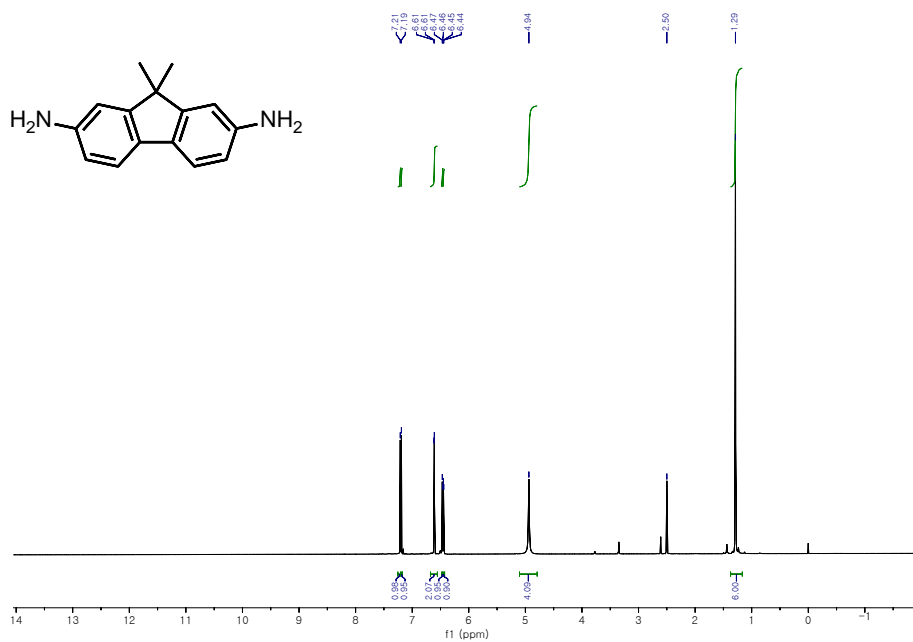


32

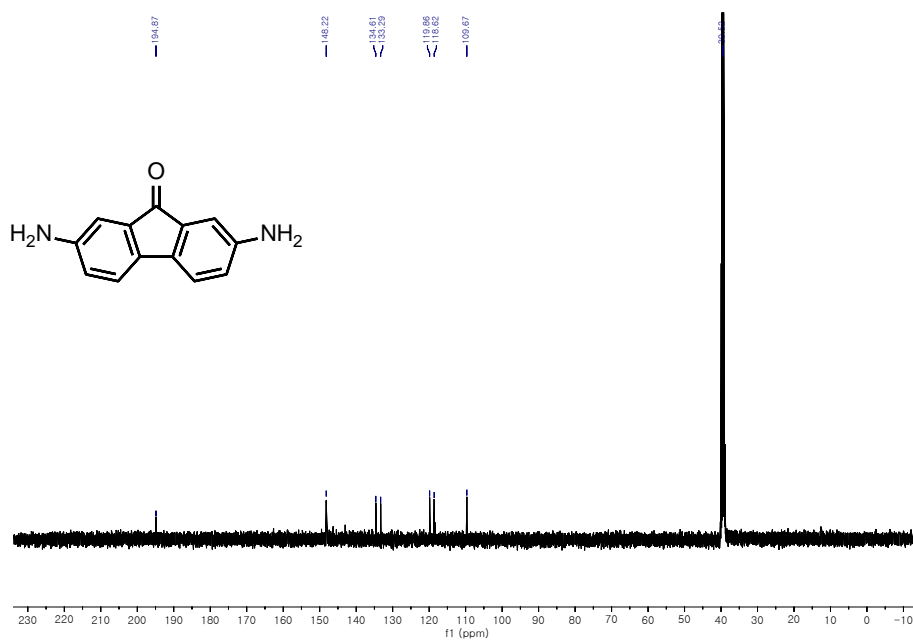
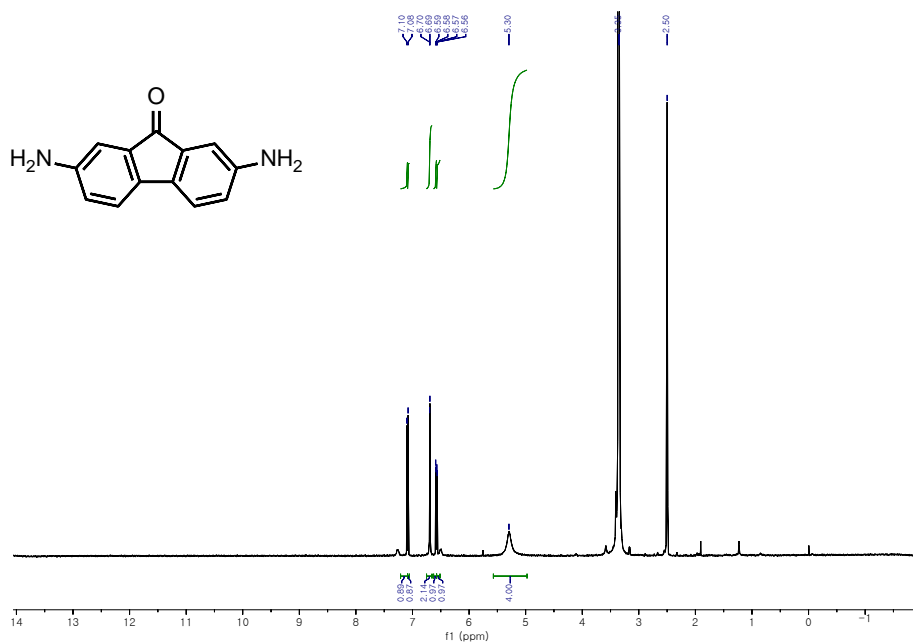


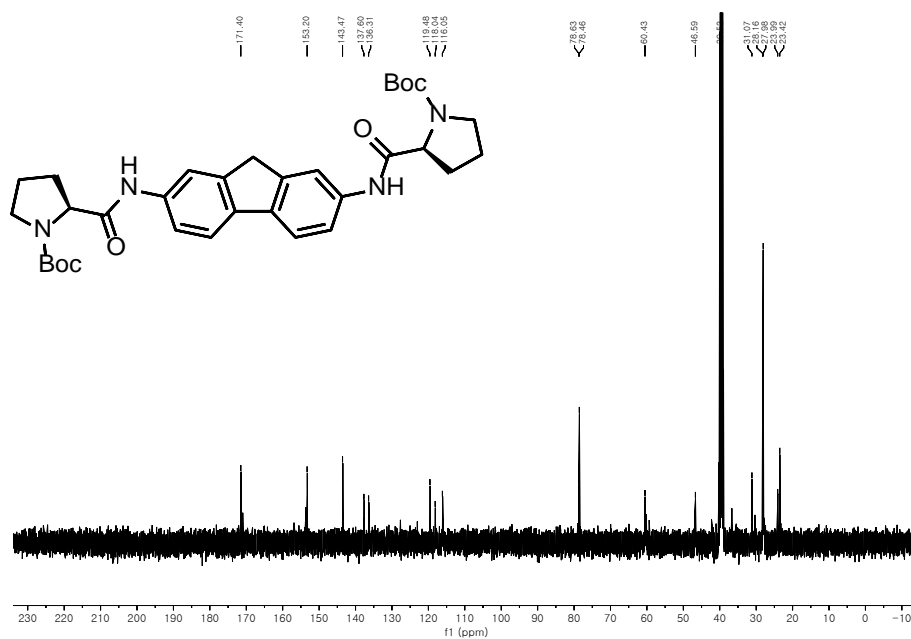
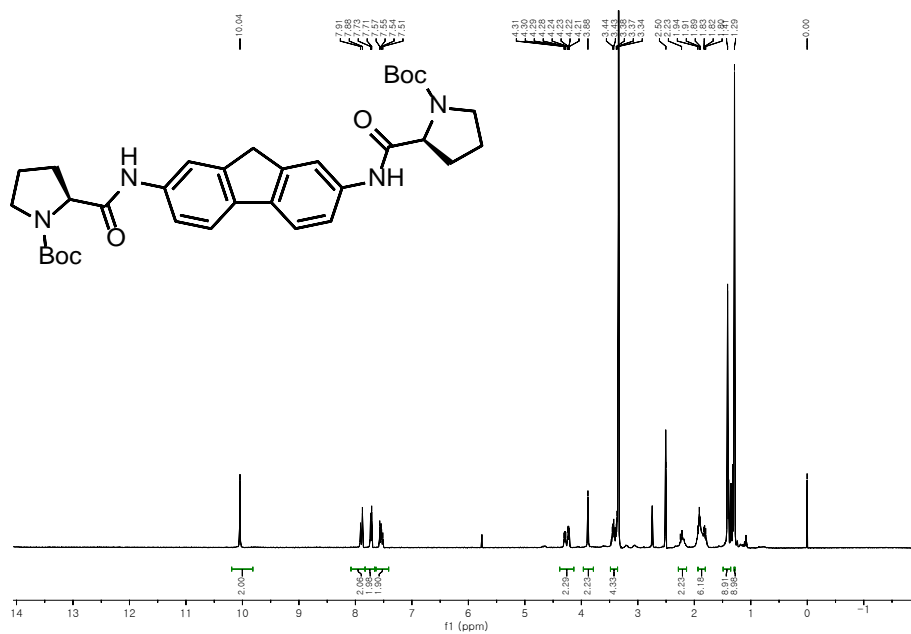
Nc1ccc2c3c(c1)c(c2)C(F)(F)C3

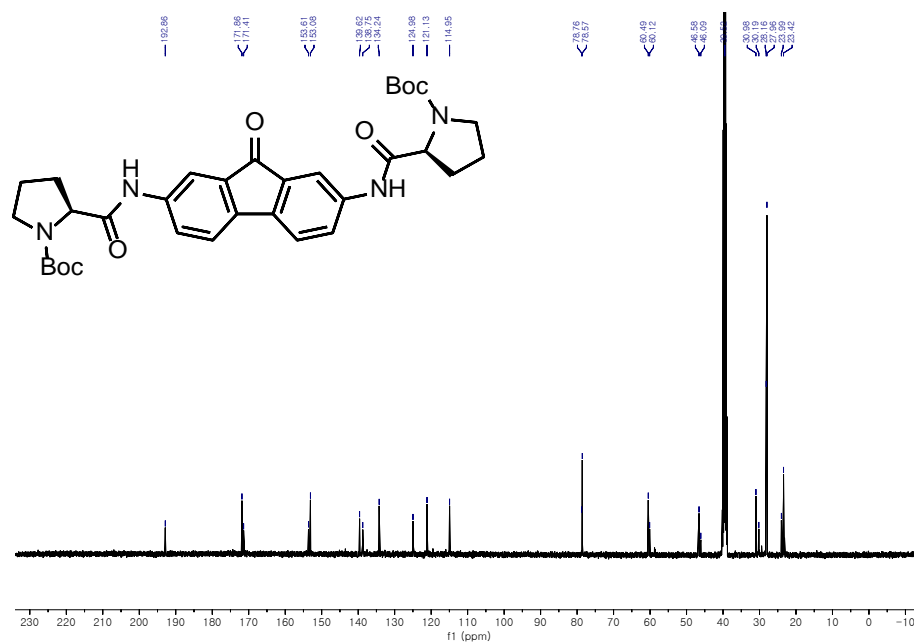
33

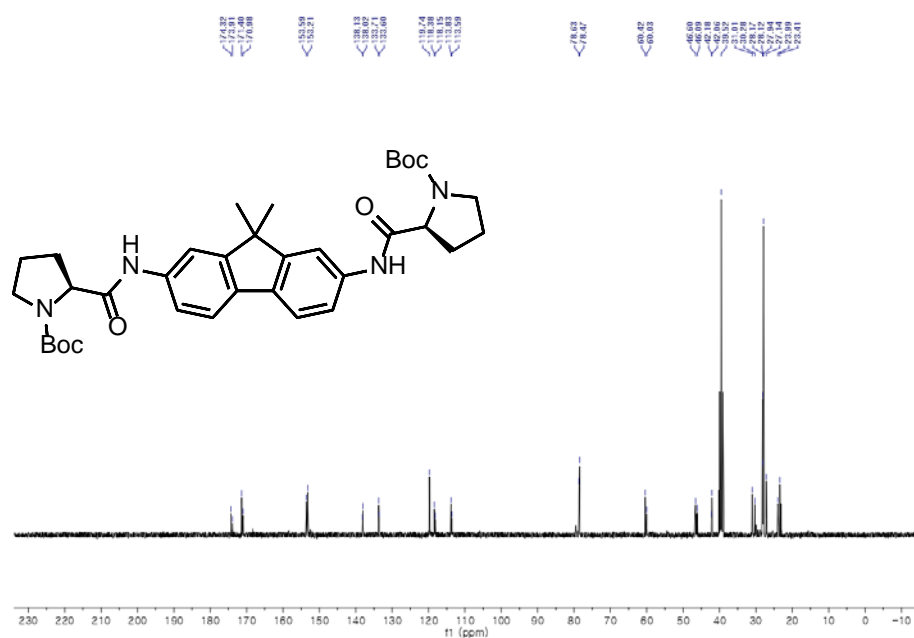


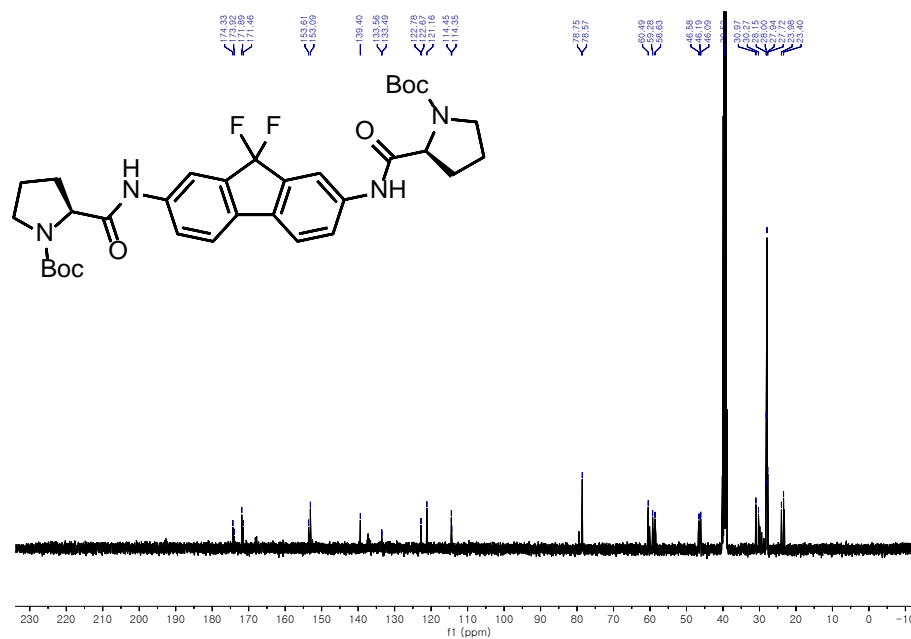
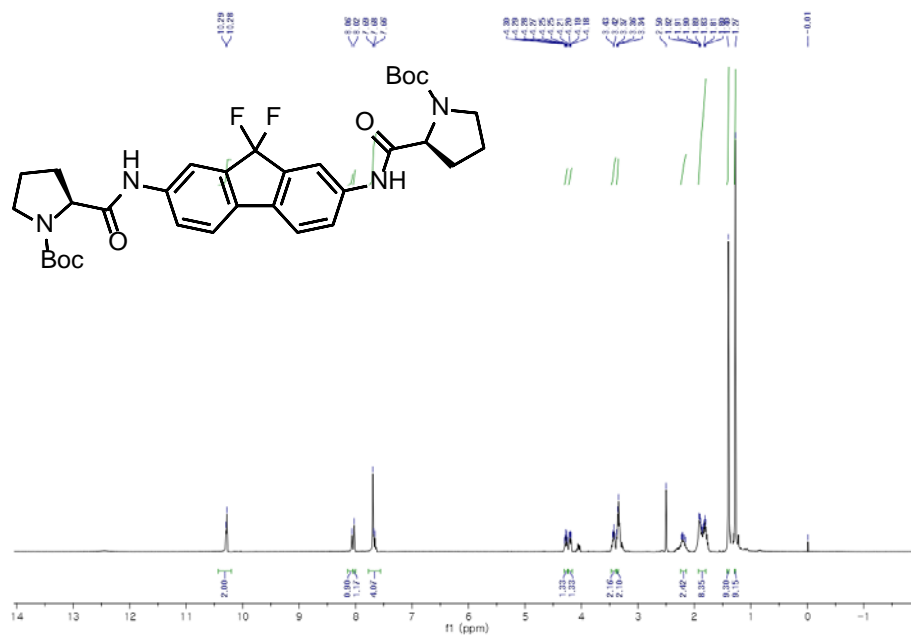
35



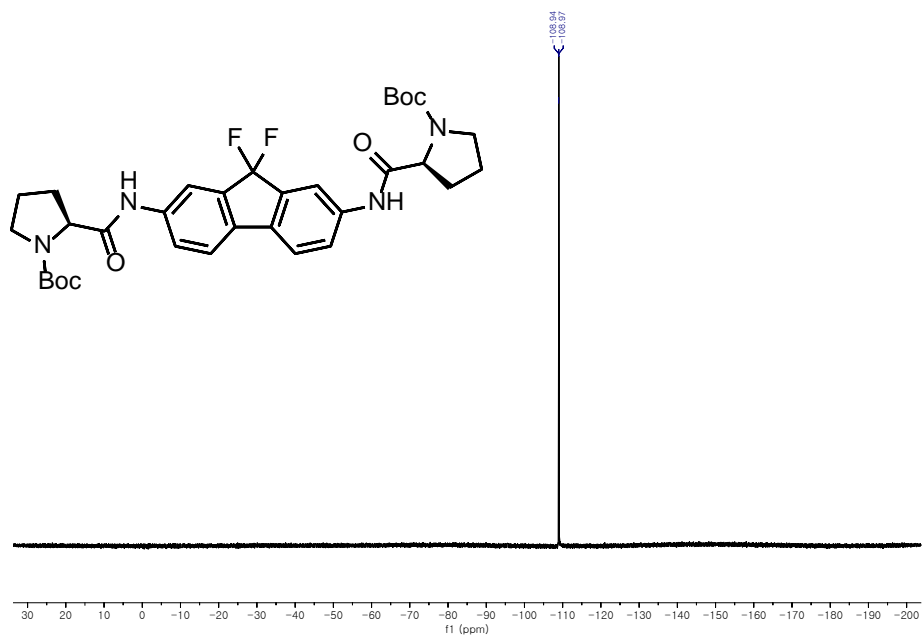




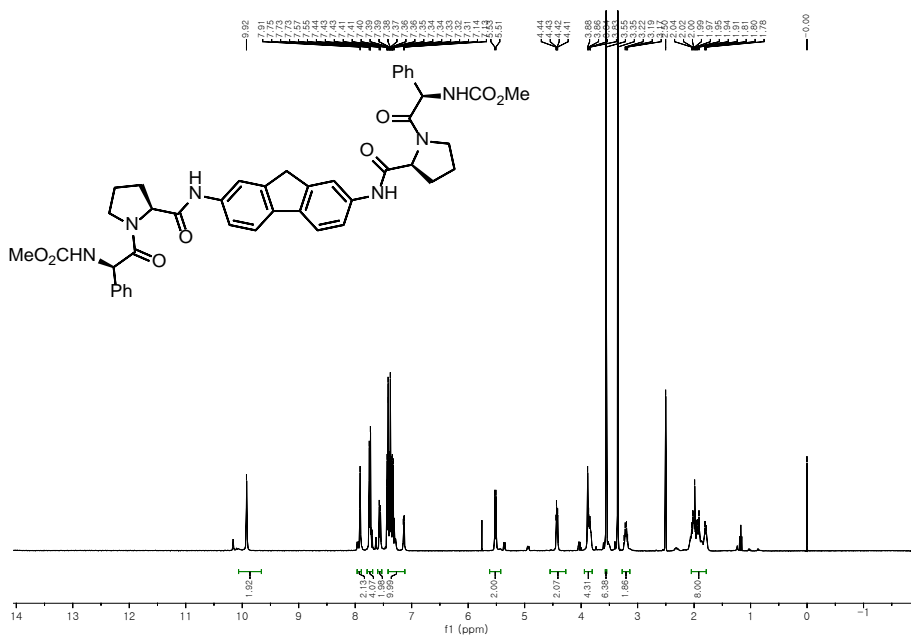


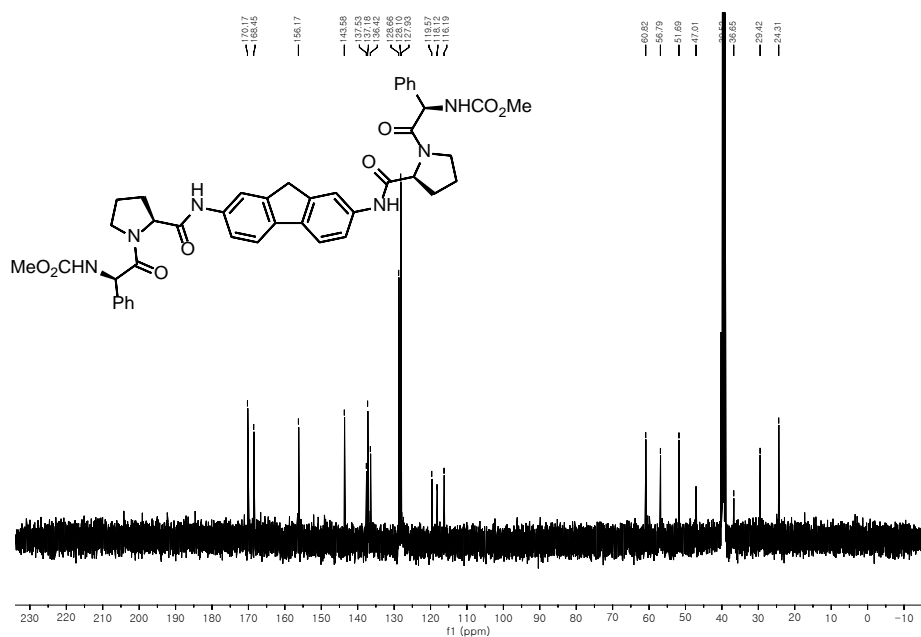


^{19}F NMR Spectrum of **39**

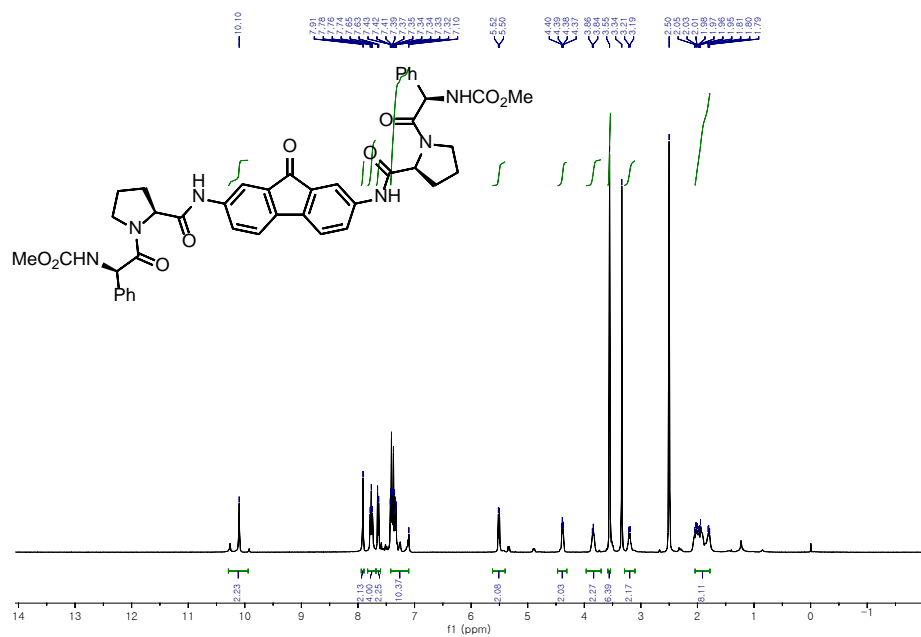


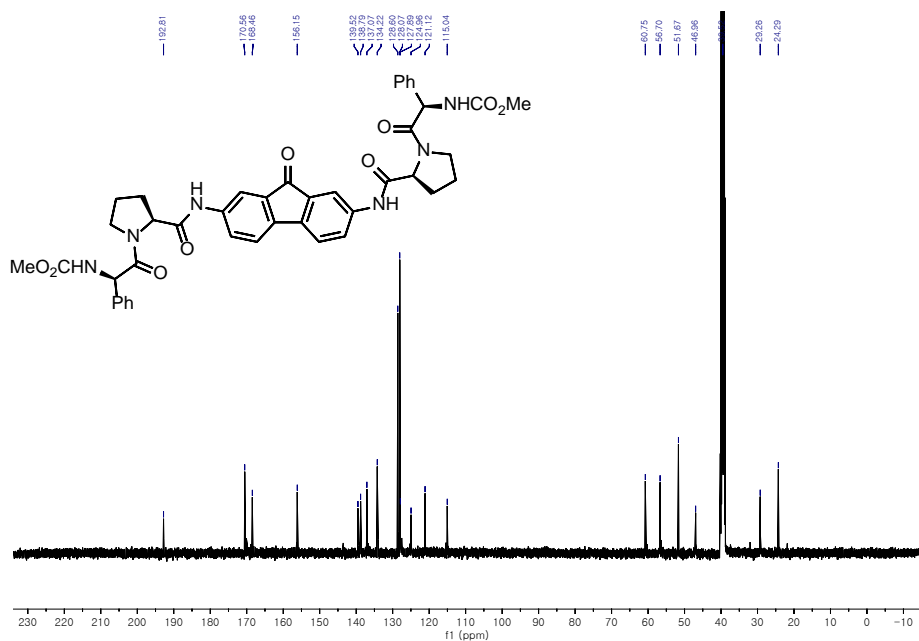
40



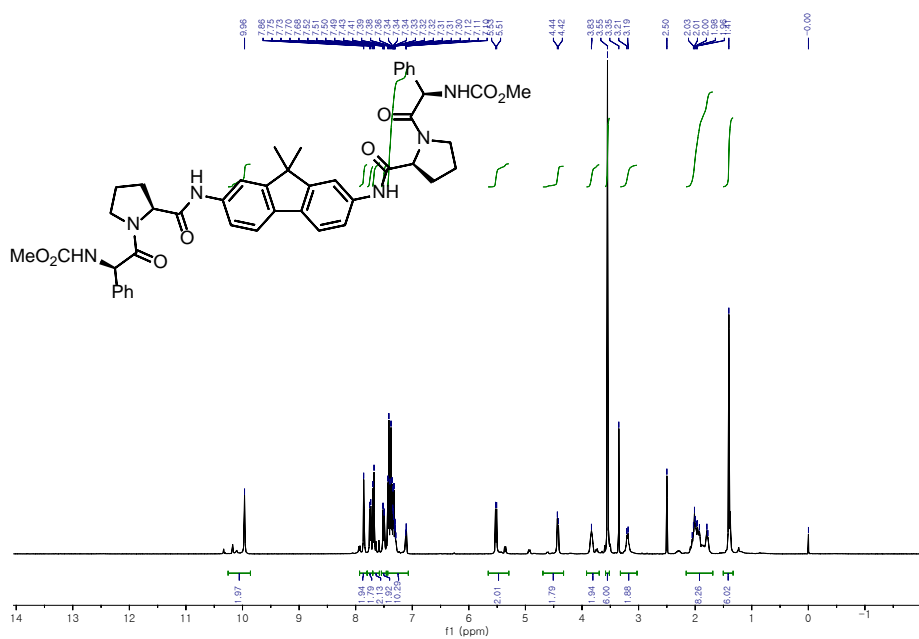


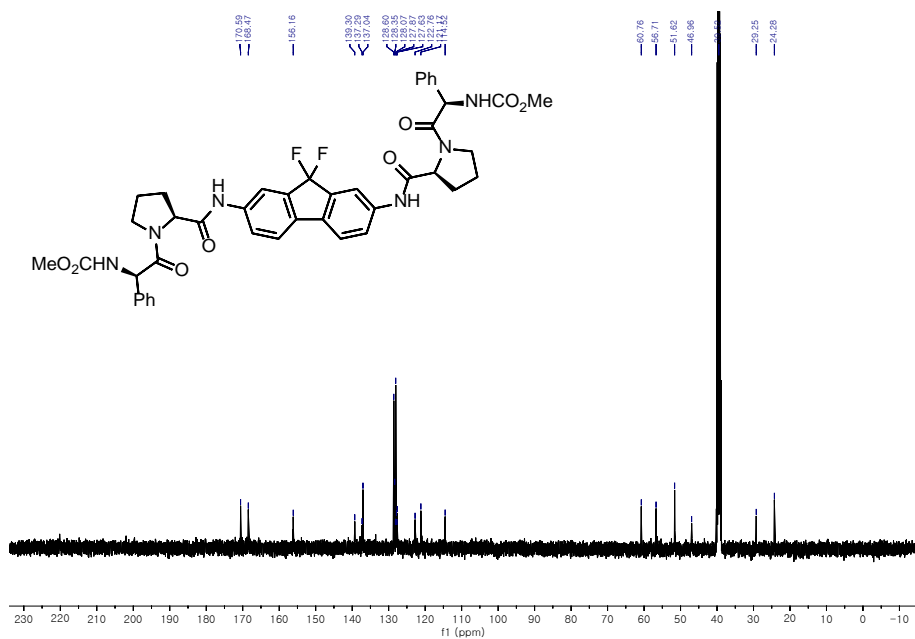
41





42





국문초록

I. NS5A 를 타겟으로 하는 C 형 간염 치료제 연구

2010 년, BMS (Bristol-Myers Squibb)사에서 개발한 디페닐계 HCV NS5A 저해제인 다클라타스비르는 여러가지 유전자형에 매우 높은 저해 활성으로 보여 혁신신약이라는 찬사를 받았다. 이에 다클라타스비르의 이미다졸 작용기를 아미이드 작용기로 치환하여, 벤지딘으로부터 3 단계 반응을 통하여 벤젠 프롤린아미이드구조의 신규 저해제를 개발하였다. 마지막부분의 캡핑기에 구조-활성 관계를 조사해본 결과, 비천연 아미노산의 페닐글라이신 형태가 가장 높은 효능을 보였다. 이를 바탕으로 마지막부분의 캡핑기를 고정한 뒤, 프롤린과 벤지딘의 유도체를 조합하여 구조-활성 관계를 다시 확인하였다. 프롤린부분은 처음에 도입하였던 천연 아미노산의 프롤린이 가장 좋은 활성을 보였고, 벤지딘은 오르토위치보다는 메타위치에 치환기가 있을 경우, 항-HCV 활성이 매우 뛰어난 것을 발견하였다. 이에 메타위치가 묶여 있는 플루오렌구조를 착안하여 신규성이 있으면서 활성이 우수한 물질을 발견하였고, 이를 토대로 타 기관과의 협업을 통한 전임상 후보물질 도출을 위한 물성조사, 약동역학 테스트 및 초기 독성 조사하였다. 그 결과, 독성이 없고 전임상을 하여도 손색이 없는 새로운 C 형간염 저해제를 제시하였다.

II. 팔라듐 산화철 나노입자를 이용한 컨쥬게이션된 폴리머 합성법

전기나 광전자의 성격에 영향을 미치는 컨쥬게이션된 폴리머를 합성하는 방법에는 루테튬을 이용한 상호 교환 반응, 구리를 이용한 클릭 화학, 팔라듐을 이용한 탄소-탄소 연결 반응 등이 있다. 이러한 반응을 이용하기 위하여 사용하는 리간드나 전이금속은 고분자의 파이-파이 상호작용을 통하여 항상 잔류하는 문제가 발생하여 고분자 고유의 성질을 파악하기가 힘들었다. 해결방안으로 반응성은 균질성의 촉매와 유사하되, 분리할 때는 비균질성 촉매의 특성을 가지는 팔라듐 산화철 나노입자를 이용하여 스즈키 중합반응을 수행하였다. 개발된 중합방법은 70 도의 비교적 낮은 온도에서도 충분히 반응성이 좋음을 밝혔고, 합성된 고분자를 하소하여 팔라듐 함량을 알아냈으며, 그 수치는 균질성 팔라듐 촉매에 비해 월등히 최소화할 수 있었다. 또한 반응이 끝난 뒤, 촉매를 자성을 이용하여 쉽게 회수할 수 있었고, 회수된 촉매는 출발물질과 염기, 용매만을 추가하여 최대 11 번까지 팔라듐이 최소화된 고분자를 얻을 수 있었다. 게다가, 11 번까지 사용한 촉매는 처음상태의 촉매처럼 일정한 나노 크기와 모양을 유지할 수 있었고 촉매의 팔라듐 함량도 크게 줄지 않았다. 개발된 고분자 중합방법론은 친환경적이어서 산업에도 충분히 이용가능 할 것으로 사료된다.